

# Algorithms and Bounds for Complex and Quaternionic Lattices With Application to MIMO Transmission

Sebastian Stern, *Member, IEEE*, Cong Ling, *Member, IEEE*, and Robert F.H. Fischer, *Senior Member, IEEE*

**Abstract**—Lattices are a popular field of study in mathematical research, but also in more practical areas like cryptography or multiple-input/multiple-output (MIMO) transmission. In mathematical theory, most often lattices over real numbers are considered. However, in communications, complex-valued processing is usually of interest. Besides, by the use of dual-polarized transmission as well as by the combination of two time slots or frequencies, four-dimensional (quaternion-valued) approaches become more and more important. Hence, to account for this fact, well-known lattice algorithms and related concepts are generalized in this work. To this end, a brief review of complex arithmetic, including the sets of Gaussian and Eisenstein integers, and an introduction to quaternion-valued numbers, including the sets of Lipschitz and Hurwitz integers, are given. On that basis, generalized variants of two important algorithms are derived: first, of the polynomial-time LLL algorithm, resulting in a reduced basis of a lattice by performing a special variant of the Euclidean algorithm defined for matrices, and second, of an algorithm to calculate the successive minima—the norms of the shortest independent vectors of a lattice—and its related lattice points. Generalized bounds for the quality of the particular results are established and the asymptotic complexities of the algorithms are assessed. These findings are extensively compared to conventional real-valued processing. It is shown that the generalized approaches outperform their real-valued counterparts in complexity and/or quality aspects. Moreover, the application of the generalized algorithms to MIMO communications is studied, particularly in the field of lattice-reduction-aided and integer-forcing equalization.

**Index Terms**—Lattices, lattice reduction, LLL algorithm, successive minima, Gaussian integers, Eisenstein integers, quaternions, Lipschitz integers, Hurwitz integers, MIMO, lattice-reduction-aided equalization, integer-forcing equalization.

## I. INTRODUCTION

THE concept of lattices has been studied for almost two centuries. Initial work was, e.g., published by Hermite [3], by Korkine and Zolotareff [4], and by Minkowski [5]. Nevertheless, lattices remained a topic of theoretical mathematical studies for quite a long time.

Sebastian Stern and Robert F.H. Fischer are with the Institute of Communications Engineering, Ulm University, 89081 Ulm, Germany (e-mail: sebastian.stern@uni-ulm.de; robert.fischer@uni-ulm.de).

Cong Ling is with the Department of Electrical and Electronic Engineering, Imperial College London, London SW7 2AZ, United Kingdom (e-mail: cling@ieee.org).

The work of Sebastian Stern and Robert F.H. Fischer has been supported in part by the Deutsche Forschungsgemeinschaft (DFG) under grant Fi 982/13-1 and the work of Cong Ling by the Engineering and Physical Sciences Research Council (EPSRC) under grant EP/S021043/1.

Parts of this work have been discussed in the conference paper [1, DOI: 10.1109/ICT.2018.8464898] presented at the 25<sup>th</sup> International Conference on Telecommunications, Saint Malo, France, 2018, and in Sebastian Stern's dissertation [2, DOI: 10.18725/OPARU-32407].

This situation dramatically changed with the advent of the digital revolution in the late 20<sup>th</sup> century. Suddenly, enough computational power was available to implement and run particular algorithms for lattice problems. The most prominent one was proposed by Lenstra, Lenstra and Lovász [6]. The LLL algorithm calculates a *reduced basis* of a lattice, i.e., a more suited mathematical description of the lattice w.r.t. some quality criteria, with only polynomial-time complexity. More powerful strategies for lattice basis reduction were addressed in the sequel, e.g., the concepts of Hermite-Korkine-Zolotareff (HKZ) reduction [7]–[9] or Minkowski reduction [9], [10], that, however, demand an exponentially-growing computational complexity for calculating the reduced basis. All above-mentioned algorithms operate over real numbers, i.e., the lattices are defined over the integer ring  $\mathbb{Z}$ .

Apart from the application of lattices in cryptological schemes [11], lattices gained popularity in the field of multiple-input/multiple-output (MIMO) communications [12]. In particular, maximum-likelihood (ML) detection was enabled by the sphere decoder [13], however, with the burden of a large computational complexity. An alternative, low-complexity strategy was given with the concept of lattice-reduction-aided (LRA) equalization [2], [14]–[19]. Here, the channel equalization is performed in a *more suited basis* which is obtained by one of the above-mentioned lattice-basis-reduction algorithms—most often, by the polynomial-time LLL algorithm. Since, for block-fading channels, this calculation has only to be done once in the beginning, the computational complexity is dramatically decreased when compared with ML detection. Besides, in comparison to straight-forward linear equalization of the MIMO channel, the noise enhancement can significantly be lowered, even resulting in the optimum diversity behavior as shown in [20].

A few years ago, the concept of integer-forcing (IF) linear (MIMO) equalization has been introduced [21]. The LRA and IF approaches share the philosophy of performing the channel equalization in a more suited representation of the channel matrix such that the noise enhancement inherently caused by equalization is lowered. However, it was found out that the restriction to lattice basis reduction—described by a unimodular integer transformation matrix—is actually not required. Instead, it is sufficient that this integer matrix has full rank—the lattice-basis-reduction problem is weakened to the so-called *successive-minima problem*. For a more detailed insight into the topic, see, e.g., [19]. These successive minima are also quite important for the derivation of bounds for lattice-basis-reduction schemes, as they serve as lower bounds for the norms of the basis vectors.

In MIMO transmission, the channel matrix is usually assumed to be complex-valued due to representation in the equivalent complex-baseband domain [22], [23]. Since the algorithms available for lattice-basis reduction have initially been real-valued, equalization was performed with an equivalent real-valued representation of the complex channel, resulting in doubled dimensions. Nevertheless, the concept can be extended to the complex case. Then, the lattice is not considered over  $\mathbb{Z}$  any more, but over the complex integers—the so-called *Gaussian integers*  $\mathcal{G}$  [24], [25]. In particular, the high-complexity HKZ and Minkowski reduction algorithms were adapted in order to run over Gaussian integers [26], [27]—mainly due to the reason that the complex-valued algorithms lower the computational complexity in comparison to their real-valued counterparts. Furthermore, it was found out that the use of another complex integer ring may be beneficial [28], [29]—of the *Eisenstein integers*  $\mathcal{E}$  [25], [30], forming the hexagonal lattice over the complex numbers. To be precise, signal constellations that form subsets of the Eisenstein integers may enable a *packing gain* [2], i.e., they cover less space in the complex plane than those based on Gaussian integers (quadrature-amplitude modulation (QAM)) with the same cardinality while the minimum distance between the signal points stays the same. Hence, the constellation's variance and the related required transmit power can be lowered.

Moreover, in recent years, four-dimensional signaling techniques have become more and more popular. In particular, in the field of optical communications, it is already quite common to employ both polarization planes of electromagnetic waves [31], resulting in a *dual-polarized* transmission. In wireless (MIMO) communications, *dual-polarized antennas* have been designed, e.g., in [32]–[34]. Besides, diversity schemes that are suited to combine the transmit symbols of two different time steps or frequencies are known for some time, e.g., the famous Alamouti scheme [35]. Given such a four-dimensional signal space, its representation over the set of *quaternion numbers* [25], [36] is quite obvious [37], [38]. Thereby, it has to be taken into account that quaternion-valued (scalar) multiplication is not commutative any more, i.e., the quaternionic numbers do not form a field but only a *skew field*. Related integer rings are given by the (non-Euclidean) set of *Lipschitz integers*  $\mathcal{L}$ —forming the quaternionic integer lattice (integers in each component)—and by the *Hurwitz integers*  $\mathcal{H}$ —enabling the Euclidean property by additionally including all quaternions with only *half-integer* components [25], [36].

Concerning the low-complexity (polynomial-time) LLL reduction algorithm [6], it is known for quite some time that it can be interpreted to form some kind of *Euclidean algorithm* for matrices [39]. Consequently, it can generally be applied w.r.t. any integer ring with Euclidean property, i.e., over rings for which a Euclidean algorithm can uniquely be defined. In [39], the possibility to apply LLL reduction over  $\mathcal{G}$ ,  $\mathcal{E}$ , and  $\mathcal{H}$  has briefly been discussed, however, only providing vague definitions of bases that can be called reduced over these particular rings. In the sequel, these criteria have been shown to be too unspecific [40]. Hence, in [40], a complex-valued (Gaussian-integer) adaption of the LLL reduction algorithm has been proposed. To this end, the real-valued quantization

operation inherently performed in the initial LLL algorithm has been replaced by a respective complex one, resulting in a stronger reduction criterion compared to [39]. In [41], an algorithm operating over the set of Eisenstein integers has been employed which is based on a further adaption of the quantization operation. Recently, in [42], LLL reduction over (other) imaginary quadratic (i.e., complex-valued) fields has been studied, again based on the adjustment of the corresponding quantization operation in the reduction algorithm. However, all those publications cover special cases rather than providing generalized criteria and algorithms. Moreover, besides the brief consideration in [39], hardly anything is known about the possibility to define an LLL reduction that operates over quaternion numbers.

Concerning algorithms that solve the successive minima problem, i.e., algorithms that calculate the matrices which are optimal w.r.t. noise enhancement for the LRA/IF receiver concepts, the situation is similar: Given the low-dimensional case, efficient algorithms have been proposed a few years ago [43]–[45]. They are, though, either completely restricted to the real-valued case or cover the complex-valued (Gaussian-integer) case by employing its equivalent real-valued representation. Besides, in [29], initial results for lattices over the Eisenstein integers have been provided that have been obtained by a particular adaption of the sphere-decoding algorithm [13]. A bound on the first successive minimum for the case of imaginary quadratic fields has been considered in [42]. Beyond that, the definition and assessment of a *generalized* successive-minima algorithm—also w.r.t. quaternionic lattices—is still an open point.

Hence, apart from a review of complex lattices and the introduction to quaternionic arithmetic, the aims and contributions of this work can be divided into three main aspects. The first point is the generalization of the LLL reduction approach based on its interpretation as Euclidean algorithm for matrices. Given the fact that the related operations are actually modulo reductions defined over Euclidean rings, generalized variants of the LLL algorithm are derived. Theoretical analysis of the related properties and parameters is provided for all real-, complex-, and quaternion-valued integer rings mentioned above. Beyond that, the application of LLL reduction given a *non-Euclidean ring*—in particular the Lipschitz integers—is discussed. Moreover, the list-based successive-minima algorithm from [44] is generalized in order to determine the successive minima for all above-mentioned complex and quaternionic (Euclidean/non-Euclidean) integer rings. All algorithms are provided in such a way that the non-commutative behavior of quaternionic multiplication is adequately taken into account.

The second main aspect deals with the generalization of quality bounds which have originally been derived for real-valued LLL reduction [6], [46] and/or the real-valued successive-minima problem [3], [9], [46]. This particularly concerns the norms of the basis vectors (and the respective successive minima), as well as the orthogonality defect of a lattice basis. It is shown that the quaternion-valued and/or complex-valued approaches may outperform their real-valued equivalents—especially if lattices over the Eisenstein or the Hurwitz integers are considered. Moreover, the asymptotic

computational complexities of the different approaches are established. Concerning the (polynomial-time) LLL lattice-basis-reduction approach, these derivations reveal that the complexity can considerably be decreased if the respective complex- or quaternion-valued variants are employed. By providing additional results from numerical simulations, it is shown that the quality bounds and complexity evaluations reflect the behavior that can be observed when i.i.d. Gaussian stochastic models are applied in practice.

Finally, the application of the derived approaches in MIMO communications, particularly in the case of (multi-user) MIMO uplink transmission [12] based on the concepts of LRA and IF equalization, is extensively studied. This includes a discussion on how the quaternion-valued concept can be employed in dual-polarized transmission, as well as in the Alamouti-like combination of two time steps or frequencies. Respective system models are derived and evaluated by means of numerical simulations for particular transmission scenarios. These results show that the theoretical derivations and bounds also reflect the behavior in practical MIMO schemes. Beyond that, the combination of the proposed strategies with advanced complex and quaternionic signal constellations—also w.r.t. soft-decision decoding approaches—is briefly discussed.

The paper is structured as follows: In Sec. II, complex integer rings are briefly reviewed and an introduction to quaternions including the sets of Lipschitz and Hurwitz integers is given. In Sec. III, the LLL algorithm as well a list-based algorithm for the determination of the successive minima of a lattice are generalized. Related quality bounds and the assessment of the computational complexities are provided in Sec. IV. In Sec. V, the particular application of the generalized algorithms is regarded in the field of MIMO communications. The paper is closed by a brief summary and an outlook in Sec. VI.

## II. TWO- AND FOUR-DIMENSIONAL EXTENSIONS OF THE REAL NUMBERS AND RELATED LATTICES

In this section, the sets of *complex numbers* and *quaternions* that form a two- and four-dimensional extension of the real numbers, respectively, are reviewed. The related algebras are presented and important subsets, particularly integer rings, are discussed. On that basis, generalized *lattices* are defined.

### A. Complex Numbers and Quaternions

First, the extension of the real numbers  $\mathbb{R}$  to complex numbers and quaternions, respectively, is reviewed. For a deeper insight into the topic, see [25], [36], [47].

1) *Complex Numbers*: The set of complex numbers

$$\mathbb{C} = \{c = \underbrace{c^{(1)}}_{\text{Re}\{c\}} + \underbrace{c^{(2)}}_{\text{Im}\{c\}} i \mid c^{(1)}, c^{(2)} \in \mathbb{R}\} \quad (1)$$

forms a *field extension* of the real numbers. It is obtained by extending the first, real component  $c^{(1)}$  (*real part*  $\text{Re}\{c\}$ ) by a second component  $c^{(2)}$  which is multiplied by the *imaginary unit*  $i = \sqrt{-1}$  (*imaginary part*  $\text{Im}\{c\}$ ).

The complex conjugate of  $c \in \mathbb{C}$  reads  $c^* = c^{(1)} - c^{(2)} i$  and the absolute value of  $c$  is given as  $|c| = \sqrt{(c^{(1)})^2 + (c^{(2)})^2}$ .

Scalar additions (and subtractions) over complex numbers are performed individually per component. The multiplication of two complex numbers  $u, v \in \mathbb{C}$  can be expressed as

$$\begin{aligned} w &= (u^{(1)} + u^{(2)} i) \cdot (v^{(1)} + v^{(2)} i) \\ &= \underbrace{(u^{(1)}v^{(1)} - u^{(2)}v^{(2)})}_{w^{(1)}} + \underbrace{(u^{(1)}v^{(2)} + u^{(2)}v^{(1)})}_{w^{(2)}} i. \end{aligned} \quad (2)$$

Hence, four multiplications and two additions/subtractions are required. Following the concept of the Karatsuba algorithm [48], this multiplication can alternatively be realized by three multiplications and five additions/subtractions. The scalar division of  $u$  by  $v$  is performed by the scalar multiplication  $u \cdot v^{-1}$  with the element  $v^{-1} = v^*/|v|^2 = v^* \cdot (v^*v)^{-1}$ .

Based on (2), an *equivalent real-valued* representation of complex matrices can be given. An  $N \times K$  matrix  $C \in \mathbb{C}^{N \times K}$  may be represented via its equivalent  $2N \times 2K$  real matrix

$$C_r = \begin{bmatrix} C^{(1)} & -C^{(2)} \\ C^{(2)} & C^{(1)} \end{bmatrix} \in \mathbb{R}^{2N \times 2K}, \quad (3)$$

where  $C^{(1)}$  and  $C^{(2)}$  denote the real and imaginary part of  $C$ , respectively. Hence, the dimensions are increased by a factor of  $D_r = 2$ . This variable also represents the number of independent real-valued components in (1). If  $N \geq K$ ,

$$\det(C^H C) = \sqrt{\det(C_r^T C_r)} \quad (4)$$

is valid [47], where  $C^H$  denotes the Hermitian of  $C$ , i.e., the conjugated transpose. Utilizing (3), the matrix addition (and subtraction)  $S = U + V$ , where  $U$  and  $V$  denote complex matrices, as well as the related complex matrix multiplication (and division)  $W = U \cdot V$ , can isomorphically be represented by the real-valued addition  $S_r = U_r + V_r$  and the real-valued multiplication  $W_r = U_r \cdot V_r$ , respectively.

2) *Quaternions*: The set of quaternions<sup>1</sup> [25], [36]

$$\begin{aligned} \mathbb{H} &= \{q = \underbrace{q^{\{1\}}}_{q^{(1)} + q^{(2)} i} + \underbrace{q^{\{2\}}}_{q^{(3)} + q^{(4)} i} j \mid q^{\{1\}}, q^{\{2\}} \in \mathbb{C}\} \\ &= \{q = q^{(1)} + q^{(2)} i + q^{(3)} j + q^{(4)} k \mid \\ &\quad q^{(1)}, q^{(2)}, q^{(3)}, q^{(4)} \in \mathbb{R}\} \end{aligned} \quad (5)$$

extends the set of complex numbers by an *additional* complex-valued component which is multiplied by the imaginary unit  $j$ . Hence, *four real-valued* components are present, where the real part of a quaternion reads  $\text{Re}\{q\} = q^{(1)}$  and its imaginary part is represented by the 3-tuple  $\text{Im}\{q\} = (q^{(2)}, q^{(3)}, q^{(4)})$ . The related imaginary *quaternion units* are given as  $i, j$ , and  $k = ij$ . The relations between these units are described by the *Hamilton equations* [36] which are stated in Table I.

From Table I, it becomes apparent that the multiplication of two quaternions is—in general—not commutative. Consequently, the quaternions do not form a field but only a *skew field*, i.e., they fulfill all conditions which are required to form a field—except for the commutativity of the multiplication.

By analogy with complex numbers, the conjugate of a quaternion  $q \in \mathbb{H}$  is given as  $q^* = q^{(1)} - q^{(2)} i - q^{(3)} j - q^{(4)} k$ .

<sup>1</sup>In honor of Sir William Rowan Hamilton, the set of quaternions is denoted by  $\mathbb{H}$ .

TABLE I  
HAMILTON EQUATIONS [36] FOR THE PRODUCT  $u \cdot v$ , WHERE  $u$  AND  $v$   
ARE QUATERNION UNITS, I.E.,  $u, v \in \{1, i, j, k\}$ .

$u \backslash v$	1	i	j	k
1	+1	+i	+j	+k
i	+i	-1	+k	-j
j	+j	-k	-1	+i
k	+k	+j	-i	-1

The absolute value of  $q$  is uniquely defined by  $|q| = \sqrt{qq^*} = \sqrt{q^*q} = \sqrt{(q^{(1)})^2 + (q^{(2)})^2 + (q^{(3)})^2 + (q^{(4)})^2}$ . Moreover, additions (and subtractions) are performed individually per component. The (non-commutative) multiplication of two quaternions  $u, v \in \mathbb{H}$  is expressed as [36]

$$\begin{aligned} u \cdot v &= (u^{(1)}v^{(1)} - u^{(2)}v^{(2)} - u^{(3)}v^{(3)} - u^{(4)}v^{(4)}) \\ &+ (u^{(1)}v^{(2)} + u^{(2)}v^{(1)} + u^{(3)}v^{(4)} - u^{(4)}v^{(3)})i \\ &+ (u^{(1)}v^{(3)} - u^{(2)}v^{(4)} + u^{(3)}v^{(1)} + u^{(4)}v^{(2)})j \\ &+ (u^{(1)}v^{(4)} + u^{(2)}v^{(3)} - u^{(3)}v^{(2)} + u^{(4)}v^{(1)})k, \end{aligned} \quad (6)$$

i.e., 16 multiplications and twelve additions/subtractions are required. Alternatively, this multiplication can be realized using eight multiplications and 28 additions/subtractions [49]. The division can be implemented via the multiplication with the inverse element  $v^{-1} = v^* \cdot (v^*v)^{-1}$ , where this choice ensures that  $vv^{-1} = 1$  (right inverse) and  $v^{-1}v = 1$  (left inverse).

Similar to the real-valued representation of complex matrices, the quaternion-valued arithmetic defined in (6) can be realized by the *equivalent complex- or real-valued matrix representation*. In particular, an  $N \times K$  matrix  $M \in \mathbb{H}^{N \times K}$  can be represented as  $2N \times 2K$  complex-valued matrix<sup>2</sup>

$$\begin{aligned} M_c &= \begin{bmatrix} M^{\{1\}} & -M^{\{2\}} \\ (M^{\{2\}})^* & (M^{\{1\}})^* \end{bmatrix} \\ &= \begin{bmatrix} M^{(1)} + M^{(2)}i & -M^{(3)} - M^{(4)}i \\ M^{(3)} - M^{(4)}i & M^{(1)} - M^{(2)}i \end{bmatrix}, \end{aligned} \quad (7)$$

where (7) directly corresponds to (3), i.e., the dimensions are increased by a factor of  $D_c = 2$ , with the only difference that an additional conjugation has to be performed in the second row. In (3), this step is not required since only real numbers are present. By plugging (7) into (3), i.e., by forming the real-valued representation of the complex matrix  $M_c$ , one would obtain one particular real-valued  $4N \times 4K$  representation of the quaternion-valued matrix  $M$ . However, for the subsequent system model, it is more convenient to form a real-valued representation according to<sup>2</sup>

$$M_r = \begin{bmatrix} M^{(1)} & -M^{(2)} & -M^{(3)} & -M^{(4)} \\ M^{(2)} & M^{(1)} & -M^{(4)} & M^{(3)} \\ M^{(3)} & M^{(4)} & M^{(1)} & -M^{(2)} \\ M^{(4)} & -M^{(3)} & M^{(2)} & M^{(1)} \end{bmatrix}, \quad (8)$$

<sup>2</sup>The complex- and real-valued representations (7) and (8), respectively, are not unique. There exist several representations that differ in the positions of the minus signs within the matrices  $M_c$  and  $M_r$ , see, e.g., [25], [50], [51]. However, all these representations isomorphically express the quaternion-valued multiplication (division) according to (6).

in which the four components are directly stacked in the left-most column. The dimensions are increased by a factor of  $D_r = 4$ , representing the four independent real-valued components in (5). Here, if  $N \geq K$ , we have<sup>3</sup>

$$\det(M^H M) = \sqrt{\det(M_c^H M_c)} = \sqrt[4]{\det(M_r^T M_r)}, \quad (9)$$

$M^H$  denoting the Hermitian (conjugated transpose) of  $M$ .

### B. Integer Rings

The set of *integers*  $\mathbb{Z} = \{\dots, -2, -1, 0, 1, 2, \dots\}$  forms a subset of the real numbers  $\mathbb{R}$  and additionally a *Euclidean ring*. Hence, for  $u, \sigma, v, \rho \in \mathbb{Z}$  and  $v \neq 0$ , a division  $u/v$  with *small remainder* according to<sup>4</sup>

$$u = \sigma \cdot v + \rho \quad (10)$$

is possible, where the term *small remainder* implicates that  $|\rho| < |v|$  is valid [52, Def. 2.5]. Consequently, the *Euclidean algorithm* [53] can be used to calculate the *greatest common divisor* (gcd) of two numbers  $u, v \in \mathbb{Z}$ . The minimum squared distance between the elements of  $\mathbb{Z}$  reads  $d_{\min, \mathbb{Z}}^2 = 1$ .

A real number  $r \in \mathbb{R}$  is quantized to its nearest integer via

$$Q_{\mathbb{Z}}\{r\} = \lfloor r \rfloor \in \mathbb{Z}, \quad (11)$$

i.e., by a simple rounding operation  $\lfloor \cdot \rfloor$ , where w.l.o.g. we assume that ties are resolved towards  $+\infty$ . The maximum squared quantization error occurs for all half-integer values ( $\mathbb{Z} + \frac{1}{2}$ ) and is given as  $\epsilon_{\mathbb{Z}}^2 = |Q_{\mathbb{Z}}\{\frac{1}{2}\} - \frac{1}{2}|^2 = \frac{1}{4}$ . The related (non-squared) error corresponds with the maximum of the remainder in (10), i.e., we have  $|\rho| \leq \frac{1}{2} < |v|$ , since  $|v| \geq 1 \forall v \in \mathbb{Z} \setminus \{0\}$ . Based on the quantization (11), the *modulo function*

$$\text{mod}_{\mathbb{Z}}\{r\} = r - Q_{\mathbb{Z}}\{r\} \quad (12)$$

yields a congruent point  $r + \lambda$ ,  $\lambda \in \mathbb{Z}$ , located within  $[-\frac{1}{2}, \frac{1}{2})$ , forming the Voronoi cell of  $\mathbb{Z}$  w.r.t. the origin [22], [25].

1) *Complex-Valued Integer Rings*: Integers in the complex plane are represented by the *Gaussian integers* [24], [25], [54]

$$\mathcal{G} = \{c = c^{(1)} + c^{(2)}i \mid c^{(1)}, c^{(2)} \in \mathbb{Z}\} = \mathbb{Z} + \mathbb{Z}i. \quad (13)$$

They are illustrated in Fig. 1 (left). The minimum squared distance between the elements reads  $d_{\min, \mathcal{G}}^2 = 1$ . The quantization of a complex number  $c \in \mathbb{C}$  to  $\mathcal{G}$  is performed as

$$Q_{\mathcal{G}}\{c\} = \lfloor c^{(1)} \rfloor + \lfloor c^{(2)} \rfloor i \in \mathcal{G}, \quad (14)$$

where the maximum squared quantization error sums up to  $\epsilon_{\mathcal{G}}^2 = |Q_{\mathcal{G}}\{\frac{1}{2} + \frac{1}{2}i\} - (\frac{1}{2} + \frac{1}{2}i)|^2 = \frac{1}{2}$ . The modulo operation  $\text{mod}_{\mathcal{G}}\{c\} = c - Q_{\mathcal{G}}\{c\}$  reduces a complex number  $c$  to the Voronoi cell of  $\mathcal{G}$  (w.r.t. the origin), which forms a square in the complex plane where all values are located within the range  $[-\frac{1}{2}, \frac{1}{2})$  per component.

<sup>3</sup>Due to the skew-field property, quaternion-valued determinants do not necessarily possess all properties which are known from real or complex ones. However, for Hermitian matrices (here, the Gramian  $M^H M$ ), they can, to a large extent, be employed just like real or complex determinants, cf. [50].

<sup>4</sup>We assume that negative remainders may occur, i.e., the modulo operation defined in (12) is assumed to be symmetric w.r.t. the origin.

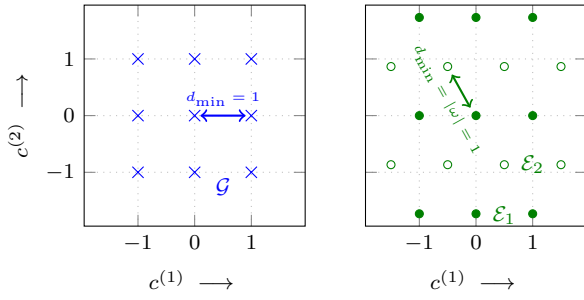


Fig. 1. Illustration of the Gaussian integers  $\mathcal{G}$  (left) and the Eisenstein integers  $\mathcal{E}$  (right). For the Eisenstein integers, the two subsets  $\mathcal{E}_1$  (filled circles) and  $\mathcal{E}_2$  (hollow circles) are shown.

The *Eisenstein integers* [25], [30]

$$\mathcal{E} = \{c = c^{(1)} + c^{(2)}\omega \mid c^{(1)}, c^{(2)} \in \mathbb{Z}\} = \mathbb{Z} + \mathbb{Z}\omega, \quad (15)$$

with the Eisenstein unit  $\omega = e^{\frac{2\pi}{3}i}$  (third root of unity), represent the hexagonal numbers ( $A_2$  lattice [25]) in the complex plane, cf. Fig. 1 (right). Without a decrease in minimum distance ( $d_{\min, \mathcal{E}}^2 = 1$ ), the elements are more densely packed (particularly, the densest packing in two-dimensions is achieved [22], [25]). The quantization is realized as [25], [55]

$$Q_{\mathcal{E}}\{c\} = \operatorname{argmin}_{Q_{\mathcal{E}_1}\{c\}, Q_{\mathcal{E}_2}\{c\}} \{|c - Q_{\mathcal{E}_1}\{c\}|, |c - Q_{\mathcal{E}_2}\{c\}|\}, \quad (16)$$

$$Q_{\mathcal{E}_1}\{c\} = Q_{\mathbb{Z}}\{c^{(1)}\} + \sqrt{3}Q_{\mathbb{Z}}\left\{\frac{c^{(2)}}{\sqrt{3}}\right\}i, \quad (17)$$

$$Q_{\mathcal{E}_2}\{c\} = Q_{\mathbb{Z}}\left\{c^{(1)} - \frac{1}{2}\right\} + \frac{1}{2} + \left(\sqrt{3}Q_{\mathbb{Z}}\left\{\frac{c^{(2)} - \frac{\sqrt{3}}{2}}{\sqrt{3}}\right\} + \frac{\sqrt{3}}{2}\right)i, \quad (18)$$

i.e., by performing a quantization to the subsets  $\mathcal{E}_1$  (filled circles in Fig. 1 (right)) and  $\mathcal{E}_2$  (hollow circles) and a subsequent decision to the point which is located closer to the original value  $c \in \mathbb{C}$ . The maximum squared quantization error reads  $\epsilon_{\mathcal{E}}^2 = \frac{1}{3}$ , cf. [2], [22], [25]. The modulo operation  $\operatorname{mod}_{\mathcal{E}}\{c\} = c - Q_{\mathcal{E}}\{c\}$  calculates a point  $c + \lambda$ ,  $\lambda \in \mathcal{E}$ , located within the *hexagonal* Voronoi cell of  $\mathcal{E}$  w.r.t. the origin.

Both Gaussian and Eisenstein integers form Euclidean rings [39]. Due to the maximum squared quantization errors, for the former,  $|\rho| \leq \frac{1}{\sqrt{2}} < |v|$ , with  $|v| \geq 1 \forall v \in \mathcal{G} \setminus \{0\}$ , is valid if the division with remainder according to (10) is performed over  $\mathcal{G}$ . For the latter,  $|\rho| \leq \frac{1}{\sqrt{3}} < |v|$ , with  $|v| \geq 1 \forall v \in \mathcal{E} \setminus \{0\}$ , holds. A division with small remainder can be performed by analogy with (10) and, thus, it is possible to define a Euclidean algorithm over the Gaussian and the Eisenstein integers.

2) *Quaternion-Valued Integer Rings*: With regard to the set of quaternions  $\mathbb{H}$ , two important subsets, in particular integer rings, can be defined. The first type are the *Lipschitz integers*

$$\begin{aligned} \mathcal{L} &= \{q = q^{(1)} + q^{(2)}i + q^{(3)}j + q^{(4)}k \mid \\ &\quad q^{(1)}, q^{(2)}, q^{(3)}, q^{(4)} \in \mathbb{Z}\} \\ &= \mathbb{Z} + \mathbb{Z}i + \mathbb{Z}j + \mathbb{Z}k, \end{aligned} \quad (19)$$

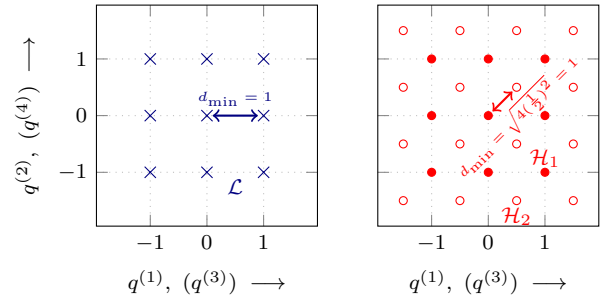


Fig. 2. Two-dimensional projection of the Lipschitz integers  $\mathcal{L}$  (left) and the Hurwitz integers  $\mathcal{H}$  (right). The components  $q^{(3)}$  and  $q^{(4)}$  are projected onto  $q^{(1)}$  and  $q^{(2)}$ , respectively. For the Hurwitz integers, the two subsets  $\mathcal{H}_1$  (filled circles) and  $\mathcal{H}_2$  (hollow circles) are shown.

i.e., following the philosophy of the Gaussian integers, integer values are present in each of the four components. A two-dimensional projection of the Lipschitz integers is illustrated in Fig. 2 (left). Again, the minimum squared distance reads  $d_{\min, \mathcal{L}}^2 = 1$ . The quantization of a quaternion  $q \in \mathbb{H}$  to the closest Lipschitz integer is realized by

$$Q_{\mathcal{L}}\{q\} = [q^{(1)}] + [q^{(2)}]i + [q^{(3)}]j + [q^{(4)}]k \in \mathcal{L}. \quad (20)$$

The modulo operation reads  $\operatorname{mod}_{\mathcal{L}}\{q\} = q - Q_{\mathcal{L}}\{q\}$ , where the Voronoi region constitutes a *hypercube* with the range  $[-\frac{1}{2}, \frac{1}{2})$  per component. The maximum squared quantization error is—in comparison to the Gaussian integers—increased to  $\epsilon_{\mathcal{L}}^2 = |\frac{1}{2} + \frac{1}{2}i + \frac{1}{2}j + \frac{1}{2}k|^2 = 1$ . A direct consequence thereof is that the division with remainder according to (10), with  $u, \sigma, v, \rho \in \mathcal{L}$ , is not a *Euclidean one* any more [36]: Here, the case  $uv^{-1} \in \mathcal{L} + (1+i+j+k)/2$  may occur. Then, for the absolute value of the remainder,  $|\rho| = |(1+i+j+k)/2| = 1 \leq |v|$ , with  $|v| \geq 1 \forall v \in \mathcal{L} \setminus \{0\}$ , is obtained. Hence,  $|\rho| = |v|$  may be present, i.e., the *inequality* required to ensure a *small* remainder is, in general, not achieved. Thus, it is *not* possible to define a Euclidean algorithm in order to calculate the gcd of two Lipschitz integers  $u, v \in \mathcal{L}$ .

Nevertheless, the non-Euclidean property of the Lipschitz integers can be “cured” by the insertion of additional points at the problematic coordinates—the half-integer values located at  $\mathcal{L} + (1+i+j+k)/2$ . Then, as depicted in Fig. 2 (right), the so-called *Hurwitz integers* [25], [36]

$$\begin{aligned} \mathcal{H} &= \left\{q = q^{(1)} + q^{(2)}i + q^{(3)}j + q^{(4)}k \mid \right. \\ &\quad \left. (q^{(1)}, q^{(2)}, q^{(3)}, q^{(4)}) \in \mathbb{Z}^4 \cup \left(\mathbb{Z} + \frac{1}{2}\right)^4\right\} \end{aligned} \quad (21)$$

are obtained, where *all* components are—at the same time—*either* integers *or* half-integers. In particular, the number of points (in quaternion space) is doubled within the same hypervolume—without a decrease in minimum squared distance, which still reads  $d_{\min, \mathcal{H}}^2 = 1$ . These points form the densest packing in four-dimensional space [25], as will be discussed in Sec. II-C. The maximum squared quantization error reads  $\epsilon_{\mathcal{H}}^2 = |\frac{1}{4} + \frac{1}{4}i + \frac{1}{4}j + \frac{1}{4}k|^2 = \frac{1}{2}$ , i.e., for the division with remainder according to (10), we have  $|\rho| \leq \frac{1}{\sqrt{2}} < |v|$ , with  $|v| \geq 1 \forall v \in \mathcal{H} \setminus \{0\}$ . As a consequence, a Euclidean ring is present and a related Euclidean algorithm can be

applied. Thereby, similar to the Eisenstein integers in (16), the quantization is performed as [25], [55]

$$Q_{\mathcal{H}}\{q\} = \underset{Q_{\mathcal{H}_1}\{q\}, Q_{\mathcal{H}_2}\{q\}}{\operatorname{argmin}} \{ |q - Q_{\mathcal{H}_1}\{q\}|, |q - Q_{\mathcal{H}_2}\{q\}| \}, \quad (22)$$

$$Q_{\mathcal{H}_1}\{c\} = Q_{\mathcal{L}}\{q\}, \quad (23)$$

$$Q_{\mathcal{H}_2}\{c\} = Q_{\mathcal{L}}\{q - o_{\mathcal{H}}\} + o_{\mathcal{H}}, \quad o_{\mathcal{H}} = \frac{1 + i + j + k}{2}. \quad (24)$$

Hence, both a quantization to all Lipschitz integers (filled circles in Fig. 2 (right)) and a quantization to all Lipschitz integers shifted by  $\frac{1}{2}$  per component (hollow circles) is done; subsequently, the closest result is chosen as the quantized value. The modulo reduction is, again, described as  $\operatorname{mod}_{\mathcal{H}}\{q\} = q - Q_{\mathcal{H}}\{q\}$ . The points are reduced to the Voronoi cell located around the origin which forms a 24-cell with 24 vertices, 96 edges, and 96 faces [25].

### C. Generalized Definition of Lattices

A lattice  $\Lambda$  is an *infinite* set of points that are distributed over the Euclidean space in such a way that an *Abelian group* w.r.t. addition is present [22], [25], [56]. Most often, lattices are considered over the real numbers. Then, a discrete (infinite) additive subgroup of  $\mathbb{R}^N$  (lattice with *dimension*  $N$ ), or equivalently the set of all integer linear combinations of a set of  $K$  independent vectors (*lattice basis* with *rank*  $K$ ; assembled in the *generator matrix*  $\mathbf{G} \in \mathbb{R}^{N \times K}$ ) is obtained.

In a more general setting, an  $N$ -dimensional lattice of rank  $K$ , with  $N \geq K$ , can be defined by

$$\Lambda(\mathbf{G}) = \left\{ \mathbf{G}\boldsymbol{\zeta} = \sum_{k=1}^K \mathbf{g}_k \zeta_k \mid \zeta_k \in \mathbb{I} \right\}, \quad (25)$$

where  $\mathbf{G} = [\mathbf{g}_1, \dots, \mathbf{g}_K]$  denotes the  $N \times K$  generator matrix of the lattice, and  $\boldsymbol{\zeta} = [\zeta_1, \dots, \zeta_K]^T$  an *integer vector* that describes linear combinations of the basis vectors based on elements drawn from the constituent integer ring  $\mathbb{I}$ .

In the real-valued case ( $\mathbf{G} \in \mathbb{R}^{N \times K}$ ), those linear combinations are expressed by real integers. The generalized definition of lattices in (25) enables the construction of lattices over complex numbers, where  $\mathbf{G} \in \mathbb{C}^{N \times K}$ . Here, both  $\mathbb{I} = \mathcal{G}$  and  $\mathbb{I} = \mathcal{E}$  are suited to express linear combinations. Moreover, lattices over quaternions, with  $\mathbf{G} = \mathbb{H}^{N \times K}$ , can be defined based on the Lipschitz integers ( $\mathbb{I} = \mathcal{L}$ ) or the Hurwitz integers ( $\mathbb{I} = \mathcal{H}$ ) as the constituent integer ring.

The basis of a lattice is not unique. Instead, there exists an infinite number of generator matrices that span the same lattice. The transformation to an alternative generator matrix can be realized by the multiplication with a *unimodular* integer matrix  $\mathbf{T} \in \mathbb{I}^{K \times K}$  according to

$$\mathbf{G}_{\text{red}} = \mathbf{G}\mathbf{T}, \quad \text{with } \det(\mathbf{T}^H \mathbf{T}) = 1. \quad (26)$$

A generator matrix is called *reduced* matrix if, by means of *lattice-reduction algorithms*, this matrix is constructed in such a way that it fulfills some desired quality criteria. Noteworthy, if the unimodularity constraint is relaxed to the full-rank constraint  $\operatorname{rank}(\mathbf{T}) = K$ , *sublattices* of the original lattice with the order  $\sqrt{\det(\mathbf{T}^H \mathbf{T})}$  may be obtained [2], [19].

To evaluate the quality of a lattice basis, the lengths (norms) of the basis vectors  $\mathbf{g}_1, \dots, \mathbf{g}_K$  are often assessed. The Euclidean norm of a vector  $\mathbf{v}$  over  $\mathbb{R}$ ,  $\mathbb{C}$ , or  $\mathbb{H}$  is given as  $\|\mathbf{v}\| = \sqrt{\mathbf{v}^H \mathbf{v}}$ . Another criterion is the *orthogonality defect* [22], [25]

$$\Omega(\mathbf{G}) = \frac{\prod_{k=1}^K \|\mathbf{g}_k\|}{\operatorname{vol}(\Lambda(\mathbf{G}))} \quad (27)$$

of a lattice basis which is given as the product of the basis vectors' norms over the volume of the lattice

$$\operatorname{vol}(\Lambda(\mathbf{G})) = \sqrt{\det(\mathbf{G}^H \mathbf{G})} \quad (28)$$

given as the volume of a related  $K$ -dimensional fundamental parallelotope. Thereby, the volume is the same for all generator matrices that span the same lattice [22], [25].

1) *Real Representation of Complex Lattices*: The Gaussian integers are isomorphic to the two-dimensional real-valued integer lattice  $\mathbb{Z}^2$  (generator matrix<sup>5</sup>  $\mathbf{G} = \mathbf{I}_2$ ), cf. [25]. Hence, a complex lattice with generator matrix  $\mathbf{G} \in \mathbb{C}^{N \times K}$  defined over  $\mathcal{G}$  is isomorphically expressed by a real lattice (over  $\mathbb{Z}$ ) with the generator matrix  $\mathbf{G}_{r,\mathcal{G}} = \mathbf{G}_r \mathbf{I}_{2K} = \mathbf{G}_r$ , cf. (3).

The Eisenstein integers are isomorphic to the real hexagonal lattice  $\mathbf{A}_2$ . Thus, a real lattice representation is obtained via [2]

$$\mathbf{G}_{r,\mathcal{E}} = \underbrace{\mathbf{G}_r}_{(3)} \underbrace{\begin{bmatrix} \mathbf{I}_K & -\frac{1}{2}\mathbf{I}_K \\ \mathbf{0}_K & \frac{\sqrt{3}}{2}\mathbf{I}_K \end{bmatrix}}_{\mathbf{G}_{\mathcal{E}}} \quad (29)$$

where, for  $K = 1$ , the right-hand-side matrix in (29) represents a generator matrix of the  $\mathbf{A}_2$  lattice [25].

2) *Real and Complex Representation of Quaternion-Valued Lattices*: The Lipschitz integers are isomorphic to the four-dimensional (real-valued) integer lattice  $\mathbb{Z}^4$  (generator matrix  $\mathbf{I}_4$ ). Quaternionic lattices over  $\mathcal{L}$  can equivalently be expressed by complex-valued lattices over  $\mathcal{G}$  via the generator matrix  $\mathbf{G}_{c,\mathcal{L}} = \mathbf{G}_c \mathbf{I}_{2K} = \mathbf{G}_c \in \mathbb{C}^{2N \times 2K}$  according to (7), or by real-valued lattices (over  $\mathbb{Z}$ ) with the corresponding generator matrix  $\mathbf{G}_{r,\mathcal{L}} = \mathbf{G}_r \mathbf{I}_{4K} = \mathbf{G}_r \in \mathbb{R}^{4N \times 4K}$  from (8).

Regarding the Hurwitz integers, an isomorphism to the four-dimensional *checkerboard lattice*  $\mathbf{D}_4$  is present [25]. This isomorphism can be exploited in order to define an equivalent real-valued representation (over  $\mathbb{Z}$ ) for lattices over  $\mathcal{H}$ . Here, the equivalent real-valued generator matrix is obtained as

$$\mathbf{G}_{r,\mathcal{H}} = \underbrace{\mathbf{G}_r}_{(8)} \underbrace{\begin{bmatrix} \mathbf{I}_K & \mathbf{0}_K & \mathbf{0}_K & \frac{1}{2}\mathbf{I}_K \\ \mathbf{0}_K & \mathbf{I}_K & \mathbf{0}_K & \frac{1}{2}\mathbf{I}_K \\ \mathbf{0}_K & \mathbf{0}_K & \mathbf{I}_K & \frac{1}{2}\mathbf{I}_K \\ \mathbf{0}_K & \mathbf{0}_K & \mathbf{0}_K & \frac{1}{2}\mathbf{I}_K \end{bmatrix}}_{\mathbf{G}_{\mathcal{H}}} \in \mathbb{R}^{4N \times 4K} \quad (30)$$

by incorporating the generator matrix of the  $\mathbf{D}_4$  lattice.<sup>6</sup> In the same way, an equivalent complex-valued representation (over  $\mathcal{G}$ ) is realized by using the generator matrix

$$\mathbf{G}_{c,\mathcal{H}} = \underbrace{\mathbf{G}_c}_{(7)} \begin{bmatrix} \mathbf{I}_K & \left(\frac{1}{2} + \frac{1}{2}i\right)\mathbf{I}_K \\ \mathbf{0}_K & \left(\frac{1}{2} + \frac{1}{2}i\right)\mathbf{I}_K \end{bmatrix} \in \mathbb{C}^{2N \times 2K}. \quad (31)$$

<sup>5</sup> $\mathbf{I}_K$  denotes the  $K \times K$  identity matrix and  $\mathbf{0}_K$  the  $K \times K$  all-zero matrix (all elements are 0).

<sup>6</sup>In particular, the generator matrix of the lattice *dual* to  $\mathbf{D}_4$  is employed that actually corresponds to a version of the original  $\mathbf{D}_4$  lattice which is scaled by a factor of  $\frac{1}{2}$  [25]. Using that strategy, the resulting points directly correspond to the set of Hurwitz integers (with half-integer values).

### III. ALGORITHMS FOR GENERALIZED LATTICE PROBLEMS

In this section, algorithms that are suited to (approximately) solve particular lattice problems are reviewed and generalized.

#### A. Lattice Basis Reduction and the LLL Algorithm

The task of lattice basis reduction is to find a *more suited basis*  $\mathbf{G}_{\text{red}} = [\mathbf{g}_{\text{red},1}, \dots, \mathbf{g}_{\text{red},K}]$  for the representation of the lattice spanned by the (unreduced) generator matrix  $\mathbf{G}$ . For generalized lattices, a unimodular integer matrix  $\mathbf{T} = [\mathbf{t}_1, \dots, \mathbf{t}_K] \in \mathbb{I}^{K \times K}$  according to (26) has to be found in such a way that particular quality criteria are fulfilled.

To assess when a lattice basis is reduced, several different criteria can be defined. One is the minimization of the orthogonality defect (27), i.e., the optimality criterion reads

$$\mathbf{T} = \underset{\substack{\mathbf{T} \in \mathbb{I}^{K \times K} \\ \det(\mathbf{T}^H \mathbf{T})=1}}{\operatorname{argmin}} \Omega(\mathbf{G}\mathbf{T}) = \underset{\substack{\mathbf{T} \in \mathbb{I}^{K \times K} \\ \det(\mathbf{T}^H \mathbf{T})=1}}{\operatorname{argmin}} \frac{\prod_{k=1}^K \|\mathbf{g}_{\text{red},k}\|}{\operatorname{vol}(\Lambda(\mathbf{G}))}. \quad (32)$$

Hence, the norms of all basis vectors are incorporated. An alternative approach is to consider the lengths of these vectors individually, e.g.,  $\|\mathbf{g}_{\text{red},1}\|$ . The minimization of the *maximum squared norm* among the basis vectors is particularly known under the name *shortest basis problem* (SBP) and described by

$$\mathbf{T} = \underset{\substack{\mathbf{T} \in \mathbb{I}^{K \times K} \\ \det(\mathbf{T}^H \mathbf{T})=1}}{\operatorname{argmin}} \max_{k=1, \dots, K} \|\mathbf{G}\mathbf{t}_k\|^2. \quad (33)$$

The LLL algorithm [6] is suboptimal w.r.t. the above lattice-basis-reduction criteria, i.e., it only approximates these optimization problems. Nevertheless, a polynomial asymptotic complexity is ensured (over  $K$ ), whereas for the exact solutions to (32) and (33) an exponential complexity is required, cf., e.g., [13], [57]. Moreover, it is possible to derive certain performance guarantees (i.e., bounds) for LLL reduction. More details will be provided in Sec. IV. In the following, the concept of LLL reduction will be generalized.

1) *Gram-Schmidt Orthogonalization*: The LLL reduction and its related criteria operate on the Gram-Schmidt orthogonalization (GSO) [58] of the generator matrix<sup>7</sup>

$$\mathbf{Q}\mathbf{R} = \mathbf{G}\mathbf{P}. \quad (34)$$

In particular,  $\mathbf{Q} = [\mathbf{q}_1, \dots, \mathbf{q}_K]$  forms an  $N \times K$  matrix with *orthogonal columns*, and  $\mathbf{R} = [r_{l,k}]$ ,  $l = 1, \dots, K$ ,  $k = 1, \dots, K$ , an upper triangular  $K \times K$  matrix with unit main diagonal ( $r_{k,k} = 1$ ,  $k = 1, \dots, K$ ). The  $K \times K$  matrix  $\mathbf{P}$  (*permutation matrix* with a single 1 per column and row and all other elements equal to 0) can be used to sort the Gram-Schmidt vectors in  $\mathbf{Q}$  according to their length during the orthogonalization process (known as *pivoting*).

The GSO procedure<sup>8</sup> is presented in Algorithm 1. In every step  $k = 1, \dots, K$ , the pivoting is performed first, i.e., the

<sup>7</sup>The matrices  $\mathbf{Q}$  and  $\mathbf{R}$  often describe the *QR decomposition* of a matrix, in which  $\mathbf{Q}$  is usually assumed to be a unitary matrix ( $\mathbf{Q}^H \mathbf{Q} = \mathbf{I}$ ). Given the GSO (without normalization), the column norms of  $\mathbf{Q}$  are then absorbed in  $\mathbf{R}$  (non-unit main diagonal). In this work, we assume that the matrix  $\mathbf{Q}$  does not have to be unitary but that  $\mathbf{R}$  is a matrix with unit main diagonal.

<sup>8</sup>To simplify the notation, we denote the selection of the elements with index  $k, \dots, l$  of a vector  $\mathbf{g}$  by  $\mathbf{g}_{k:l}$ . Given a matrix  $\mathbf{G}$ , the selection of a submatrix composed of the rows  $k, \dots, l$  and the columns  $m, \dots, n$  is denoted as  $\mathbf{G}_{k:l, m:n}$ .

shortest of the remaining columns  $\mathbf{q}_k, \dots, \mathbf{q}_K$  is inserted at position  $k$  (and removed at its original position). Afterwards, the remaining columns are projected onto the orthogonal complement of  $\mathbf{q}_k$ . In contrast to other implementations, e.g., [40], [58], all multiplications are defined in such a way that a non-commutative behavior, e.g., for the case of quaternion numbers, is taken into account. Hence, the procedure can be used for real-, complex-, or quaternion-valued numbers.

2) *Generalized LLL Reduction Criteria*: In the initial publication on real-valued LLL (RLLL) reduction, the matrices  $\mathbf{R}$  and  $\mathbf{Q}$  have been evaluated w.r.t. two conditions: i) the property  $|r_{l,k}| \leq \frac{1}{2}$ ,  $1 \leq l < k \leq K$ , has to be fulfilled for the upper triangular part of  $\mathbf{R}$ , known as *size-reduction* condition, and ii) postulating a size-reduced matrix  $\mathbf{R}$ , the Lovász condition  $\|\mathbf{q}_k\|^2 \geq (\delta - |r_{k-1,k}|^2) \cdot \|\mathbf{q}_{k-1}\|^2$  has to hold for the norms of the columns of  $\mathbf{Q}$ . The parameter  $\delta$  is used as a quality parameter and enables a trade-off between reduction quality and the runtime of the algorithm.

Taking a closer look at the size-reduction condition, it becomes apparent that the LLL algorithm [6] can be interpreted to form some kind of Euclidean algorithm for matrices, see also [39]. In particular, this condition is forced by a modulo reduction according to (12), i.e., by a (Euclidean) division as defined in (10) with the divisor  $v = 1$ , where the resulting remainder  $r_{l,k} = \rho$  is a *small remainder* since  $|r_{l,k}| \leq \frac{1}{2} < |v| = 1$ . The size-reduction condition is alternatively expressed by  $\mathbb{Q}_{\mathbb{Z}}\{r_{l,k}\} = 0$ , i.e., all non-zero, non-diagonal values in  $\mathbf{R}$  have to be located within the Voronoi cell of  $\mathbb{Z}$  w.r.t. the origin.

Taking advantage of the interpretation that the size-reduction operation forms a modulo reduction over the particular Euclidean ring and the fact that the Lovász condition is generally valid for Euclidean rings as it compares norms of vectors, *generalized LLL reduction criteria* can be defined.

**Definition 1** (Generalized LLL Reduction). *A generator matrix  $\mathbf{G} = \mathbf{Q}\mathbf{R}$  that spans a lattice over the Euclidean integer ring  $\mathbb{I}$  is LLL-reduced over  $\mathbb{I}$ , if*

i)  $\mathbf{R}$  is size-reduced according to

$$\mathbb{Q}_{\mathbb{I}}\{r_{l,k}\} = 0, \quad 1 \leq l < k \leq K, \quad (35)$$

ii) the respective Lovász condition

$$\|\mathbf{q}_k\|^2 \geq (\delta - |r_{k-1,k}|^2) \cdot \|\mathbf{q}_{k-1}\|^2 \quad (36)$$

is fulfilled. The quality parameter can be chosen according to

$$\delta \in (\epsilon_{\mathbb{I}}^2, 1], \quad (37)$$

where  $\epsilon_{\mathbb{I}}^2$  denotes the maximum squared quantization error for elements quantized to the Euclidean integer ring  $\mathbb{I}$ .

*Proof.* Since, after size reduction,  $\mathbb{Q}_{\mathbb{I}}\{r_{l,k}\} = 0$  is valid,  $r_{l,k}$  forms the remainder  $\rho$  of the division with the divisor  $v = 1$  as defined in (10). If  $\mathbb{I}$  is a Euclidean ring,  $|r_{l,k}| \leq \epsilon_{\mathbb{I}} < |v| = 1$ , i.e., a *small remainder* is present. Hence, the Lovász condition becomes operative if  $0 < (\delta - \epsilon_{\mathbb{I}}^2) \leq 1$ , i.e., if  $\delta \in (\epsilon_{\mathbb{I}}^2, 1]$ .  $\square$

**Remark.** For the integer lattice  $\mathbb{Z}$ , we have  $\delta \in (\frac{1}{4}, 1]$  since  $\epsilon_{\mathbb{Z}}^2 = \frac{1}{4}$ . This result is identical to the range initially derived in [6], [59]. Given  $\mathbb{I} = \mathcal{G}$ ,  $\delta \in (\frac{1}{2}, 1]$  is valid as  $\epsilon_{\mathcal{G}}^2 = \frac{1}{2}$ ,



**Algorithm 1** Gram–Schmidt Orthogonalization with Pivoting.

---

```

[ $\mathbf{Q}, \mathbf{R}, \mathbf{P}$ ] = GSO( $\mathbf{G}$ )
1:  $\mathbf{Q} = \mathbf{G}, \mathbf{R} = \mathbf{I}_K, \mathbf{P} = \mathbf{I}_K$ 
2: for  $k = 1, \dots, K$  do
3:    $k_m = \operatorname{argmin}_{l=k, \dots, K} \|\mathbf{q}_l\|$ 
4:   if  $k_m \neq k$  then ▷ pivoting
5:      $\mathbf{Q} = [\mathbf{q}_{1:k-1}, \mathbf{q}_{k_m}, \mathbf{q}_{k:k_m-1}, \mathbf{q}_{k_m+1:K}]$ 
6:      $\mathbf{P} = [\mathbf{p}_{1:k-1}, \mathbf{p}_{k_m}, \mathbf{p}_{k:k_m-1}, \mathbf{p}_{k_m+1:K}]$ 
7:     In the upper  $k-1$  rows of  $\mathbf{R}$  (index  $1 : k-1$ ):
8:        $\mathbf{R} = [\mathbf{r}_{1:k-1}, \mathbf{r}_{k_m}, \mathbf{r}_{k:k_m-1}, \mathbf{r}_{k_m+1:K}]$ 
9:   end if
10:  for  $l = k+1, \dots, K$  do ▷ orthogonalization
11:     $r_{k,l} = \mathbf{q}_k^H \mathbf{q}_l \cdot \|\mathbf{q}_k\|^{-2}$ 
12:     $\mathbf{q}_l = \mathbf{q}_l - \mathbf{q}_k r_{k,l}$ 
13:  end for

```

---

cf. [40]. For lattices over  $\mathcal{E}$ ,  $\delta \in (\frac{1}{3}, 1]$  is obtained due to  $\epsilon_{\mathcal{E}}^2 = \frac{1}{3}$ . Considering lattices over the Hurwitz integers  $\mathcal{H}$ ,  $\delta \in (\frac{1}{2}, 1]$  as  $\epsilon_{\mathcal{H}}^2 = \frac{1}{2}$ . Since the Lipschitz integers do not form a Euclidean ring, an LLL reduction over  $\mathcal{L}$  can—in general—not be defined. This can be seen if the maximum squared quantization error  $\epsilon_{\mathcal{L}}^2$  is inserted into the Lovász condition: even when  $\delta = 1$ ,  $\delta - |r_{k-1,k}|^2 = 0$  if  $|r_{k-1,k}| = 1$ , i.e., the reduction may become inoperative.

A generalization of the size-reduction operation from [6], [40] is provided in Algorithm 2—given the (reduced) basis  $\mathbf{G}_{\text{red}}$ , its related matrix  $\mathbf{R}$ , the transformation matrix  $\mathbf{T}$ , the indices  $l$  and  $k$ , and the integer ring  $\mathbb{I}$  as input variables. For lattices over  $\mathbb{Z}$  and  $\mathcal{G}$ , the operations are equivalent to the ones defined in the RLLL algorithm [6] and the complex LLL (CLLL) algorithm [40], respectively. However, the generalized definition also enables an LLL reduction over the Eisenstein integers (ELLL algorithm), over the Hurwitz integers (QLLL algorithm, “Q” for quaternions), and over other Euclidean rings.

Given complex and quaternion-valued matrices, the reduction can alternatively be performed w.r.t. their equivalent real- and real-/complex-valued matrix representations, as defined in (3), (8), and (7). Then, the reduction has to be done with real-valued and/or complex-valued algorithms. However, during the GSO, the particular structure of these matrices (and the isomorphism) is destroyed, i.e., the resulting reduced basis and the related integer matrix cannot be reconverted into equivalent complex/quaternion-valued representations, see also [2]. Consequently, the quality of the reduction will not necessarily be the same. More details will be given in Sec. IV.

3) *Generalized LLL Reduction Algorithm:* In Algorithm 3, a generalized variant of the LLL algorithm is provided. In contrast to other implementations, e.g., in [40], all multiplications are performed in the right order to account for non-commutative behavior. In particular, in the first line, a GSO with pivoting is calculated. The pivoting is not necessarily required, but it is well-known that sorted Gram–Schmidt vectors may speed up the following reduction process [60]. In the loop, the size reduction for the element  $r_{k-1,k}$  (over the particular ring  $\mathbb{I}$ ) is done first. Then, the respective Lovász condition can be checked. If it is not fulfilled, the columns  $k-1$  and  $k$  are swapped in  $\mathbf{G}_{\text{red}}$  and the (unimodular) transformation

**Algorithm 2** Generalized Size Reduction.

---

```

[ $\mathbf{G}_{\text{red}}, \mathbf{R}, \mathbf{T}$ ] = SIZERED( $\mathbf{G}_{\text{red}}, \mathbf{R}, \mathbf{T}, l, k, \mathbb{I}$ )
1:  $r_q = \mathbb{Q}_{\mathbb{I}}\{r_{l,k}\}$ 
2: if  $r_q \neq 0$  then
3:    $\mathbf{g}_{\text{red},k} = \mathbf{g}_{\text{red},k} - \mathbf{g}_{\text{red},l} r_q$ 
4:    $\mathbf{t}_k = \mathbf{t}_k - \mathbf{t}_l r_q$ 
5:   In the upper  $l$  rows of  $\mathbf{R}$  (index  $1 : l$ ):
6:      $\mathbf{r}_k = \mathbf{r}_k - \mathbf{r}_l r_q$ 
7: end if

```

---

**Algorithm 3** Generalized LLL Reduction.

---

```

[ $\mathbf{G}_{\text{red}}, \mathbf{Q}, \mathbf{R}, \mathbf{T}$ ] = LLL( $\mathbf{G}, \delta, \mathbb{I}$ )
1: [ $\mathbf{Q}, \mathbf{R}, \mathbf{T}$ ] = GSO( $\mathbf{G}$ ) ▷ initial GSO with pivoting
2:  $\mathbf{G}_{\text{red}} = \mathbf{G}\mathbf{T}, k = 2$ 
3: while  $k \leq K$  do
4:   [ $\mathbf{G}_{\text{red}}, \mathbf{R}, \mathbf{T}$ ] = SIZERED( $\mathbf{G}_{\text{red}}, \mathbf{R}, \mathbf{T}, k-1, k, \mathbb{I}$ )
5:   if  $\|\mathbf{q}_k\|^2 < (\delta - |r_{k-1,k}|^2) \cdot \|\mathbf{q}_{k-1}\|^2$  then ▷ swap
6:      $\mathbf{G}_{\text{red}} = [\mathbf{g}_{\text{red},1:k-2}, \mathbf{g}_{\text{red},k}, \mathbf{g}_{\text{red},k-1}, \mathbf{g}_{\text{red},k+1:K}]$ 
7:      $\mathbf{T} = [\mathbf{t}_{1:k-2}, \mathbf{t}_k, \mathbf{t}_{k-1}, \mathbf{t}_{k+1:K}]$ 
8:     [ $\mathbf{Q}, \mathbf{R}$ ] = UPDATEQR( $\mathbf{Q}, \mathbf{R}, k$ )
9:      $k = \max(2, k-1)$ 
10:  else ▷ Lovász condition fulfilled
11:    for  $l = k-2, k-3, \dots, 1$  do
12:      [ $\mathbf{G}_{\text{red}}, \mathbf{R}, \mathbf{T}$ ] = SIZERED( $\mathbf{G}_{\text{red}}, \mathbf{R}, \mathbf{T}, l, k, \mathbb{I}$ )
13:    end for
14:     $k = k+1$ 
15:  end if
16: end while

```

---

**Algorithm 4** GSO update if columns  $k$  and  $k-1$  are swapped.

---

```

[ $\mathbf{Q}, \mathbf{R}$ ] = UPDATEQR( $\mathbf{Q}, \mathbf{R}, k$ )
1:  $\tilde{\mathbf{q}}_{k-1} = \mathbf{q}_{k-1}, \tilde{\mathbf{q}}_k = \mathbf{q}_k, \tilde{\mathbf{R}} = \mathbf{R}$  ▷ temporal variables
2:  $\mathbf{q}_{k-1} = \mathbf{q}_k + \mathbf{q}_{k-1} r_{k-1,k}$ 
3:  $\mathbf{r}_{k-1,k} = r_{k-1,k}^* \cdot \|\tilde{\mathbf{q}}_{k-1}\|^2 \cdot \|\mathbf{q}_{k-1}\|^{-2}$ 
4:  $\mathbf{q}_k = \tilde{\mathbf{q}}_{k-1} - \mathbf{q}_{k-1} r_{k-1,k}$ 
5: for  $l = k+1, \dots, K$  do
6:    $r_{k-1,l} = r_{k-1,k} r_{k-1,l} + r_{k,l} \cdot \|\tilde{\mathbf{q}}_k\|^2 \cdot \|\mathbf{q}_{k-1}\|^{-2}$ 
7:    $r_{k,l} = \tilde{r}_{k-1,l} - \tilde{r}_{k-1,k} r_{k,l}$ 
8: end for
9: for  $l = 1, \dots, k-2$  do
10:   $r_{l,k-1} = r_{l,k}$ 
11:   $r_{l,k} = \tilde{r}_{l,k-1}$ 
12: end for

```

---

matrix  $\mathbf{T}$ . As a consequence, the matrices  $\mathbf{Q}$  and  $\mathbf{R}$  have to be updated. This can either be done by a complete recalculation of the GSO, or by the procedure in Algorithm 4 that restricts the recalculation to all elements which have to be updated. It is an adapted variant of the procedure in [40], additionally taking the right order of all multiplications into account. If the check of the Lovász condition is successful, the elements  $r_{l,k}$ ,  $l = k-2, k-3, \dots, 1$ , are finally reduced and the algorithm continues with the next reduction step until  $k = K$ .

4) *Pseudo-QLLL Reduction:* Even though an LLL reduction over the Lipschitz integers can—due to the non-existent Euclidean property—not be defined in general, a *pseudo-QLLL reduction* can be defined instead. In particular, the reduction only becomes inoperative if  $|r_{k-1,k}| = 1$ . Hence, choosing  $\delta = 1$ , the LLL algorithm can be applied if the probability that  $|r_{k-1,k}| = 1$  tends to zero.

Such a case is, e.g., present if the elements of the generator matrix are drawn i.i.d.ly from a continuous distribution (e.g.,



an i.i.d. Gaussian one). Then, if the quantization in the size-reduction steps is performed w.r.t.  $\mathbb{I} = \mathcal{L}$  and if additionally the parameter  $\delta = 1$  is chosen, a pseudo-QLLL-reduced basis is obtained. Obviously, no general performance guarantees or bounds can be derived in that case—however, it is at least ensured that the Lovász condition is still operative and that, thus, some kind of “optimized” basis is produced.

### B. Shortest Independent Vectors in Lattices

Another important lattice problem is the determination of the shortest linearly independent vectors in lattices. They are related to the so-called *successive minima*. In particular, the  $k^{\text{th}}$  successive minimum of a lattice with  $N \times K$  generator matrix  $\mathbf{G}$ ,  $k = 1, \dots, K$ , is defined as [5], [61]

$$\mu_k = \inf\{\mu \mid \dim\{\text{span}\{\Lambda(\mathbf{G}) \cap \mathbb{B}_N(\mu)\}\} = k\}, \quad (38)$$

where  $\mathbb{B}_N(\mu)$  denotes the  $N$ -dimensional ball with hyperradius  $\mu$  centered at the origin. In words,  $\mu_k$  denotes the smallest radius in which  $k$  linearly independent vectors can be found within the hyperball. The related lattice points with

$$\mu_k = \|\lambda_{m,k}\|, \quad k = 1, \dots, K, \quad (39)$$

form the  $K$  linearly independent vectors with the shortest (Euclidean) norms.

Closely related to the *successive-minima problem* (SMP)—the determination of the  $K$  shortest independent vectors in a lattice—is the *shortest independent vector problem* (SIVP). Here, only the maximum of the (squared) norms has to be short as possible, cf. the SBP in (33). Hence, the (generalized) SIVP is a weakened variant of the SMP and defined as

$$\mathbf{T} = \underset{\substack{\mathbf{T} \in \mathbb{I}^{K \times K} \\ \text{rank}(\mathbf{T})=K}}{\text{argmin}} \max_{k=1, \dots, K} \|\mathbf{G}\mathbf{t}_k\|^2. \quad (40)$$

Obviously, every optimal solution for the successive-minima problem is also optimal w.r.t. the SIVP [43], [62].

As becomes apparent from (40), the  $K$  independent lattice vectors do not necessarily form a basis of the lattice spanned by  $\mathbf{G}$ . In particular, if the  $K$  integer vectors  $\mathbf{t}_k$  are combined into the integer transformation matrix  $\mathbf{T} = [\mathbf{t}_1, \dots, \mathbf{t}_K]$ , the transformed generator matrix  $\mathbf{G}_{\text{tra}} = \mathbf{G}\mathbf{T}$  may only define a *sublattice* of the original one: the integer vectors  $\mathbf{t}_k$  are only required to be linearly independent, but they do not have to form a unimodular transformation matrix in combination. Hence,  $\mathbf{T}$  may only have full rank, resulting in a “thinned” lattice when multiplied by  $\mathbf{G}$ , depending on the particular determinant  $\det(\mathbf{T})$ . Further details can, e.g., be found in [2], [19]. Consequently, the successive minima can be used as lower bounds for the norms of the basis vectors of any (alternative) basis for a lattice spanned by a particular generator matrix  $\mathbf{G}$ .

1) *Generalized Successive Minima*: Even though the successive minima have initially been considered for real-valued lattices over  $\mathbb{Z}$ , e.g., in [5], [61], it is quite obvious that they can also be determined if other integer rings  $\mathbb{I}$  are present. The only condition is that the shortest  $K$  linearly independent lattice vectors are found—no additional constraints as, e.g., a Euclidean property of the particular ring are imposed.

In contrast to LLL reduction, the isomorphism of a complex or quaternionic matrix  $\mathbf{G}$  and its equivalent real-valued representation  $\mathbf{G}_r$  according to (3) and (8), respectively, holds for the successive minima as shown in the following Theorem.

**Theorem 1** (Successive Minima of Complex and Quaternionic Lattices). *Given an  $N \times K$  generator matrix  $\mathbf{G}$  for which the successive minima over  $\mathbb{I}$  are given as*

$$\boldsymbol{\mu}_{\mathbb{I}} = [\mu_1, \mu_2, \dots, \mu_K] \in \mathbb{R}^K, \quad (41)$$

*the successive minima of the equivalent  $D_r N \times D_r K$  real-valued generator matrix  $\mathbf{G}_{r,\mathbb{I}} = \mathbf{G}_r \mathbf{G}_{\mathbb{I}}$ , where  $\mathbf{G}_r$  denotes the  $D_r N \times D_r K$  real-valued representation of  $\mathbf{G}$ ,  $\mathbf{G}_{\mathbb{I}}$  the  $D_r K \times D_r K$  real-valued generator matrix of the integer ring  $\mathbb{I}$ , and  $D_r$  the number of (real-valued) components per scalar, cf. (3) and (8), are obtained as*

$$\boldsymbol{\mu}_{r,\mathbb{I}} = \left[ \underbrace{\mu_1, \dots, \mu_1}_{D_r \text{ times}}, \underbrace{\mu_2, \dots, \mu_2}_{D_r \text{ times}}, \dots, \underbrace{\mu_K, \dots, \mu_K}_{D_r \text{ times}} \right] \in \mathbb{R}^{D_r K}, \quad (42)$$

*i.e., each successive minimum from (41) occurs  $D_r$  times. This property is valid for complex lattices ( $D_r = 2$ ) over both Gaussian and Eisenstein integers, as well as for quaternionic lattices ( $D_r = 4$ ) over both Lipschitz and Hurwitz integers.*

*Proof.* We start with the complex case ( $D_r = 2$ ). Given  $\mathbf{G}_r$  according to (3), pairs of orthogonal (and, thus, linearly independent) column vectors occur at the indices  $k$  and  $k + K$ , which additionally possess the norms  $\|\mathbf{g}_{r,k}\| = \|\mathbf{g}_{r,k+K}\| = \|\mathbf{g}_k\|$ ,  $k = 1, \dots, K$ . The same is obviously valid for the matrix  $\mathbf{G}_{r,\mathcal{G}} = \mathbf{G}_r \mathbf{I}_{2K}$ , but also for the matrix  $\mathbf{G}_{r,\mathcal{E}} = \mathbf{G}_r \mathbf{G}_{\mathcal{E}}$ : Since  $\mathbf{G}_{\mathcal{E}}$  from (29) is a non-singular matrix,  $\text{rank}(\mathbf{G}_{r,\mathcal{E}}) = \text{rank}(\mathbf{G}_r)$ , i.e., the columns of  $\mathbf{G}_{r,\mathcal{E}}$  are still independent. Concerning its column norms, the left half (index  $1, \dots, K$ ) does not change in comparison to  $\mathbf{G}_r$  due to the identity part in  $\mathbf{G}_{\mathcal{E}}$ . Regarding the right half of the columns ( $K + 1, \dots, 2K$ ), we obtain the squared norms  $\|\mathbf{g}_{r,\mathcal{E},k}\|^2 = \frac{1}{4}\|\mathbf{g}_k^{(1)}\|^2 + \frac{3}{4}\|\mathbf{g}_k^{(2)}\|^2 + \frac{1}{4}\|\mathbf{g}_k^{(2)}\|^2 + \frac{3}{4}\|\mathbf{g}_k^{(1)}\|^2 = \|\mathbf{g}_k^{(1)} + \mathbf{g}_k^{(2)}\|^2 = \|\mathbf{g}_k\|^2$ , i.e., these norms do not change either.<sup>9</sup> Hence, each lattice vector in  $\Lambda(\mathbf{G}_{r,\mathbb{I}})$  has a linearly independent counterpart with the same length; both of them isomorphically represent one lattice vector of  $\Lambda(\mathbf{G})$  (with the same norm). As a consequence, for  $\mathbf{G}_{r,\mathbb{I}}$ , pairs of linearly independent lattice vectors  $\lambda_{m,k}$  and  $\lambda_{m,k+1}$  are obtained that yield successive minima with the same value, i.e.,  $\mu_k = \mu_{k+1}$ ,  $k = 1, 3, \dots, 2K - 1$ .

For quaternion-valued matrices ( $D_r = 4$ ), the proof is similar: In  $\mathbf{G}_r$  according to (8), orthogonal vectors with  $\|\mathbf{g}_{r,k}\| = \|\mathbf{g}_{r,k+K}\| = \|\mathbf{g}_{r,k+2K}\| = \|\mathbf{g}_{r,k+3K}\| = \|\mathbf{g}_k\|$  are present. Given the ring of Lipschitz integers, the same holds for the matrix  $\mathbf{G}_{r,\mathcal{L}} = \mathbf{G}_r \mathbf{I}_{4K}$ . Considering lattices over Hurwitz integers, we have  $\mathbf{G}_{r,\mathcal{H}} = \mathbf{G}_r \mathbf{G}_{\mathcal{H}}$ , where  $\text{rank}(\mathbf{G}_{r,\mathcal{H}}) = \text{rank}(\mathbf{G}_r)$ . The non-singular matrix  $\mathbf{G}_{\mathcal{H}}$  defined in (30) consists of an identity part for the column indices  $1, \dots, 3K$ . For the rightmost part ( $3K + 1, \dots, 4K$ ),

<sup>9</sup>Interpretation: The right part in (29) represents the *Eisenstein unit*  $\omega = e^{\frac{2\pi}{3}i} = -\frac{1}{2} + \frac{\sqrt{3}}{2}i$  with  $|\omega| = 1$ , i.e., only a rotation in the complex plane is performed. The left (identity) part corresponds to the  $0^{\text{th}}$  root of unity  $e^0 = 1$ .

we obtain the squared norms  $\|\mathbf{g}_{r,\mathcal{H},k}\|^2 = 4 \cdot \frac{1}{4} \cdot \|\mathbf{g}_k^{(1)} + \mathbf{g}_k^{(2)} + \mathbf{g}_k^{(3)} + \mathbf{g}_k^{(4)}\|^2 = \|\mathbf{g}_k\|^2$ , i.e., they remain the same.<sup>10</sup> Hence,  $\mu_k = \mu_{k+1} = \mu_{k+2} = \mu_{k+3}$ ,  $k = 1, 5, \dots, 4K - 3$ , is obtained.  $\square$

**Remark.** *Given lattices over the Gaussian integers, this isomorphism has been recognized earlier, e.g., in [43]. To the best of our knowledge, all other integer rings have not been considered before.*

*In the quaternion-valued case, an isomorphism based on the equivalent complex-valued representation (7) can be derived in an analogous way. Then, the successive minima are repeated two times in the complex description.*

Due to Theorem 1, the successive minima and the related lattice points and integer vectors can isomorphically be determined by solving the problem for the equivalent real-valued representation. Hence, a permutation of the real or complex integer vectors can be found such that an integer transformation matrix  $T_r$  is formed that possesses the particular structure defined in (3) or (8). Then, this matrix can be reconverted to a complex or quaternion-valued representation, see also [2, Example 4.3]. Both the “direct” determination of the successive minima over  $\mathbb{C}$  or  $\mathbb{H}$ , and their “indirect” determination over  $\mathbb{R}$ , finally lead to the same result. Please note that, given lattices over Eisenstein or Hurwitz integers, a reversion is required at the end to compensate for the matrices  $\mathbf{G}_{\mathcal{E}}$  and  $\mathbf{G}_{\mathcal{H}}$  in (29) and (30), respectively. This reversion process will be described below (and, additionally, in Appendix A).

### C. Generalized Determination of the Successive Minima

For the determination of the successive minima, a special  $K$ -dimensional variant of the shortest-vector problem has to be solved. It is well-known that already the classical shortest-vector problem is NP-hard, i.e., that the computational complexity grows exponentially with the dimension  $K$ . Nevertheless, at least for small dimensions, algorithms have been proposed which can efficiently solve the shortest-vector problem. The most prominent one is the so-called *sphere decoder* [13].

To solve the SMP, several algorithms have been proposed within the last few years [43]–[45]. One possible strategy applied in [43] is to solve the shortest-vector problem  $K$  times. Another strategy employed in [44], [45] is to solve an adapted variant thereof once in the beginning, afterwards only operating on the initial result.

In this work, we address the list-based approach initially proposed in [44] which has been shown to perform well w.r.t. runtime behavior if moderate dimensions are present ( $K < 20$  in the real-valued case), see also the comparison in [45]. In particular, in that approach, the sphere decoder [13] is initially applied to generate a list that contains all lattice points within a hyperball of a predefined search radius. Then, among those candidates, the shortest linearly independent ones are selected.

<sup>10</sup>Interpretation: The rightmost part in (30) represents the *Hurwitz unit*  $\frac{1}{2}(1 + i + j + k)$  with  $|\frac{1}{2}(1 + i + j + k)| = 1$ , i.e., only a rotation in quaternionic space is performed. The left (identity) part corresponds to the units 1,  $i$ , and  $j$ .

### Algorithm 5 List-Based Determination of Successive Minima.

---

```

 $[\mathbf{G}_{\text{tra}}, \mathbf{T}] = \text{SMP}(\mathbf{G}, \mathbb{I})$ 
1:  $\mathbf{G}_{r,\mathbb{I}} = \text{RINGTOZ}(\mathbf{G}, \mathbb{I})$  ▷ real-valued representation
2:  $[\mathbf{G}_{\text{red}}, \mathbf{T}_{\text{LLL}}] = \text{LLL}(\mathbf{G}_{r,\mathbb{I}}, 1, \mathbb{Z})$  ▷ reduced basis
3:  $\mathbf{C}_t = \text{LISTSPHEREDECODER}(\mathbf{G}_{\text{red}}, \max_k \|\mathbf{g}_{\text{red},k}\|^2)$ 
4:  $\mathbf{C} = \mathbf{T}_{\text{LLL}} \mathbf{C}_t$  ▷ convert to original basis
5:  $\mathbf{C}_u = \text{ZTORING}(\mathbf{C}, \mathbb{I})$  ▷ go back to ring  $\mathbb{I}$ 
6:  $\mathbf{C}_s = \text{SORT}(\mathbf{C}_u, \mathbf{G}\mathbf{C}_u)$  ▷ sort w.r.t. norm
7:  $\mathbf{i} = \text{ROWECHELON}(\mathbf{C}_s)$  ▷ indices of row-echelon form
8:  $\mathbf{T} = [\mathbf{c}_{i_1}, \dots, \mathbf{c}_{i_K}]$  ▷ shortest independent vectors
9:  $\mathbf{G}_{\text{tra}} = \mathbf{G}\mathbf{T}$  ▷ transformed generator matrix

```

---

The generalized concept is provided in Algorithm 5. As mentioned above, a list-based variant of the sphere decoder is initially applied. As the sphere decoder [13] in combination with Schnorr–Euchner enumeration [8] only operates over real numbers, the generator matrix  $\mathbf{G}$  has to be converted to its equivalent real-valued representation (given the integer ring  $\mathbb{I}$ ). This is done with the procedure RINGTOZ which is listed in Algorithm 6 in Appendix A. For the list sphere decoder, an initial search radius has to be provided. The naive approach would be to use the maximum (squared) column norm of  $\mathbf{G}_{r,\mathbb{I}}$  as the (squared) radius, since the (squared) solution to the SMP can never be worse than that value. However, the search radius (and the related complexity) can significantly be decreased by applying a reduced basis via the LLL algorithm (Line 2) instead, using the quality parameter  $\delta = 1$ . Since this call has a low complexity [59], it is negligible in comparison to the call of the list sphere decoder, which is subsequently applied [13, Algorithm ALLCLOSESTPOINTS]. It results in a matrix of integer candidate vectors  $\mathbf{C}_t \in \mathbb{Z}^{D_r K \times N_c}$ , where  $N_c$  denotes the list size. A list of respective candidate vectors w.r.t. the unreduced basis  $\mathbf{G}_{r,\mathbb{I}}$  is subsequently calculated by the multiplication with  $\mathbf{T}_{\text{LLL}}$  (Line 4). The integer candidate vectors over the original ring  $\mathbb{I}$  are finally obtained by the procedure ZTORING which is listed in Algorithm 7 in Appendix A. In particular, in that procedure, the original complex- or quaternion-valued representations are reconstructed from the real-valued ones. In Line 6 of Algorithm 5, the candidate vectors are then sorted in ascending order w.r.t. their norms. This can be done by a standard sorting algorithm [58]. In the procedure ROWECHELON, which is listed in Appendix A (Algorithm 8), the matrix of sorted candidate vectors is transformed to row-echelon form. At the particular indices  $\mathbf{i} = [i_1, \dots, i_K]$  where a new dimension is established (“steps” in the row-echelon form), the vector resulting in the  $k^{\text{th}}$  successive minimum is found as it leads to the shortest vector that is independent from the previous  $k - 1$  ones. The related transformation matrix  $\mathbf{T}$  is formed in Line 8, and the respective transformed generator matrix  $\mathbf{G}_{\text{tra}}$  finally in Line 9.

The reversion to the original ring  $\mathbb{I}$  (as performed in Line 5 in Algorithm 5) can alternatively be performed *after* the calculation of the matrices  $\mathbf{T}$  and  $\mathbf{G}_{\text{tra}}$  (defined over  $\mathbb{Z}$  and  $\mathbb{R}$ ) takes place. However, then, for complex- and quaternion-valued lattices, the calculation of the row-echelon form has to be performed over real numbers with the equivalent  $2K \times 2N_c$  and  $4K \times 4N_c$  representation  $\mathbf{C}$ , respectively.

#### IV. GENERALIZED QUALITY BOUNDS AND ASYMPTOTIC COMPUTATIONAL COMPLEXITY

Based on the generalized criteria and algorithms discussed previously, quality bounds are derived and compared to each other in this section. In addition, the asymptotic complexity of both above-mentioned (generalized) algorithms is evaluated.

##### A. Bounds on the Norms

The norms of the basis vectors are suited quantities to assess the quality of a lattice basis. Since the respective successive minima are given as the norms of the shortest independent vectors in the particular lattice, they serve as lower bounds on the norms resulting from any lattice-basis-reduction scheme.

To solve the SIVP (40) and the SBP (33), respectively, it is required that the *maximum* of the  $K$  norms has to be as small as possible. However, as stated in [46, p. 35], it is generally not possible to derive bounds for the  $K^{\text{th}}$  successive minimum and any other of them except from the first. In particular,  $\mu_2, \dots, \mu_K$  can become arbitrarily large in comparison to the lattice volume. It is quite obvious that the same holds for the norms of the basis vectors  $\mathbf{g}_2, \dots, \mathbf{g}_K$ . Nevertheless, for the first successive minimum  $\mu_1$  and the related basis vector  $\mathbf{g}_1$ , bounds can in general be given.

1) *First Successive Minimum*: Given a real-valued lattice ( $\mathbb{I} = \mathbb{Z}$ ) with generator matrix  $\mathbf{G} \in \mathbb{R}^{N \times K}$ , the squared first successive minimum is bounded according to *Minkowski's first theorem* [3], [9], [46]

$$\mu_{\mathbb{Z},1}^2 \leq \eta_K \text{vol}^{\frac{2}{K}}(\mathbf{A}(\mathbf{G})), \quad (43)$$

where the factor  $\eta_K$ , which depends on the particular dimension, is called Hermite's constant. It is only known for dimensions up to  $K = 8$  as well as  $K = 24$ , cf. [46, Table on p. 33]. However, it has been shown that Hermite's constant can be upper-bounded by the term [63]

$$\eta_K \leq \frac{2}{\pi} \Gamma\left(2 + \frac{K}{2}\right)^{\frac{2}{K}}, \quad (44)$$

where  $\Gamma(x) = (x-1)!$  denotes the Gamma function.

Minkowski's first theorem is generalized in the following Theorem.

**Theorem 2** (Generalized Bound on the First Successive Minimum). *In lattices with  $N \times K$  generator matrix  $\mathbf{G}$  that are defined over the integer ring  $\mathbb{I}$  and for which  $D_r$  denotes the number of real-valued components per scalar, the first successive minimum is bounded by*

$$\mu_{\mathbb{I},1}^2 \leq \eta_{D_r,K} |\det(\mathbf{G}_{\mathbb{I}})|^{\frac{2}{D_r K}} \text{vol}^{\frac{2}{K}}(\mathbf{A}(\mathbf{G})). \quad (45)$$

*Proof.* According to Theorem 1, we have  $\mu_{\mathbb{I},1}^2 = \mu_{r,\mathbb{Z},1}^2$ , the latter denoting the first successive minimum of the equivalent  $D_r N \times D_r K$  real-valued representation  $\mathbf{G}_r$ . Moreover,

$\text{vol}^{\frac{2}{D_r K}}(\mathbf{A}(\mathbf{G}_r)) = \text{vol}^{\frac{2}{K}}(\mathbf{A}(\mathbf{G}))$ , cf. (4), (9), and (28). Hence, applying Minkowski's first theorem (43) w.r.t.  $\mu_{r,\mathbb{Z},1}^2$ , we obtain

$$\begin{aligned} \mu_{\mathbb{I},1}^2 &\leq \eta_{D_r,K} \text{vol}^{\frac{2}{D_r K}}(\mathbf{A}(\mathbf{G}_{r,\mathbb{I}})) \\ &= \eta_{D_r,K} \det^{\frac{1}{D_r K}}(\mathbf{G}_{r,\mathbb{I}}^T \mathbf{G}_{r,\mathbb{I}}) \\ &= \eta_{D_r,K} \det^{\frac{1}{D_r K}}(\mathbf{G}_{\mathbb{I}}^T \mathbf{G}_r^T \mathbf{G}_r \mathbf{G}_{\mathbb{I}}) \\ &= \eta_{D_r,K} |\det(\mathbf{G}_{\mathbb{I}})|^{\frac{2}{D_r K}} \det^{\frac{1}{D_r K}}(\mathbf{G}_r^T \mathbf{G}_r) \\ &= \eta_{D_r,K} |\det(\mathbf{G}_{\mathbb{I}})|^{\frac{2}{D_r K}} \text{vol}^{\frac{2}{K}}(\mathbf{A}(\mathbf{G})) \end{aligned} \quad (46)$$

since the equivalent real-valued generator matrix of the integer ring  $\mathbb{I}$ , denoted as  $\mathbf{G}_{\mathbb{I}}$ , is a non-singular matrix.  $\square$

**Remark.** *Given lattices over  $\mathbb{Z}$  ( $D_r = 1$ ),  $\mathcal{G}$  ( $D_r = 2$ ), or  $\mathcal{L}$  ( $D_r = 4$ ), the matrix  $\mathbf{G}_{\mathbb{I}}$  is an identity matrix, i.e.,  $\det(\mathbf{G}_{\mathbb{I}}) = 1$ . For complex lattices defined over  $\mathcal{E}$  we have  $\det(\mathbf{G}_{\mathcal{E}}) = (\sqrt{3}/2)^K$ , cf. (29), and for quaternionic ones over  $\mathcal{H}$ ,  $\det(\mathbf{G}_{\mathcal{H}}) = (1/2)^K$ , see (30). Hence, we obtain  $|\det(\mathbf{G}_{\mathcal{E}})|^{\frac{2}{D_r K}} = \sqrt{3}/2$  and  $|\det(\mathbf{G}_{\mathcal{H}})|^{\frac{2}{D_r K}} = 1/\sqrt{2}$ , respectively.*

*Noteworthy, for the set of Eisenstein integers, (45) is equivalent to the bound that has been derived for the special case of imaginary quadratic fields in [42].*

When comparing the two types of complex lattices considered in this work, it can be recognized that the bound (45) is smaller for  $\mathbb{I} = \mathcal{E}$  than for  $\mathbb{I} = \mathcal{G}$  since  $\frac{\sqrt{3}}{2} \approx 0.866$ . Hence, in general, the first successive minimum is expected to be smaller. Given quaternion-valued lattices, the bound for  $\mathcal{H}$  is lowered by a factor of  $\frac{1}{\sqrt{2}} \approx 0.707$  in comparison to the bound for  $\mathcal{L}$ .

2) *First Basis Vector of an LLL Basis*: In the initial publication on LLL reduction over  $\mathbb{Z}$  [6], it has been shown that the squared norm of the first basis vector can be bounded. Below, this bound is generalized for lattices over integer rings  $\mathbb{I}$ .

**Theorem 3** (Generalized Bound on the First Vector Norm of an LLL Basis). *Given a lattice with  $N \times K$  generator matrix  $\mathbf{G}$  which is LLL-reduced over the particular Euclidean integer ring  $\mathbb{I}$ , the first basis vector is bounded as*

$$\mu_{\mathbb{I},1}^2 \leq \|\mathbf{g}_{\mathbb{I},1}\|^2 \leq \left(\frac{1}{\delta - \epsilon_{\mathbb{I}}^2}\right)^{\frac{K-1}{2}} \text{vol}^{\frac{2}{K}}(\mathbf{A}(\mathbf{G})), \quad (47)$$

where  $\epsilon_{\mathbb{I}}^2$  denotes the particular maximum squared quantization error.

*Proof.* The lower bound is obvious as  $\mu_{\mathbb{I},1}$  is the norm of the shortest non-zero lattice vector. The upper bound is, similar to [6], derived as follows: Due to the Lovász condition (36),

$$\|\mathbf{q}_k\|^2 \leq \frac{1}{\delta - \epsilon_{\mathbb{I}}^2} \|\mathbf{q}_{k+1}\|^2. \quad (48)$$

Hence, since in the (unsorted) GSO  $\mathbf{q}_1 = \mathbf{g}_1$ ,

$$\|\mathbf{g}_{\mathbb{I},1}\|^2 \leq \left(\frac{1}{\delta - \epsilon_{\mathbb{I}}^2}\right)^{k-1} \|\mathbf{q}_k\|^2, \quad k = 1, \dots, K. \quad (49)$$

Taking the product over all indices  $K$ , we obtain

$$\|\mathbf{g}_{\mathbb{I},1}\|^{2K} \leq \left(\frac{1}{\delta - \epsilon_{\mathbb{I}}^2}\right)^{\frac{K(K-1)}{2}} \prod_{k=1}^K \|\mathbf{q}_k\|^2. \quad (50)$$

Since  $\prod_{k=1}^K \|\mathbf{q}_k\|^2 = \text{vol}^2(\Lambda(\mathbf{G}))$ , see, e.g., [6],

$$\|\mathbf{g}_{\mathbb{I},1}\|^2 \leq \left( \frac{1}{\delta - \epsilon_{\mathbb{I}}^2} \right)^{\frac{K-1}{2}} \text{vol}^{\frac{2}{K}}(\Lambda(\mathbf{G})). \quad (51)$$

□

**Remark.** The bounds derived in [6] ( $\mathbb{Z}$ ) and [40] ( $\mathcal{G}$ ) cover special cases in which the particular maximum squared quantization errors  $\epsilon_{\mathbb{Z}}^2 = \frac{1}{4}$  and  $\epsilon_{\mathcal{G}}^2 = \frac{1}{2}$  have already been incorporated. Via (47), the additional bounds for  $\mathcal{E}$  ( $\epsilon_{\mathcal{E}}^2 = \frac{1}{3}$ ) and  $\mathcal{H}$  ( $\epsilon_{\mathcal{H}}^2 = \frac{1}{2}$ ) are readily obtained.

3) *Comparison of the Bounds:* The above upper bounds on the first successive minimum and the first vector norm of an LLL basis are—normalized to the volume of the lattice—illustrated in Fig. 3. In the upper plot, the complex case is considered. In the bottom plot, quaternion-valued matrices are regarded. To this end, the exact value for Hermite’s constant has been chosen for all dimensions where it is exactly known; otherwise, the approximation (44) has been used. For LLL reduction, the (optimal) parameter  $\delta = 1$  is assumed.

Considering the first successive minimum, the superiority of lattices over  $\mathcal{E}$  and  $\mathcal{H}$ , in comparison to lattices over  $\mathcal{G}$  and  $\mathcal{L}$ , or their isomorphic real- and complex-valued representations over  $\mathbb{Z}$  and  $\mathcal{G}$ , respectively, is clearly visible. For  $N \times 2$  matrices, in both the complex- and quaternion-valued case, the LLL-reduced first vector norms are identical to the respective first successive minima. This is not a surprise since an LLL reduction with  $\delta = 1$  is equivalent to a Gaussian reduction, cf. [14], [40]. It is quite obvious that this relation does not hold any more if the LLL reduction is applied to the equivalent  $2N \times 4$  or  $4N \times 8$  isomorphic representations. When increasing the dimensions, the loss of the LLL approach in comparison to the successive minima becomes more and more apparent. Among all variants of LLL reduction, given  $\delta = 1$ , the QLLL one ( $\mathbb{I} = \mathcal{H}$ ) performs the best, followed by the ELLL one ( $\mathbb{I} = \mathcal{E}$ ). The RLLL approach ( $\mathbb{I} = \mathbb{Z}$ ) already shows a significant gap, and the CLLL one ( $\mathbb{I} = \mathcal{G}$ ) performs the worst.

In Fig. 3, the quality parameter  $\delta = 1$  is considered. Still the question remains which type of LLL reduction is—depending on  $\delta$ —the best-performing one in an asymptotic manner. This comparison is expressed by the following Corollary.

**Corollary 1** (Comparison of the First Vector Norm of LLL Variants). *Given two variants of LLL reduction operating over lattices of rank  $K_1$  and  $K_2$ , and related Euclidean integer rings with the maximum squared quantization errors  $\epsilon_1^2$  and  $\epsilon_2^2$ , the first one has a smaller asymptotic ( $K_1, K_2 \rightarrow \infty$ ) upper bound (47) for the first basis vector than the second one if*

$$\frac{(\delta - \epsilon_2^2)^{K_2-1}}{(\delta - \epsilon_1^2)^{K_1-1}} < 1. \quad (52)$$

In Appendix B, (52) is briefly derived and the particular comparisons are listed for all considered LLL variants. The main conclusions are: Given complex matrices ( $\mathbf{G} \in \mathbb{C}^{N \times K}$ ), the ELLL approach generally performs better than the CLLL one, and it also leads to a smaller bound when compared with the RLLL one (within the relevant range of  $\delta$ ). In contrast, the CLLL algorithm performs worse than the RLLL one,

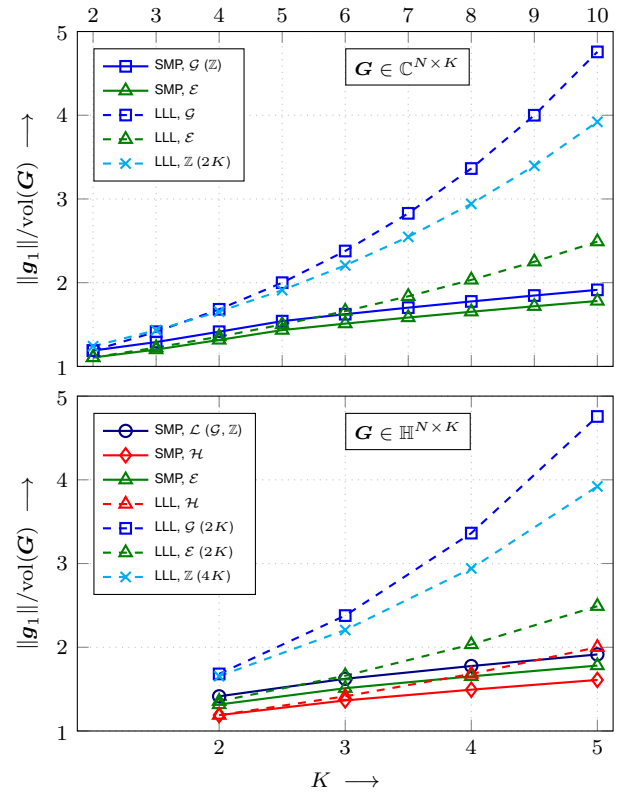


Fig. 3. Upper bounds on the normalized first successive minimum (solid lines) and the normalized first vector norm of an LLL-reduced basis with parameter  $\delta = 1$  (dashed lines) over the dimension  $K$ . Top: complex-valued lattices. Bottom: quaternion-valued lattices.

except from the case when  $\delta = \frac{3}{4}$ , see also [40]. Given quaternionic lattices ( $\mathbf{G} \in \mathbb{H}^{N \times K}$ ), it can be stated that the QLLL algorithm shows better bounds than its CLLL, ELLL, and RLLL counterparts within the relevant range of  $\delta$ . Hence, its use is highly recommendable in the quaternion-valued case.

## B. Bounds on the Product of the Norms

Even though the above bounds are restricted to the first vectors, it is possible to gain some indirect knowledge on all vectors. In particular, bounds on their *product* can be given.

1) *Product of the Successive Minima:* According to Minkowski’s second theorem [46], [64], for  $L = 1, \dots, K$ , the product of the first  $L$  squared successive minima is bounded by

$$\prod_{l=1}^L \mu_{\mathbb{Z},l}^2 \leq \eta_K^L \text{vol}^{\frac{2L}{K}}(\Lambda(\mathbf{G})). \quad (53)$$

Since, for  $L = K$ ,

$$\prod_{k=1}^K \mu_{\mathbb{Z},k}^2 \leq \eta_K^K \text{vol}^2(\Lambda(\mathbf{G})), \quad (54)$$

a bound on the orthogonality defect (27) of the transformed matrix  $\mathbf{G}_{\text{tra},\mathbb{Z}} = \mathbf{G}\mathbf{T}_{\mathbb{Z}}$  containing the shortest independent lattice vectors (cf. Sec. III) is readily obtained.

**Theorem 4** (Bound on the Orthogonality Defect of the Shortest Independent Vectors in a Real-Valued Lattice). *The orthogonality defect of the transformed matrix  $\mathbf{G}_{\text{tra}}$  is upper bounded by*

$$\Omega(\mathbf{G}_{\text{tra},\mathbb{Z}}) \leq \eta_K^{\frac{K}{2}}. \quad (55)$$

*Proof.* If  $\mathbf{T}_{\mathbb{Z}}$  is unimodular, (55) directly follows from (54) since  $\Lambda(\mathbf{G}_{\text{tra},\mathbb{Z}}) = \Lambda(\mathbf{G})$  is valid. If  $\mathbf{T}_{\mathbb{Z}}$  is non-unimodular,  $\Lambda(\mathbf{G}_{\text{tra},\mathbb{Z}}) \neq \Lambda(\mathbf{G})$ . However, since then,  $\sqrt{\det(\mathbf{T}_{\mathbb{Z}}^H \mathbf{T}_{\mathbb{Z}})} > 1$ , we have  $\text{vol}(\Lambda(\mathbf{G}_{\text{tra},\mathbb{Z}})) > \text{vol}(\Lambda(\mathbf{G}))$ . Consequently,

$$\Omega^2(\mathbf{G}_{\text{tra},\mathbb{Z}}) = \frac{\prod_{k=1}^K \mu_{\mathbb{Z},k}^2}{\text{vol}^2(\Lambda(\mathbf{G}_{\text{tra},\mathbb{Z}}))} < \frac{\prod_{k=1}^K \mu_{\mathbb{Z},k}^2}{\text{vol}^2(\Lambda(\mathbf{G}))}, \quad (56)$$

i.e., (55) still follows from (54).  $\square$

**Theorem 5** (Generalized Bound on the Product of the Successive Minima and the Related Orthogonality Defect). *In lattices with  $N \times K$  generator matrix  $\mathbf{G}$  that are defined over the integer ring  $\mathbb{I}$  and for which  $D_r$  denotes the number of real-valued components per scalar, the product of the first  $L$  successive minima is bounded by*

$$\prod_{l=1}^L \mu_{\mathbb{I},l}^2 \leq \eta_{D_r,K}^L |\det(\mathbf{G}_{\mathbb{I}})|^{\frac{2L}{D_r K}} \text{vol}^{\frac{2L}{K}}(\Lambda(\mathbf{G})), \quad (57)$$

and the orthogonality defect by

$$\Omega(\mathbf{G}_{\text{tra},\mathbb{I}}) = \eta_{D_r,K}^{\frac{K}{D_r}} |\det(\mathbf{G}_{\mathbb{I}})|^{\frac{1}{D_r}}. \quad (58)$$

*Proof.* The argumentation can be done equivalently to the derivations which are given in the proofs for Theorem 2 and Theorem 4.  $\square$

**Remark.** *Given lattices over  $\mathbb{Z}$  ( $D_r = 1$ ),  $\mathcal{G}$  ( $D_r = 2$ ), or  $\mathcal{L}$  ( $D_r = 4$ ),  $|\det(\mathbf{G}_{\mathbb{I}})|^{\frac{2L}{D_r K}} = |\det(\mathbf{G}_{\mathbb{I}})|^{\frac{1}{D_r}} = 1$ . For complex lattices defined over  $\mathcal{E}$  we have  $|\det(\mathbf{G}_{\mathcal{E}})|^{\frac{2L}{D_r K}} = (\sqrt{3}/2)^L$  and  $|\det(\mathbf{G}_{\mathcal{E}})|^{\frac{1}{D_r}} = (3/4)^{\frac{K}{4}}$ . For quaternionic ones over  $\mathcal{H}$ ,  $|\det(\mathbf{G}_{\mathcal{H}})|^{\frac{2L}{D_r K}} = (1/\sqrt{2})^L$ , and  $|\det(\mathbf{G}_{\mathcal{H}})|^{\frac{1}{D_r}} = (1/2)^{\frac{K}{4}}$ .*

When employing complex lattices over  $\mathcal{E}$ , the upper bound on the orthogonality defect shrinks by a factor of  $(3/4)^{\frac{K}{4}}$  in comparison to lattices over  $\mathcal{G}$ . In contrast to the bound on the first successive minimum in (45), the expected gain grows with the dimension  $K$ . For quaternion-valued lattices over  $\mathbb{I} = \mathcal{H}$ , the gap to the bound over  $\mathbb{I} = \mathcal{L}$  grows by a factor of  $(1/2)^{\frac{K}{4}}$ .

2) *Product of the Vector Norms of an LLL Basis:* A bound for the product of the norms of an LLL-reduced basis can be derived in a similar way. In particular, it is known that at least the product over *all* basis vectors is bounded [6], [46]. This fact is generalized in the following Theorem.

**Theorem 6** (Generalized Bound on the Product of the Norms of an LLL-Reduced Basis and its Related Orthogonality Defect). *Given a lattice  $\Lambda(\mathbf{G})$  spanned by the  $N \times K$  generator matrix  $\mathbf{G}$ , the product of the norms of the basis vectors of an equivalent LLL-reduced matrix  $\mathbf{G}_{\text{red},\mathbb{I}}$  obtained over the integer ring  $\mathbb{I}$  w.r.t. the quality parameter  $\delta$  is bounded as*

$$\prod_{k=1}^K \mu_{\mathbb{I},k}^2 \leq \prod_{k=1}^K \|\mathbf{g}_{\mathbb{I},k}\|^2 \leq \text{vol}^2(\Lambda(\mathbf{G})) \cdot \underbrace{\left( \frac{1}{\delta - \epsilon_{\mathbb{I}}^2} \right)^{\frac{K(K-1)}{2}}}_{\geq \Omega^2(\mathbf{G}_{\text{red},\mathbb{I}})}. \quad (59)$$

Thereby, the rightmost term defines an upper bound on the squared orthogonality defect of  $\mathbf{G}_{\text{red},\mathbb{I}}$ .

*Proof.* The lower bound is readily obtained since  $\mu_{\mathbb{I},k}$  represents the norms of the shortest independent vectors in the

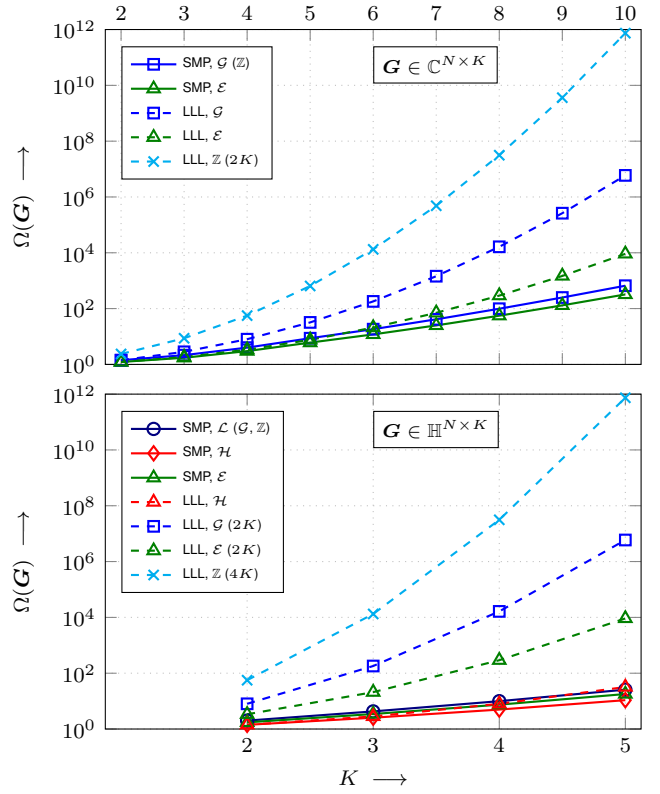


Fig. 4. Upper bounds on the orthogonality defect of the transformed matrix  $\mathbf{G}_{\text{tra},\mathbb{I}}$  formed by the shortest independent vectors of the lattice (solid lines) and on the orthogonality defect of the LLL-reduced basis  $\mathbf{G}_{\text{red},\mathbb{I}}$  with parameter  $\delta = 1$  (dashed lines) over the dimension  $K$ . Top: complex-valued lattices. Bottom: quaternion-valued lattices.

particular lattice. The upper bound is, similar to the proof of the original bound in [6], given as follows: After LLL reduction, the  $k^{\text{th}}$  basis vector can be written as

$$\begin{aligned} \|\mathbf{g}_{\mathbb{I},k}\|^2 &= \|\mathbf{q}_k\|^2 + \sum_{l=1}^{k-1} |r_{k,l}|^2 \|\mathbf{q}_l\|^2 \\ &\leq \|\mathbf{q}_k\|^2 + \sum_{l=1}^{k-1} \epsilon_{\mathbb{I}}^2 \left( \frac{1}{\delta - \epsilon_{\mathbb{I}}^2} \right)^{k-l} \|\mathbf{q}_k\|^2 \\ &= \left( 1 + \epsilon_{\mathbb{I}}^2 \sum_{l=1}^{k-1} \left( \frac{1}{\delta - \epsilon_{\mathbb{I}}^2} \right)^{k-l} \right) \cdot \|\mathbf{q}_k\|^2 \\ &\leq \left( \frac{1}{\delta - \epsilon_{\mathbb{I}}^2} \right)^{k-1} \cdot \|\mathbf{q}_k\|^2. \end{aligned} \quad (60)$$

Forming the product over all basis vectors, we obtain

$$\prod_{k=1}^K \|\mathbf{g}_{\mathbb{I},k}\|^2 \leq \left( \frac{1}{\delta - \epsilon_{\mathbb{I}}^2} \right)^{\frac{K(K-1)}{2}} \underbrace{\prod_{k=1}^K \|\mathbf{q}_k\|^2}_{\text{vol}^2(\Lambda(\mathbf{G}))}. \quad (61)$$

$\square$

3) *Comparison of the Bounds:* In Fig. 4, the different bounds on the orthogonality defect are depicted (Top: complex lattices; Bottom: quaternionic lattices). Again, the exact Hermite's constant has been chosen if it is known for the particular



dimension; otherwise, it has been approximated by (44). The quality parameter  $\delta = 1$  is assumed for LLL reduction.

Considering the orthogonality defect of the transformed matrix  $\mathbf{G}_{\text{tra},\mathbb{I}}$  formed by the shortest independent vectors, the superiority of lattices over  $\mathcal{E}$  (Fig. 4 Top) and  $\mathcal{H}$  (Fig. 4 Bottom) in comparison to lattices defined over  $\mathcal{G}$  and  $\mathcal{L}$ , respectively, is clearly visible. In the quaternion-valued case, the QLLL reduction approaches the orthogonality defect of  $\mathbf{G}_{\text{tra},\mathcal{H}}$  quite well. In general, the QLLL reduction shows the best reduction quality, followed by the ELLL one. Interestingly, the CLLL approach ( $\mathbb{I} = \mathcal{G}$ ) performs better than the RLLL one ( $\mathbb{I} = \mathbb{Z}$ ). This is contrary to the behavior for the bounds on the first vector depicted in Fig. 3, for which the RLLL reduction performed better. The reason is the additional factor  $K$  in the exponent of (59) in comparison to (47), i.e., the doubled dimension carries great weight in the RLLL approach.

Given a particular quality parameter  $\delta$ , the asymptotic behavior of the different types of LLL reduction still has to be analyzed. This can be done with the following Corollary.

**Corollary 2** (Comparison of the Orthogonality Defect of LLL Variants). *Given two variants of LLL reduction operating over lattices of rank  $K_1$  and  $K_2$ , and related Euclidean integer rings with the maximum squared quantization errors  $\epsilon_1^2$  and  $\epsilon_2^2$ , the first one has a smaller asymptotic ( $K_1, K_2 \rightarrow \infty$ ) upper bound on the orthogonality defect in (59) than the second one if*

$$\frac{(\delta - \epsilon_2^2)^{K_2(K_2-1)}}{(\delta - \epsilon_1^2)^{K_1(K_1-1)}} < 1. \quad (62)$$

This inequality is straightforwardly obtained from (59).

The particular comparisons are provided in Appendix C. We briefly summarize the main results w.r.t. the asymptotic behavior of the orthogonality defect: Regarding complex matrices, the CLLL approach performs better than the RLLL one, cf. the discussion above. This is a novel result that has not been recognized in the original CLLL paper [40]. It is also quite obvious that the ELLL approach performs better than the RLLL one for most  $\delta$  except from  $\delta \approx \frac{1}{3}$ . Besides, the ELLL strategy generally performs better than the CLLL one. Given quaternionic lattices, the QLLL reduction is more powerful than the CLLL one. Moreover, it performs better than the ELLL reduction and also better than the RLLL reduction, except from a small range where  $\delta \approx \frac{1}{2}$ .

### C. Asymptotic Computational Complexity

The asymptotic computational complexity is studied next. This includes a general discussion on the complexity as well as a comparison of the different variants, i.e., of the complexity if different types of integer rings are applied.

1) *Complexity of the List-Based Determination of the Successive Minima:* In Algorithm 5, three main steps can be identified: i) the call of the (real-valued) LLL algorithm to find short initial basis vectors, ii) the call of the list sphere decoder that provides all points within a hypersphere where the maximum norm of the basis vectors defines the radius, and iii) the calculation of the row-echelon form.

Even if  $\delta = 1$ , the LLL algorithm has a polynomial complexity given a particular dimension [59]; hence, it can efficiently be performed, see also the discussion below. Moreover, the transformation to row-echelon form (Algorithm 8) that applies a simple Gaussian elimination has a polynomial complexity over  $K$  as well as the list size  $N_c$ . In particular, its asymptotic complexity reads  $\mathcal{O}(K^2 N_c)$ , since (less than)  $K$  rows of  $\mathbf{C}_s$  have to be updated  $K$  times, particularly each time when an independent vector was found.

Hence, the crucial point in the algorithm is the call of the sphere decoder [13], which is known to have an exponential complexity (over  $K$ ). In [44], it has been stated that the number of candidates, i.e., the number of points within a *real-valued* hypersphere, can be approximated by

$$N_{c,\mathbb{Z}} \approx \frac{(\pi\psi^2)^{\frac{K}{2}}}{\frac{K}{2}! \text{vol}(\Lambda(\mathbf{G}))} \quad (63)$$

for the real-valued generator matrix  $\mathbf{G} \in \mathbb{R}^{N \times K}$ , see also [25], where  $\psi^2$  denotes the squared search radius which is defined as  $\psi^2 = \max_k \|\mathbf{g}_{\text{red},k}\|^2$ . Since the maximum norm of an LLL-reduced basis (as well as the  $K^{\text{th}}$  successive minimum) cannot be bounded, the list size cannot be bounded, too. This list size is generalized in the following Corollary.

**Corollary 3** (Approximative List Size in the Generalized Determination of the Successive Minima). *In lattices with  $N \times K$  generator matrix  $\mathbf{G}$  that are defined over the integer ring  $\mathbb{I}$  and for which  $D_r$  denotes the number of real-valued components per scalar, the list size in the determination of the successive minima is approximated by*

$$\begin{aligned} N_{c,\mathbb{I}} &\approx \frac{(\pi\psi^2)^{\frac{D_r K}{2}}}{\frac{D_r K}{2}! \text{vol}(\Lambda(\mathbf{G}_{r,\mathbb{I}}))} \\ &= \frac{(\pi\psi^2)^{\frac{D_r K}{2}}}{\frac{D_r K}{2}! |\det(\mathbf{G}_{\mathbb{I}})| \text{vol}^{D_r}(\Lambda(\mathbf{G}))}. \end{aligned} \quad (64)$$

**Remark.** *In the denominator,  $\text{vol}(\Lambda(\mathbf{G}_{r,\mathbb{I}}))$  has to be incorporated since the search is actually performed with the  $D_r N \times D_r K$  real-valued representation  $\mathbf{G}_{r,\mathbb{I}}$  of  $\mathbf{G}$  with  $\text{vol}(\mathbf{G}_{r,\mathbb{I}}) = |\det(\mathbf{G}_{\mathbb{I}})| \text{vol}^{D_r}(\mathbf{G})$ , cf. Secs. II and III.*

For lattices over Eisenstein and Hurwitz integers, we have  $\det(\mathbf{G}_{\mathcal{E}}) = (\sqrt{3}/2)^K$  and  $\det(\mathbf{G}_{\mathcal{H}}) = (1/2)^K$ , respectively. Hence, the number of candidates is increased in comparison to lattices over Gaussian and Lipschitz integers, for which the determinant is one. This is quite obvious as the Eisenstein as well as the Hurwitz integers constitute denser packings—within the same hypervolume, more points are located. However, please note that the initial RLLL reduction is then performed with  $\mathbf{G}_{r,\mathcal{E}}$  or  $\mathbf{G}_{r,\mathcal{H}}$ . Thereby, lower search radii may be obtained (see the above bounds), counteracting the increase in list size.

2) *Complexity of LLL Reduction:* The computational complexities of the different LLL approaches are finally assessed and compared to each other. They are evaluated w.r.t. the number of *real-valued multiplications* since, in hardware implementation, multiplications are usually much more costly than additions.

It has been shown in the literature that an upper bound on the number of iterations in the LLL algorithm, i.e., on

the number of runs of the code lines within the while-loop in Algorithm 3, can be given [57], [65]. To this end, the elements of the generator matrix have to be assumed to be drawn from a real-valued unit-variance uniform [57] or Gaussian [65] distribution. Then, the asymptotic number of iterations reads  $\mathcal{O}(K \log_{\frac{1}{\delta}}(K))$  if  $\delta < 1$ , where the base of the logarithm is the inverse of the quality parameter  $\delta$ . For the case when  $\delta = 1$ , see [59]. It has been derived in [65] that the same behavior holds for the complex case if a circular-symmetric unit-variance Gaussian distribution is present. Adapting the derivation in [65] to the quaternion-valued case, it can straightforwardly be shown that a circular-symmetric unit-variance quaternionic Gaussian distribution leads to the same result.

It is well-known that the complexity inside the while loop of the LLL algorithm—assuming an efficient implementation of the Gram–Schmidt update—is dominated by the for-loop for size reduction (Lines 11–13 in Algorithm 3), which has an asymptotic complexity of  $\mathcal{O}(NK)$ , cf., e.g., [40]. Hence, in total,<sup>11</sup> this leads to the famous result that the LLL reduction as implemented in Algorithm 3 has the asymptotic complexity  $\mathcal{O}(K^3 N \log_{\frac{1}{\delta}}(K))$ . Noteworthy, this complexity analysis holds for all types of LLL reduction described in this work—under the assumption that the operations are performed in the particular real-, complex-, or quaternion-valued arithmetic.

A complexity comparison of different LLL variants w.r.t the number of totally required *real-valued* multiplications, denoted as  $M_r$ , is of interest. In [40], such a comparison was given for complex matrices and CLLL vs. RLLL reduction. This comparison is generalized in the following Corollary.

**Corollary 4** (Comparison of the Complexity of LLL Variants). *Given two variants of LLL reduction operating over lattices of rank  $K_1$  and  $K_2$ , and related Euclidean integer rings  $\mathbb{I}_1$  and  $\mathbb{I}_2$  for which  $N_{r,\mathbb{I}}$  denotes the number of real-valued multiplications required to implement a multiplication in the respective field, their ratio of the number of real-valued multiplications in the particular LLL algorithm  $M_{r,\mathbb{I}}$  reads*

$$\frac{M_{r,\mathbb{I}_1}}{M_{r,\mathbb{I}_2}} \approx \frac{N_{r,\mathbb{I}_1}}{N_{r,\mathbb{I}_2}} \cdot \frac{K_1^3 N_1 \log_{\frac{1}{\delta}}(K_1)}{K_2^3 N_2 \log_{\frac{1}{\delta}}(K_2)} \cdot \xi_{\mathbb{I}_1,\mathbb{I}_2}, \quad (65)$$

where  $\xi_{\mathbb{I}_1,\mathbb{I}_2} = \Pr\{Q_{\mathbb{I}_1}\{r_{l,k}\} \neq 0\} / \Pr\{Q_{\mathbb{I}_2}\{r_{l,k}\} \neq 0\}$  denotes the ratio between the probabilities that the particular size-reduction operation has to be performed.

In an asymptotic view, (65) simplifies to

$$\lim_{K_1, K_2 \rightarrow \infty} \frac{M_{r,\mathbb{I}_1}}{M_{r,\mathbb{I}_2}} \approx \frac{N_{r,\mathbb{I}_1}}{N_{r,\mathbb{I}_2}} \cdot \frac{K_1^3 N_1}{K_2^3 N_2} \cdot \xi_{\mathbb{I}_1,\mathbb{I}_2}, \quad (66)$$

since  $\log_{\frac{1}{\delta}}(K_1) / \log_{\frac{1}{\delta}}(K_2) \rightarrow 1$ .

**Remark.** *To account for the fact that the size reduction only has to be performed if  $Q_{\mathbb{I}}\{r_{l,k}\} \neq 0$ , cf. Algorithm 2, the ratio  $\xi_{\mathbb{I}_1,\mathbb{I}_2}$  is incorporated. As stated in [66] for complex matrices, the real value  $r_{l,k}$  in the RLLL algorithm and the complex components  $r_{l,k}^{(1)}$  and  $r_{l,k}^{(2)}$  in the CLLL one, which can*

<sup>11</sup>The initial GSO (with pivoting) according to Algorithm 1 is not relevant in the analysis of the asymptotic behavior of the LLL algorithm as it only has a complexity of  $\mathcal{O}(NK)$  required once in the beginning. Besides, even if a naive update of the GSO is performed within the while-loop, the total asymptotic complexity of one iteration still reads  $\mathcal{O}(NK)$ .

be assumed to be independent in a radial-symmetric model, have quite similar statistics. Hence,  $\Pr\{Q_{\mathcal{G}}\{r_{l,k}\} \neq 0\} \approx 2 \Pr\{Q_{\mathcal{Z}}\{r_{l,k}\} \neq 0\}$ , i.e.,  $\xi_{\mathcal{G},\mathcal{Z}} \approx 2$ .

Considering the ELLL approach, in the size-reduction step, the quantization is not performed w.r.t. a square Voronoi cell as in the CLLL approach but w.r.t. a hexagonal one. The latter covers less space ( $\text{vol}(\mathcal{E}) = \text{vol}(\mathbf{A}_2) = \frac{\sqrt{3}}{2}$ ) than the former ( $\text{vol}(\mathcal{G}) = \text{vol}(\mathbb{Z}^2) = 1$ ). However, the hexagonal cell is more similar to a two-dimensional hypersphere, i.e., a circle, than the square one. Hence, it covers a circular-symmetric (Gaussian) distribution more precisely. It can be expected that both effects roughly compensate each other. Thus,  $\xi_{\mathcal{E},\mathcal{G}} \approx 1$ .

For quaternionic lattices, four independent components  $r_{l,k}^{(1)}$ ,  $r_{l,k}^{(2)}$ ,  $r_{l,k}^{(3)}$ , and  $r_{l,k}^{(4)}$  can be assumed if the QLLL algorithm is applied. However, here it has to be taken into account that the Voronoi cell of  $\mathcal{H}$  forms a 24-cell as mentioned in Sec. II, which covers less volume ( $\text{vol}(\mathcal{H}) = \frac{1}{2}$ ) than a four-dimensional hypercube ( $\text{vol}(\mathcal{L}) = \text{vol}(\mathbb{Z}^4) = 1$ ). Nevertheless, the former covers a circular-symmetric (Gaussian) distribution in a better way, cf. above. Hence, we can again assume that  $\xi_{\mathcal{H},\mathcal{L}} \approx 1$  and, as a consequence, that  $\xi_{\mathcal{H},\mathcal{G}} \approx 2$  and  $\xi_{\mathcal{H},\mathcal{Z}} \approx 4$ .

We briefly evaluate the asymptotic complexity ratios according to (66). To this end, please note that for the straightforward multiplication of complex numbers in (2), four real-valued multiplications are required. For the quaternionic multiplication as defined in (6), 16 real-valued multiplications are necessary. Hence, we obtain  $N_{r,\mathbb{Z}} = 1$ ,  $N_{r,\mathcal{G}} = N_{r,\mathcal{E}} = 4$ , and  $N_{r,\mathcal{H}} = 16$ . Assuming complex matrices, the asymptotic ratios of the required real multiplications calculate to  $\frac{M_{r,\mathcal{G}}}{M_{r,\mathbb{Z}}} \approx \frac{M_{r,\mathcal{E}}}{M_{r,\mathbb{Z}}} \approx \frac{1}{2}$  for the comparison of complex and real-valued processing (given  $K_2 = 2K_1$ ,  $N_2 = 2N_1$ , and  $\xi_{\mathcal{G},\mathbb{Z}} \approx \xi_{\mathcal{E},\mathbb{Z}} \approx 2$ ). Hence, for the former, the complexity is roughly halved, see also [40]. Assuming quaternionic matrices, we obtain the ratios  $\frac{M_{r,\mathcal{H}}}{M_{r,\mathcal{G}}} \approx \frac{M_{r,\mathcal{H}}}{M_{r,\mathcal{E}}} \approx \frac{1}{2}$  for quaternionic vs. complex processing as  $\xi_{\mathcal{H},\mathcal{G}} \approx \xi_{\mathcal{H},\mathcal{E}} \approx 2$ . Comparing quaternionic and real-valued processing,  $\frac{M_{r,\mathcal{H}}}{M_{r,\mathbb{Z}}} \approx \frac{1}{4}$ , since  $K_2 = 4K_1$ ,  $N_2 = 4N_1$ , and  $\xi_{\mathcal{H},\mathbb{Z}} \approx 4$ . Thus, the complexity is significantly reduced by using the QLLL algorithm instead of its real/complex counterparts.

Finally, we briefly consider the complexity ratios for the case when “advanced” multiplication schemes are applied. As mentioned in Sec. II, a complex-valued multiplication can be implemented by only  $N_r = 3$  real-valued multiplications, and a quaternion-valued multiplication by only  $N_r = 8$  ones. Hence, for complex- vs. real-valued processing, the ratios  $\frac{M_{r,\mathcal{G}}}{M_{r,\mathbb{Z}}} \approx \frac{M_{r,\mathcal{E}}}{M_{r,\mathbb{Z}}} \approx \frac{3}{8}$  are obtained. For quaternion-valued vs. complex-valued processing, the complexity ratios are given as  $\frac{M_{r,\mathcal{H}}}{M_{r,\mathcal{G}}} \approx \frac{M_{r,\mathcal{H}}}{M_{r,\mathcal{E}}} \approx \frac{1}{3}$ , and for quaternion-valued vs. real-valued processing, the number of required multiplications is reduced to  $\frac{M_{r,\mathcal{H}}}{M_{r,\mathbb{Z}}} \approx \frac{1}{8}$ . Please note that these decreased numbers of multiplications are accompanied by increased numbers of required additions. Hence, the best-performing strategy largely depends on the particular hardware architecture.

#### D. Numerical Evaluation and Comparison

To complement the theoretical derivations provided in this section, numerical simulations have been performed. In partic-



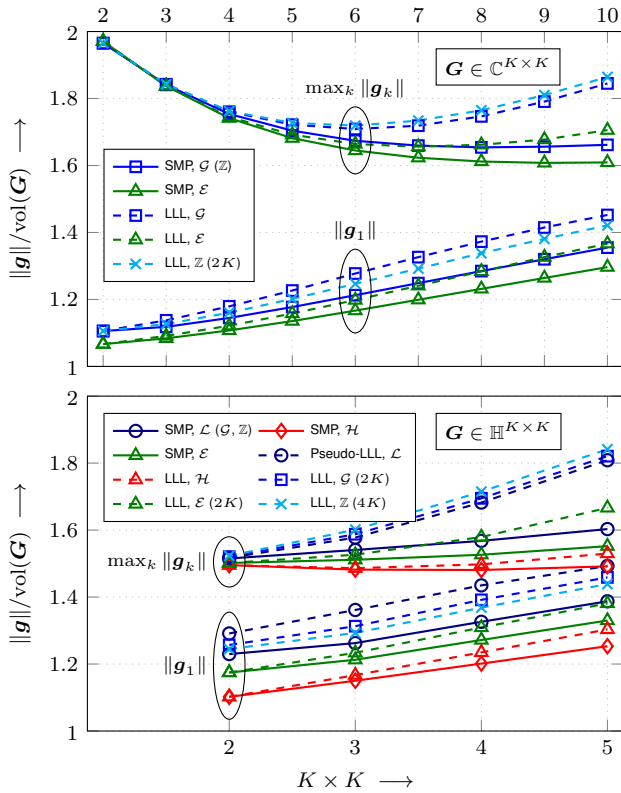


Fig. 5. 0.99-quantiles for the normalized first successive minimum (solid lines) and the normalized first vector norm of an LLL-reduced basis with parameter  $\delta = 1$  (dashed lines) as well as the related maximum values among all vectors over the dimensions  $K \times K$  obtained from numerical simulations. Top: complex-valued lattices. Bottom: quaternion-valued lattices.

ular, for both the complex- and the quaternion-valued case,  $10^6$  i.i.d. unit-variance complex or quaternionic Gaussian random matrices have been considered. Since we are interested in upper bounds on the quality and complexity, the assessment is performed by evaluating the 0.99-quantiles of the particular quantities, i.e., the values which are surpassed by exactly 1% of the observed realizations. Again, for LLL reduction, the optimal quality parameter  $\delta = 1$  is assumed.

1) *Norms of the Vectors:* In Fig. 5, the 0.99-quantiles of the normalized norms are illustrated, cf. Fig. 3 (Top: complex matrices; Bottom: quaternionic matrices). In addition to the norms of the first vectors, their maximum values are shown. The maximum among the vector norms, which can only be evaluated numerically (see above), is the relevant quantity for the SBP (33) and the SIVP (40).

Restricting the considerations to the norms of the first vectors in Fig. 5, the conclusions follow the ones that were drawn for the theoretical upper bounds in Fig. 3: Lattices over  $\mathcal{E}$  and  $\mathcal{H}$  possess lower first successive minima than lattices over  $\mathcal{G}$  and  $\mathcal{L}$ , respectively. The LLL reductions over  $\mathcal{E}$  and  $\mathcal{H}$  show the best quality; their respective quantiles may even fall below the ones of the successive minima over  $\mathcal{G}$  and  $\mathcal{L}$  for small dimensions. Among the “genuine” LLL approaches, the reduction over  $\mathcal{G}$  performs the worst. In the quaternion-valued case, only the curve for pseudo-QLLL reduction (over  $\mathcal{L}$ ) possesses higher quantiles. However, for statistical models

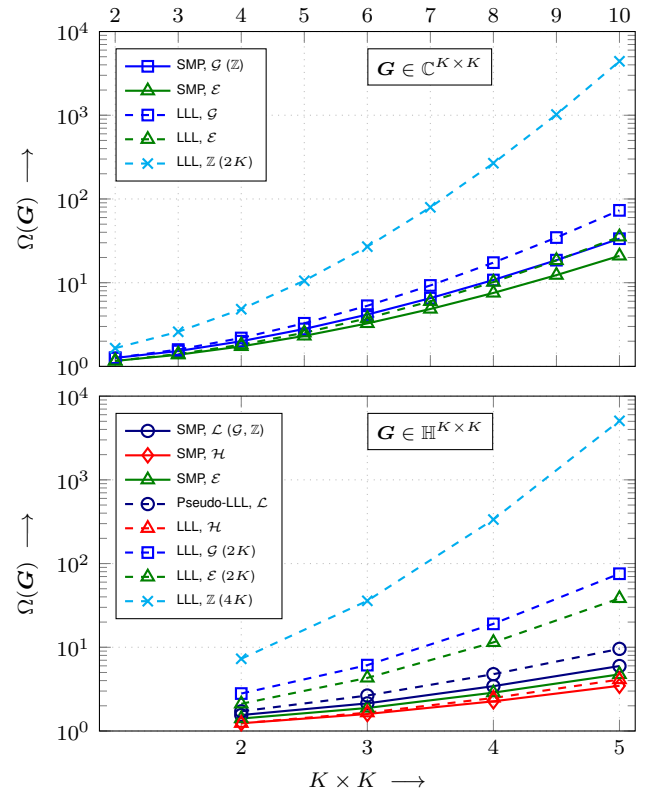


Fig. 6. 0.99-quantiles for the orthogonality defect of the matrix formed by the shortest independent vectors of the lattice (solid lines) as well as the related basis vectors of an LLL-reduced basis with parameter  $\delta = 1$  (dashed lines) over the dimensions  $K \times K$  obtained from numerical simulations. Top: complex-valued lattices. Bottom: quaternion-valued lattices.

like the i.i.d. Gaussian one at hand, its application still results in a reasonable performance, though alternative approaches may be more appropriate if the first vector is relevant.

For the maximum of the vector norms in Fig. 5, similar conclusions can be drawn—except for two important observations: First, in contrast to the first vector and similar to the theoretical bounds on the orthogonality defect in Fig. 4, the CLLL reduction performs better than the RLLL reduction. Second, in the quaternion-valued case, the pseudo-QLLL reduction even possesses lower quantiles than the CLLL or RLLL reduction. Hence, concerning an approximate solution for the SBP and the SIVP, respectively, the application of the pseudo-QLLL reduction over  $\mathcal{L}$  may even be beneficial in practice, if and only if the “genuine” QLLL reduction over  $\mathcal{H}$  is not desired.

2) *Orthogonality Defect:* In Fig. 6, the 0.99-quantile of the orthogonality defect is plotted as the statistical quantity. Again, the complex case is shown at the top and the quaternionic case at the bottom.

The shapes of the curves correspond to the behavior that can be expected when the theoretical bounds from Fig. 4 are regarded. For the complex case, the orthogonality defect of the matrix formed by the shortest independent vectors over  $\mathcal{E}$  is the lowest one, whereas the application of the RLLL algorithm results in the worst quality.

For quaternion-valued lattices, the successive minima over  $\mathcal{H}$  as well as the related LLL reduction are accompanied by

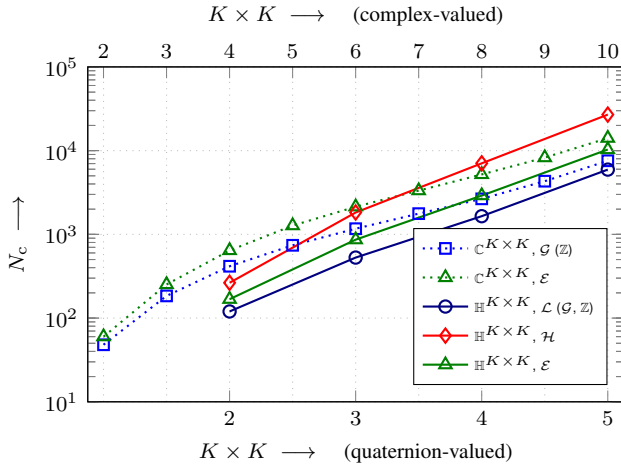


Fig. 7. 0.99-quantiles of the list size  $N_c$  for the determination of the successive minima according to Algorithm 5 over different integer rings  $\mathbb{I}$  obtained by numerical simulations. Dashed curves: complex-valued lattices with generator matrix  $\mathbf{G} \in \mathbb{C}^{K \times K}$ . Solid curves: quaternion-valued lattices with generator matrix  $\mathbf{G} \in \mathbb{H}^{K \times K}$ .

the smallest orthogonality defects. Again, the classical LLL reduction over  $\mathbb{Z}$  shows the worst quality. Surprisingly, at least w.r.t. the orthogonality defect, the pseudo-QLLL reduction over  $\mathcal{L}$  results in quite a good performance. In particular, the orthogonality defect falls significantly below the one of any equivalent complex or real-valued strategy.

3) *List Sizes of the Successive-Minima Algorithm:* Fig. 7 depicts the 0.99-quantiles of the list size  $N_c$  for the list-based determination of the successive minima of a lattice as described in Sec. III-B. Both the complex-valued ( $\mathbf{G} \in \mathbb{C}^{K \times K}$ ) and the quaternion-valued case ( $\mathbf{G} \in \mathbb{H}^{K \times K}$ ) are considered.

With regard to complex lattices, the determination of the successive minima over  $\mathcal{E}$  is accompanied by a slightly increased list size in comparison to  $\mathcal{G}$ . As explained in Sec. IV-C1, this increase in complexity is caused by an increased number of lattice points within a given search radius due to the denser packing. Obviously, even though the initial search radius obtained by *real-valued* LLL reduction may be lowered a little bit for lattices over Eisenstein integers, the denser packing seems to be the more dominating point.

The same holds for the quaternion-valued case: here, lattices over  $\mathcal{L}$  result in the lowest quantiles for the list size, whereas lattices over  $\mathcal{H}$  are—due to the densest packing in four dimensions—accompanied by the largest quantities. If the successive minima w.r.t.  $\mathcal{E}$  are calculated for the equivalent complex-valued representation, the list size is located in between the one of  $\mathbb{I} = \mathcal{L}$  and  $\mathbb{I} = \mathcal{H}$ , as the packing is denser than the one of  $\mathcal{G}^2$ , but sparser than the one of  $\mathcal{H}$ .

4) *Multiplications within the LLL Algorithm:* Finally, we assess the 0.99-quantiles of the numbers of real-valued multiplications  $M_r$  that are required to run the (generalized) LLL reduction as defined in Algorithm 3. To this end, the numbers are shown in Fig. 8 (Top: complex lattices; Bottom: quaternionic lattices). Both the standard multiplication approaches (2) and (6), respectively, with  $N_r = 4$  and  $N_r = 16$  real-valued multiplications (solid lines), and the reduced-complexity variants

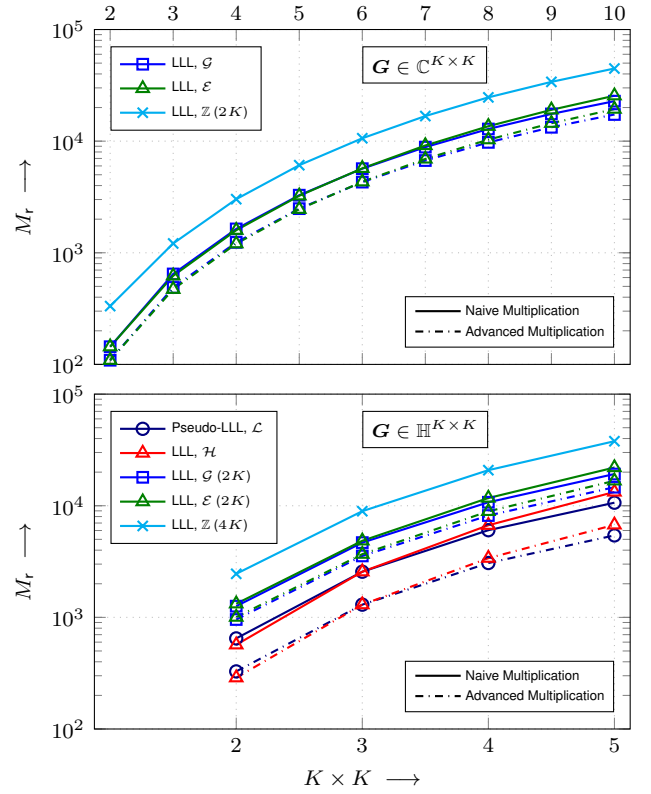


Fig. 8. 0.99-quantiles for the number of real-valued multiplications  $M_r$  within the generalized LLL reduction approach as stated in Algorithm 3 obtained by numerical simulations. Over each integer ring, the quality parameter  $\delta = 1$  was used. Solid lines indicate the naive implementation of the complex or quaternion-valued multiplication operations, dashed-dotted ones the implementation with reduced numbers of real-valued multiplications. Top: complex-valued lattices. Bottom: quaternion-valued lattices.

with  $N_r = 3$  and  $N_r = 8$  multiplications (dashed-dotted lines), are evaluated.

Given the complex case in Fig. 8 (Top), it is clearly visible that the CLLL and the ELLL algorithm roughly possess the same number of multiplications, which are halved in comparison to the RLLL approach if the standard multiplication strategy is applied, cf. Sec. IV-C2. If the advanced complex multiplication with  $N_r = 3$  is used instead, these ratios are reduced to about  $\frac{3}{8}$  like predicted by the asymptotic assessment of the complexity.

For the quaternion-valued case in Fig. 8 (Bottom), the following conclusions can be drawn: Pseudo-QLLL reduction over  $\mathcal{L}$  and QLLL reduction over  $\mathcal{H}$  possess about the same number of real-valued multiplications. The same is valid for the CLLL and the ELLL algorithm, using the equivalent complex-valued representation. Restricting to the standard quaternion-valued multiplication approach, the number of multiplications can roughly be halved in comparison to the CLLL and the ELLL approach, and roughly be reduced to one fourth in comparison to the RLLL approach, if the reduction is performed over  $\mathcal{L}$  or  $\mathcal{H}$ . When using the advanced multiplication scheme for quaternionic numbers, these ratios can further be reduced to one third and one eighth, respectively, as already derived in the theoretical analysis in Sec. IV-C2.

## V. APPLICATION TO MIMO TRANSMISSION

In this section, it is studied in which ways the generalized algorithms derived and analyzed in the previous sections can be applied to the field of MIMO communications. To this end, the system model of complex MIMO transmission is reviewed and extended to the quaternion-valued case. Particular scenarios for the use of quaternion-valued arithmetic are identified. In addition, lattice-based channel equalization is adapted to the situation at hand.

### A. SISO Fading Channel

In wireless transmission, the fading model is quite popular to represent non-line-of-sight connections. In the simplest case, only one transmit and one receive antenna are used, i.e., a single-input/single-output (SISO) fading channel is present. It can be modeled by the system equation<sup>12</sup>

$$y = h \cdot x + n. \quad (67)$$

Thereby,  $x$  is a transmit symbol taken from the finite set of symbols  $\mathcal{A}$  (signal constellation),  $h$  denotes the fading coefficient (multiplicative distortion),  $n$  represents Gaussian noise (additive distortion), and  $y$  is the disturbed receive symbol.

1) *Complex-Valued Transmission:* Most often, (67) is considered to be a complex-valued equation that models radio-frequency transmission in the equivalent complex baseband [22], [23]. Then, a (zero-mean) QAM constellation  $\mathcal{A} \subset \mathbb{C}$  with the variance  $\sigma_{x,c}^2$  and the cardinality  $M_c = |\mathcal{A}|$  is most commonly applied. These constellations form (shifted) subsets of the Gaussian integers [19], [44]. Alternatively, constellations based on the Eisenstein integers can be employed [2], [19], [28], [30]. In accordance, the fading coefficient is complex (*Rayleigh* fading [67], usually normalized to  $\sigma_{h,c}^2 = 1$ ), and we have to deal with (radial-symmetric) complex Gaussian noise with some variance  $\sigma_{n,c}^2$ .

Taking advantage of (3), the SISO Rayleigh-fading channel can equivalently be modeled by a real-valued system with the system equation<sup>13</sup>

$$\begin{bmatrix} y^{(1)} \\ y^{(2)} \end{bmatrix} = \begin{bmatrix} h^{(1)} & -h^{(2)} \\ h^{(2)} & h^{(1)} \end{bmatrix} \begin{bmatrix} x^{(1)} \\ x^{(2)} \end{bmatrix} + \begin{bmatrix} n^{(1)} \\ n^{(2)} \end{bmatrix}, \quad (68)$$

where the noise components  $n^{(1)}$  and  $n^{(2)}$  have the variance  $\sigma_{n,r}^2 = \frac{1}{2}\sigma_{n,c}^2$  and the variances of the constellation's components read  $\sigma_{x,r}^2 = \frac{1}{2}\sigma_{x,c}^2$  if the components are independent (e.g., in QAM).

2) *Quaternion-Valued Transmission:* On the basis of (67), a *quaternion-valued* SISO fading channel model can be defined. Then, the transmit symbols are consistently drawn from a quaternion-valued signal constellation  $\mathcal{A} \subset \mathbb{H}$  with the (4D) cardinality  $M_q = |\mathcal{A}|$ . The signal points can, e.g., be chosen as a subset of the Lipschitz or the Hurwitz integers [1], [68].

<sup>12</sup>In order to simplify the notation, the time index is omitted in all system equations, i.e., one particular time step (modulation step) is considered.

<sup>13</sup>For  $x$  and  $n$ , only the left column of the equivalent real-valued representation (3) is employed, as the right column is completely redundant and not required to obtain the final result (left column) of  $y$ .

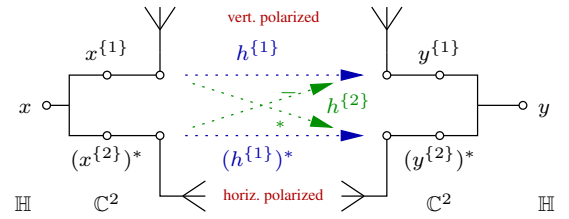


Fig. 9. Transmission with dual-polarized antennas over the SISO fading channel according to (71). At the transmitter and receiver, antenna pairs are present that transmit and receive electromagnetic waves which carry information in both the vertical polarization plane (top) and the horizontal polarization plane (bottom). In the quaternion-valued fading factor  $h = h^{\{1\}} + h^{\{2\}}j$ , both the direct gain  $h^{\{1\}}$  and the cross-polar gain  $h^{\{2\}}$  are contained.

The related variance reads  $\sigma_{x,q}^2$ . The fading coefficient is given as

$$h = \underbrace{(h^{\{1\}} + h^{\{2\}}i)}_{h^{\{1\}}} + \underbrace{(h^{\{3\}} + h^{\{4\}}i)}_{h^{\{2\}}}j, \quad (69)$$

i.e., it consists of *four independent real-valued* or *two independent complex-valued* ones, respectively. Since two independent unit-variance Rayleigh-fading coefficients are present, the variance reads  $\sigma_{h,q}^2 = 2\sigma_{h,c}^2 = 4\sigma_{h,r}^2 = 2$ . In the same way, the noise is represented by

$$n = \underbrace{(n^{\{1\}} + n^{\{2\}}i)}_{n^{\{1\}}} + \underbrace{(n^{\{3\}} + n^{\{4\}}i)}_{n^{\{2\}}}j, \quad (70)$$

where  $\sigma_{n,q}^2 = 2\sigma_{n,c}^2 = 4\sigma_{n,r}^2$ . A disturbed receive symbol  $y \in \mathbb{H}$  is finally obtained.

Benefiting from (7), the quaternion-valued SISO fading channel is equivalently expressed by the complex-valued  $2 \times 2$  system equation

$$\begin{bmatrix} y^{\{1\}} \\ (y^{\{2\}})^* \end{bmatrix} = \begin{bmatrix} h^{\{1\}} & -h^{\{2\}} \\ (h^{\{2\}})^* & (h^{\{1\}})^* \end{bmatrix} \begin{bmatrix} x^{\{1\}} \\ (x^{\{2\}})^* \end{bmatrix} + \begin{bmatrix} n^{\{1\}} \\ (n^{\{2\}})^* \end{bmatrix}. \quad (71)$$

This complex  $2 \times 2$  system equation and its quaternion-valued (scalar) representation, respectively, are well-suited to model particular transmission scenarios:

- i) Transmission with *dual-polarized antennas*: as illustrated in Fig. 9, (71) models the (SISO) transmission with one dual-polarized antenna at both the transmitter and the receiver side. In particular, both horizontal and vertical polarization of the electromagnetic wave are then used for the orthogonal transmission of *two* complex-valued symbols at the same time and on the same frequency band. Thereby, the first complex fading factor  $h^{\{1\}}$  describes the *direct gain* within the same polarization plane, whereas  $h^{\{2\}}$  represents the *cross-polar gain*, i.e., the crosstalk to the other polarization plane. Moreover, the noise samples  $n^{\{1\}}$  and  $n^{\{2\}}$  describe the additive noise which is present at the vertically and horizontally polarized receive antenna, respectively. Further details can be found in [1], [37], [38].
- ii) Transmission with Alamouti (space-time) coding: the system equation (71) corresponds to the one of the Alamouti scheme as a diversity technique [35]. Then, the complex symbols  $x^{\{1\}}$  and  $x^{\{2\}}$  may actually be

radiated at different time steps (or, e.g., frequencies), but are processed jointly. Diversity is obtained if the channel gains  $h^{\{1\}}$  and  $h^{\{2\}}$  (representing the two time steps, frequencies, ...) are independent. The quaternion-valued SISO fading model can be seen as an alternative (scalar) representation of the  $2 \times 2$  space-time coding scheme. For further details and a deeper comparison of dual-polarized transmission and Alamouti coding, see [69].

### B. MIMO Fading Channel (Uplink Transmission)

The complex- or quaternion-valued SISO fading models can be generalized to respective MIMO ones. In this work, *MIMO uplink transmission*—aka *MIMO multiple-access channel*—is treated in an exemplary way.

$K$  uncoordinated single-antenna user devices transmit their data—at the same time and on the same frequency—to *one* central receiver which is equipped with  $N \geq K$  antennas. The related system equation is given as

$$\mathbf{y} = \mathbf{H} \cdot \mathbf{x} + \mathbf{n}. \quad (72)$$

Here,  $\mathbf{x} = [x_1, \dots, x_K]^T$  denotes the vector of transmit symbols sent by the users,  $\mathbf{H}$  the  $N \times K$  MIMO channel matrix,  $\mathbf{n} = [n_1, \dots, n_N]^T$  a vector with  $N$  noise samples, and  $\mathbf{y} = [y_1, \dots, y_N]^T$  the vector of  $N$  symbols which are received at the central unit.

1) *Complex-Valued Transmission*: Most often, a complex-valued MIMO channel is considered. A popular model is that the channel matrix

$$\mathbf{H} = [h_{n,k}]_{\substack{n=1,\dots,N \\ k=1,\dots,K}} \in \mathbb{C}^{N \times K} \quad (73)$$

contains i.i.d. complex Gaussian unit-variance channel gains  $h_{n,k} \in \mathbb{C}$  that describe (in equivalent complex baseband representation) the links between the user  $k$  and the receive antenna  $n$ . At each receive antenna, complex Gaussian noise with the (same) variance  $\sigma_{n,c}^2$  is assumed.

Given the assumption that the transmit symbols  $x_1, \dots, x_K$  are drawn from a complex-valued integer ring  $\mathbb{I}$ , i.e.,  $x_k \in \mathcal{G}$  or  $x_k \in \mathcal{E}$ ,  $k = 1, \dots, K$ , and neglecting the noise, the receive symbols are drawn from (a subset of) a complex-valued lattice as defined in (25). Thereby, the generator matrix is given as  $\mathbf{G} = \mathbf{H}$ .

The complex-valued system equation is equivalently expressed by the real-valued equation

$$\underbrace{\begin{bmatrix} \mathbf{y}^{(1)} \\ \mathbf{y}^{(2)} \end{bmatrix}}_{\mathbf{y}_r} = \underbrace{\begin{bmatrix} \mathbf{H}^{(1)} & -\mathbf{H}^{(2)} \\ \mathbf{H}^{(2)} & \mathbf{H}^{(1)} \end{bmatrix}}_{\mathbf{H}_r} \underbrace{\begin{bmatrix} \mathbf{x}^{(1)} \\ \mathbf{x}^{(2)} \end{bmatrix}}_{\mathbf{x}_r} + \underbrace{\begin{bmatrix} \mathbf{n}^{(1)} \\ \mathbf{n}^{(2)} \end{bmatrix}}_{\mathbf{n}_r}. \quad (74)$$

Consequently, given the case that  $\mathbf{x} \in \mathcal{G}^K$ , an equivalent  $2N \times 2K$  real-valued lattice (over  $\mathbb{I} = \mathbb{Z}$ ) with the generator matrix  $\mathbf{H}_r$  is spanned, where  $\mathbf{x}_r \in \mathbb{Z}^{2K}$ . Lattices over  $\mathbb{I} = \mathcal{E}$  can be expressed according to (29).

2) *Quaternion-Valued Transmission*: It is possible to extend the complex-valued MIMO uplink model to the quaternion-valued case. Then, the channel matrix is represented as

$$\mathbf{H} = [h_{n,k}]_{\substack{n=1,\dots,N \\ k=1,\dots,K}} \in \mathbb{H}^{N \times K}, \quad (75)$$

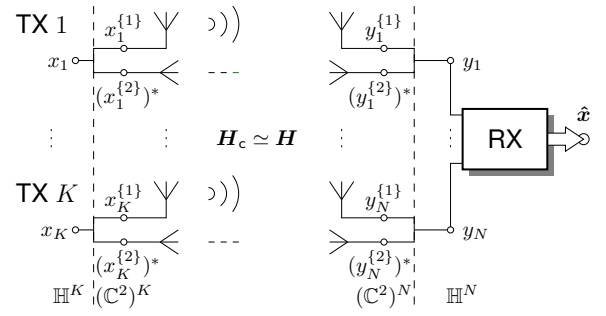


Fig. 10. Quaternion-valued MIMO uplink transmission (MIMO multiple-access channel) with dual-polarized antennas.  $K$  uncoordinated pairs of transmit antennas (in each TX, one for vertical and one for horizontal polarization) radiate the users' data symbols to the  $N$  pairs of receive antennas. The quaternion-valued receive symbols  $y_1, \dots, y_N$  are processed jointly in a central receive unit (RX) in order to obtain estimates of the transmit symbols  $x_1, \dots, x_K$ .

i.e., it contains i.i.d. quaternion-valued Gaussian channel gains  $h_{n,k} \in \mathbb{H}$  (Gaussian distribution in each component) with the total variance  $\sigma_{h,q}^2 = 2\sigma_{h,c}^2 = 2$ , i.e., unit-variance channel gains per complex component as often considered in MIMO communications. Under the assumption that the transmit symbols  $x_1, \dots, x_K$  are now chosen from a quaternion-valued integer ring  $\mathbb{I}$ , i.e.,  $x_k \in \mathcal{L}$  or  $x_k \in \mathcal{H}$ ,  $k = 1, \dots, K$ , and neglecting the noise, the receive symbols form a subset of a quaternion-valued lattice according to (25) with  $\mathbf{G} = \mathbf{H}$ .

Given the scenario of MIMO uplink transmission via dual-polarized antennas as depicted in Fig. 10, the quaternion-valued channel gains describe the links between the *transmit-antenna pairs*  $k$ ,  $k = 1, \dots, K$ , and the *receive-antenna pairs*  $n$ ,  $n = 1, \dots, N$ . At each receive-antenna pair, quaternion-valued noise samples with the (total) variance  $\sigma_{n,q}^2$  are assumed that contain the noise of both polarization planes. When using the quaternionic model for the representation of the Alamouti coding scheme, the horizontally-polarized antennas can be replaced by “virtual” antennas that represent the transmission at another time step or in another frequency band instead.

As becomes apparent from Fig. 10, the quaternion-valued transmission is actually realized by the equivalent  $2N \times 2K$  complex-valued system model

$$\underbrace{\begin{bmatrix} \mathbf{y}^{\{1\}} \\ (\mathbf{y}^{\{2\}})^* \end{bmatrix}}_{\mathbf{y}_c} = \underbrace{\begin{bmatrix} \mathbf{H}^{\{1\}} & -\mathbf{H}^{\{2\}} \\ (\mathbf{H}^{\{2\}})^* & (\mathbf{H}^{\{1\}})^* \end{bmatrix}}_{\mathbf{H}_c} \underbrace{\begin{bmatrix} \mathbf{x}^{\{1\}} \\ (\mathbf{x}^{\{2\}})^* \end{bmatrix}}_{\mathbf{x}_c} + \underbrace{\begin{bmatrix} \mathbf{n}^{\{1\}} \\ (\mathbf{n}^{\{2\}})^* \end{bmatrix}}_{\mathbf{n}_c}. \quad (76)$$

Hence, if  $\mathbf{x} \in \mathcal{L}^K$ , the quaternion-valued lattice  $\Lambda(\mathbf{H})$  is isomorphically represented by a complex lattice ( $\mathbb{I} = \mathcal{G}$ ) with the generator matrix  $\mathbf{G} = \mathbf{H}_c$ . In the same way, on the basis of (8), an equivalent real-valued lattice ( $\mathbb{I} = \mathbb{Z}$ ) can be defined. A quaternion-valued transmission with symbols drawn from  $\mathbb{I} = \mathcal{H}$  can be represented by equivalent lattices over  $\mathbb{I} = \mathbb{Z}$  and  $\mathbb{I} = \mathcal{G}$  according to (30) and (31), respectively.

### C. Lattice-Reduction-Aided and Integer-Forcing Equalization

In the MIMO (uplink) scenario, handling the (multi-user) interference is a crucial point. It is well-known that (purely)

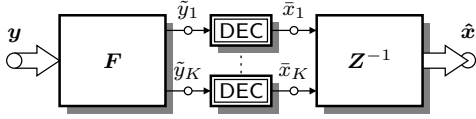


Fig. 11. General receiver structure of LRA/IF linear equalization [19]. The receive symbols in  $\mathbf{y}$  are linearly equalized via the filter matrix  $\mathbf{F}$  before channel decoding (DEC) w.r.t. linear combinations  $\tilde{x}_k$  of the transmit symbols is applied. The remaining interference is resolved via the inverse of the integer matrix  $\mathbf{Z}$ , resulting in estimates  $\hat{x}_k$  of the original transmit symbols.

linear channel equalization according to the zero-forcing (ZF) or the minimum mean-square error (MMSE) criterion does not achieve a satisfactory performance since it does not exploit the MIMO channel's (spatial) diversity, see, e.g., [12], [70].

In contrast, the concepts of *lattice-reduction-aided* (LRA) linear equalization [14], [15], [18] and the closely related integer-forcing (IF) linear equalization [21] are suited in order to achieve the receive diversity of the MIMO channel [20], see also the discussion below. In the following, a universal description thereof is provided that enables a lattice-based channel equalization over all above-mentioned integer rings  $\mathbb{I}$ . To that end, please note that both the LRA and the IF receiver share the same equalization task; they only differ in the way the integer interference is treated in combination with the channel code, see [19] or the section on soft-decision decoding given below.

The generalized concept is described as follows: The transmit symbols  $x_1, \dots, x_K$  are chosen from a subset  $\mathcal{A}$  of the integer ring  $\mathbb{I}$ . Then, as illustrated in Fig. 11, the channel matrix  $\mathbf{H}$  is *not directly* equalized by its pseudoinverse<sup>14</sup>  $\mathbf{H}^+$ . Instead, a *transformed* channel  $\mathbf{H}_{\text{tra}}$  is first handled via the  $K \times N$  filter matrix  $\mathbf{F} = [\mathbf{f}_1^H, \dots, \mathbf{f}_K^H]^H$  with the rows  $\mathbf{f}_1, \dots, \mathbf{f}_K$ . Assuming the ZF criterion, the filter matrix is obtained as<sup>15</sup> [19], [20]

$$\mathbf{F}^H = \mathbf{H}_{\text{tra}}^{+H} = \mathbf{H}^{+H} \underbrace{\mathbf{Z}^H}_{\mathbf{T}}, \quad (77)$$

where the transformation is expressed by the *integer matrix*  $\mathbf{T} \in \mathbb{I}^{K \times K}$ . In particular, the matrix  $\mathbf{F}$  *shapes* the interference in such a way that only *integer interference* is left before decoding—this integer interference is particularly expressed by the integer matrix  $\mathbf{Z} = \mathbf{T}^H \in \mathbb{I}^{K \times K}$  and finally reversed via the matrix  $\mathbf{Z}^{-1} = \mathbf{T}^{-H}$  as illustrated in Fig. 11.

In (77), the transformation matrix  $\mathbf{T}$  (and, thus,  $\mathbf{Z}$ ) should be chosen in a way that the row norms of  $\mathbf{F}$  are minimized. In the presence of additive white Gaussian noise with the variance  $\sigma_n^2$ , they determine the *noise variances*

$$\sigma_{n,k}^2 = \|\mathbf{f}_k\|^2 \cdot \sigma_n^2, \quad k = 1, \dots, K, \quad (78)$$

and, thus, the individual signal-to-noise ratios (SNRs) and the related mean-square errors (MSEs) before decoding. In order to minimize the MSEs, the ZF criterion applied in (77) is

<sup>14</sup>The  $K \times N$  (left) pseudoinverse of an  $N \times K$  matrix  $\mathbf{G}$  is calculated as  $\mathbf{G}^+ = (\mathbf{G}^H \mathbf{G})^{-1} \mathbf{G}^H$ . If  $N = K$ ,  $\mathbf{G}^+ = \mathbf{G}^{-1}$ . The Hermitian of  $\mathbf{G}^+$  is denoted as  $\mathbf{G}^{+H} = (\mathbf{G}^+)^H$ , and as  $\mathbf{G}^{-H}$  if  $\mathbf{G}$  is a square matrix.

<sup>15</sup>The lattice spanned by  $\mathbf{G} = \mathbf{H}^{+H}$  is the lattice which is *dual* to the one spanned by  $\mathbf{G} = \mathbf{H}$ , cf. [19], [25], [66].

not the optimum strategy. They can be lowered by employing the *MMSE criterion*. To this end, the matrices in (77) can be replaced by their *augmented ones* [17], [71] according to [19], [44]

$$\mathcal{F}^H = \mathcal{H}_{\text{tra}}^{+H} = \underbrace{\begin{bmatrix} \mathbf{H} \\ \frac{\sigma_n}{\sigma_x} \mathbf{I}_K \end{bmatrix}^{+H}}_{\mathcal{H}^{+H}} \underbrace{\mathbf{Z}^H}_{\mathbf{T}}, \quad (79)$$

where  $\mathcal{H}$  denotes the  $(N+K) \times K$  augmented channel matrix in which the (square root of the) *inverse SNR* is incorporated.<sup>16</sup> The filter matrix  $\mathbf{F}$  for MMSE linear equalization is then given as the  $K \times N$  *left part* of the  $K \times (N+K)$  *augmented filter matrix*  $\mathcal{F}$ , and the noise variances in (78) are determined by the (complete) rows of  $\mathcal{F}$  instead of  $\mathbf{F}$  [2].

The crucial performance criterion is usually the *worst-link SNR*, i.e., the lowest SNR among the  $K$  data streams *before decoding*. It dominates the error curves in case of uncoded transmission (spatial *diversity order* [12]) as well as the coded performance expressed in achievable bit rate according to Shannon [21]. Considering the worst-link SNR as the performance criterion and applying the MMSE criterion according to (79), the optimization problem reads

$$\underbrace{\mathbf{Z}}_{\mathbf{T}^H} = \underset{\mathbf{Z} \in \mathbb{I}^{K \times K}}{\text{argmin}} \max_{k=1, \dots, K} \left\{ \|\underbrace{\mathcal{H}^{+H}}_{\mathbf{G}} \mathbf{z}_k^H\|^2 \right\}, \quad (80)$$

where the rows of  $\mathbf{Z}$  correspond to the columns of its Hermitian matrix  $\mathbf{Z}^H = [\mathbf{z}_1^H, \dots, \mathbf{z}_K^H]$ .

In the initial publications on lattice-based equalization [14], [15], see also [18], the integer matrix  $\mathbf{Z}$  from (80) is restricted to the set of unimodular matrices, i.e.,  $\det(\mathbf{Z}^H \mathbf{Z}) = 1$ , in order to ensure the existence of an inverse matrix  $\mathbf{Z}^{-1} \in \mathbb{I}^{K \times K}$  for integer equalization. Then, (80) corresponds to the SBP as defined in (33) which can be solved (approximately) by lattice-basis-reduction algorithms like the LLL one.

However, this unimodularity constraint is actually not required [19], [21]. If  $\mathbf{Z}$  describes a *full-rank integer linear combination* of the transmit symbols, i.e., if the constraint  $\text{rank}(\mathbf{Z}) = K$  is imposed,  $\mathbf{G} = \mathcal{F}^H$  may only define a *sublattice* of  $\mathbf{G} = \mathcal{H}^{+H}$ , cf. Sec. II-C. Hence, after linear equalization via  $\mathbf{F}$ , the vector of linear combinations of the transmit symbols,  $\mathbf{Z}\mathbf{x}$ , may be drawn from a *subspace* of  $\mathbb{I}^K$ . Nevertheless, only valid lattice points are obtained. Using a suited lattice-decoding strategy, the linear combinations can still successfully be reconstructed, and the non-unimodular relaxation does not impair the equalization approach. Consequently, the SIVP (40) has to be solved w.r.t. the generator matrix  $\mathbf{G} = \mathcal{H}^{+H}$ . As discussed in Sec. III, this is optimally performed by the calculation of the successive-minima vectors.

#### D. Diversity Orders and Asymptotic Rates

The *diversity order* describes the slope of the symbol error curve of *uncoded* transmission if *the average over all possible*

<sup>16</sup>Instead of using the augmented matrix  $\mathcal{H}$ , often the Cholesky square root  $\mathbf{L}^H$  of  $\mathbf{L}\mathbf{L}^H = (\mathbf{H}^H \mathbf{H} + \sigma_n^2 / \sigma_x^2)$  is applied to calculate the MMSE variant of the channel transformation in (77). Both approaches are equivalent since  $\mathcal{H}$  is an alternative square-root of  $\mathbf{L}\mathbf{L}^H$  [2], [19].



*channel realizations and users* is considered. Given the symbol error ratio (SER) over the SNR  $\sigma_x^2/\sigma_n^2$ , it is defined as [12]

$$\Delta = - \lim_{\frac{\sigma_x^2}{\sigma_n^2} \rightarrow \infty} \frac{\log_{10} \text{SER}}{\log_{10} \left( \frac{\sigma_x^2}{\sigma_n^2} \right)}. \quad (81)$$

Hence, the SER drops by  $\Delta$  decades per 10 dB SNR increase.

It has been proven in [20] that LRA equalization exploits the MIMO channel's receive diversity. To this end, a bound on the product of the norms of the basis vectors over the volume has to exist. According to Theorem 6, this property is fulfilled for all (generalized) variants of LLL reduction and the related successive-minima vectors.

The achievable receive diversity can be generalized to

$$\Delta_{\text{rec}} = \frac{D_r}{2} N, \quad (82)$$

where  $D_r = 1$  is valid for real,  $D_r = 2$  for complex, and  $D_r = 4$  for quaternionic Gaussian MIMO channels. As a consequence, the diversity is doubled for quaternionic channels in comparison to complex ones. This can either be derived from the fact that the number of independent Gaussian random variables per scalar coefficient is doubled as well [72], or from the point of view that its equivalent complex-valued MIMO representation (76) actually forms an Alamouti code—if the complex channel gains are independent in both planes, the diversity in the Alamouti scheme is doubled [35], see also the discussion in [69].

The *asymptotic (bit) rate* often serves as a quantity for quality assessment in *coded transmission*. It describes the maximum bit rate *for the worst-case user*<sup>17</sup> and *one particular channel realization*. In the LRA/IF setting, it is given as the Shannon capacity for an infinite-dimensional modulo channel [21], [73]. In the setup at hand, it is universally expressed by

$$R = \frac{D_r}{2} \max_{k=1, \dots, K} \log_2 \left( \frac{\sigma_x^2}{\|\mathbf{f}_k\|^2 \cdot \sigma_n^2} \right). \quad (83)$$

### E. Lattice Constellations and Soft-Decision Decoding

We briefly review different types of lattice constellations, i.e., finite subsets  $\mathcal{A} \subset \mathbb{I}$  that are used as signal sets in lattice-based MIMO transmission, including their properties and gains.

In complex transmission, most often QAM constellations are employed that form (shifted) subsets of  $\mathcal{G}$ . Besides, especially in optical communications, *dual-polarized QAM* [31] is popular which corresponds to (shifted) subsets of  $\mathcal{L}$  if interpreted over quaternion space. Alternatively, lattice-based constellations can be defined as  $\mathcal{A} \subset \mathcal{E}$  [2], [28], [41], [42] and  $\mathcal{A} \subset \mathcal{H}$  [1], [31], [68], [74]–[76], respectively. Since these rings constitute denser packings than their related  $\mathbb{Z}^{D_r}$ -based ones, the number of signal points within a certain hypervolume is increased, i.e., a *packing gain* is achieved. This gain can either be used to increase the cardinality (data rate) keeping the SNR fixed, or to lower the SNR (constellation's variance) for a fixed cardinality/rate. Noteworthy, in LRA/IF equalization, this

packing gain directly adds up to the SNR gain obtained from solving the SBP/SMP over the particular ring  $\mathbb{I}$  (*factorization or equalization gain*), cf. Sec. IV.

The packing gain has to be distinguished from the *shaping gain* that is present if the finite constellation is not bounded by a hypercube but by other geometric shapes like a hexagonal Voronoi cell or even hyperspheres. This gain does, in general, not depend on the particular signal lattice  $\mathbb{I}$  (and is not even restricted to lattice-based constellations). It additionally adds up to the other two gains mentioned above.

If lattice-based equalization is combined with hard-decision decoding, no additional constraint on the (lattice) constellation is imposed; the decoding operation in Fig. 11 is realized by the quantization  $Q_{\mathbb{I}}\{\cdot\}$  followed by the decoding algorithm after integer equalization. The situation changes when soft-decision decoding is applied: in the LRA/IF receiver, linear combinations of transmit symbols have to be decoded directly, see also [2], [19], [21]. Two different strategies have been derived to handle this situation: As initially proposed in the IF concept [21], an isomorphism can be established between the constellation points and the code symbols. It is enabled by *p-ary algebraic constellations*,  $p$  prime, that are constructed by a special interaction between signal lattice and shaping region (see above). Such constellations have been proposed and assessed over Gaussian and Eisenstein integers in [2], [24], [30], [41]. Moreover, first results on Hurwitz-based algebraic constellations are available [74]–[76]. An alternative approach is based on a special kind of multilevel-coding scheme [77], [78] in which the addition of Gaussian integers corresponds to the addition with carry over binary arithmetic [78] and the addition of Eisenstein integers to the addition with carry over ternary arithmetic [79]. An adaption to other rings like the Hurwitz integers is still an open point.

### F. Numerical Evaluation and Comparison

The performance of the generalized lattice algorithms in the MIMO uplink scenario is finally assessed by means of numerical simulations. To this end,  $10^6$  i.i.d. complex and quaternionic Gaussian *channel matrices* have been generated according to (73) and (75), respectively. Please note that—in contrast to the numerical evaluations in Sec. IV-D—those matrices do not directly form the generator matrices of the lattices to be considered. Instead, since we assume that the MMSE criterion is applied and that the filter matrix is calculated as defined in (79), the generator matrices are given by the pseudoinverses of the respective augmented channel matrices (*MMSE dual-lattice approach*, cf. [19]). Hence, the statistical distributions differ from the straightforward evaluation of i.i.d. Gaussian matrices. The channel equalization is performed using the LRA/IF receiver as explained in Sec. V-C. For all kinds of LLL reduction, the optimal quality parameter  $\delta = 1$  is assumed once again.

1) *Symbol Error Ratios in Uncoded Transmission*: We start with the assessment of the different SERs which are obtained in case of uncoded transmission. These curves are not only relevant in terms of the quality of the different lattice algorithms, but are also suited to evaluate the different diversity

<sup>17</sup>If all users are assumed/forced to employ the same channel code and the same signal constellation, they usually share the same rate, see, e.g., [21].

behavior, cf. Sec. V-D. In order to simulate a block-fading environment, bursty transmissions with  $10^3$  symbols/noise samples per channel matrix have been performed. Due to uncoded transmission, the decoders in Fig. 11 are realized by the quantization to the particular integer ring  $\mathbb{I}$ , see above. The data symbols are finally estimated by an ML decision based on the signal constellation  $\mathcal{A}$ . Please note that we focus on the comparison of the *equalization performance*, i.e., we are not interested in shaping or packing gains obtained by different constellations. Since, in the comparisons, all constellations possess the same variance  $\sigma_x^2$ , all gains are enabled by a superior performance of the algorithms given particular rings.

First, we restrict to the complex-valued case. For lattices defined over the Gaussian integers, the zero-mean 4-ary QAM constellation  $\mathcal{A}_G = \{\pm 1 \pm i\} \subset \mathcal{G}$  with variance  $\sigma_x^2 = 2$  has been employed. Since its components are independent, they can individually be processed using the equivalent real-valued representation according to (3), i.e., if algorithms over  $\mathbb{Z}$  are considered.<sup>18</sup> Hence, the same constellation is present in both representations. Unfortunately,  $\mathcal{A}_G \not\subset \mathcal{E}$ , i.e., we cannot employ this constellation for lattices over  $\mathcal{E}$  any more. Thus, the zero-mean signal constellation  $\mathcal{A}_E = \{1, -1, \sqrt{3}i, -\sqrt{3}i\}$ , with  $\sigma_x^2 = 2$ , has been used. Since both signal constellations possess the same variance, a fair comparison is enabled, i.e., a packing or shaping gain is not present.

In Fig. 12 (Top), the SER is plotted over the SNR for complex transmission and two scenarios with  $N = K = 4$  and  $N = K = 8$ , respectively. The expected diversity orders  $\Delta_{\text{rec}} = 4$  and  $\Delta_{\text{rec}} = 8$  are clearly visible. If  $N = K = 4$ , all curves are still quite similar. However, in the high-SNR regime, the use of the Eisenstein lattice may even be disadvantageous. This is due to the fact that the application of the particular algorithms yields almost the same result since the dimensions are low, i.e., nearly the same (maximum) noise enhancement is present over  $\mathcal{G}$  and  $\mathcal{E}$ . However, the quantization to  $\mathcal{E}$  results in a higher probability for false quantization due to six nearest neighbors instead of four (cf. Sec. II). In coded transmission, this effect becomes irrelevant. Regarding the case  $N = K = 8$ , the decreased maximum noise enhancement for  $\mathcal{E}$  is now the dominating part. It has a positive impact such that a horizontal (SNR) gain is achieved if the ELLL algorithm is applied or if the respective successive-minima vectors are calculated. In summary, as expected from the results provided in Sec. IV, the potential gains increase with the dimensions even though the statistical model slightly differs from a Gaussian one (MMSE dual-lattice approach (79)).

Next, we consider the case of quaternion-valued transmission. To this end, the 16-ary constellation  $\mathcal{A}_L = \{\pm 1 \pm i \pm j \pm k\}$  (4QAM per complex component) with  $\sigma_x^2 = 4$  has been employed for which  $\mathcal{A}_L \subset \mathcal{L} \simeq \mathcal{G}^2 \simeq \mathbb{Z}^4$  as well as  $\mathcal{A}_L \subset \mathcal{H}$  are valid, since  $\mathcal{L} \subset \mathcal{H}$ . Hence, this constellation can be used in combination with lattices over  $\mathcal{L}$ ,  $\mathcal{H}$ ,  $\mathcal{G}$ , and  $\mathbb{Z}$ . The related SER curves are illustrated in Fig. 12 (Bottom) for two particular scenarios with  $N = K = 2$  and  $N = K = 4$ .

<sup>18</sup>Please note that, in this work, one symbol error is always defined w.r.t. the original complex or quaternion-valued signal constellation  $\mathcal{A}$ .

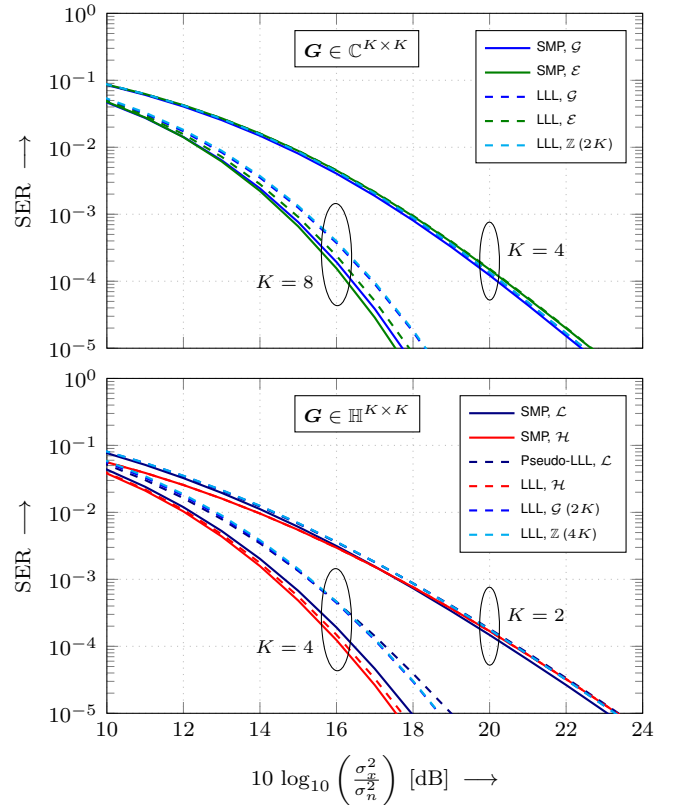


Fig. 12. Symbol error ratio over the SNR in dB for  $K \times K$  uncoded MIMO uplink transmission and LRA/IF equalization (MMSE criterion) over different integer rings and algorithms obtained by numerical simulations. For LLL reduction, the optimal parameter  $\delta = 1$  is assumed. Top: complex-valued transmission with the signal constellations  $\mathcal{A}_G = \{\pm 1 \pm i\}$  and  $\mathcal{A}_E = \{1, -1, \sqrt{3}i, -\sqrt{3}i\}$ . Bottom: quaternion-valued transmission with the constellation  $\mathcal{A}_L = \{\pm 1 \pm i \pm j \pm k\}$ .

First, we see that, in accordance with (82), the diversity orders are the same as in Fig. 12 (Top), even though the dimensions  $K$  are halved. For  $N = K = 2$ , the curves are again quite the same. Moreover, we also have the effect that the quantization to  $\mathcal{H}$  may be more erroneous than the one to  $\mathcal{L}$  due to the increased number of nearest neighbors (24 instead of 8). In contrast, for  $N = K = 4$ , the Hurwitz lattice achieves a significant gain over  $\mathcal{L}$ , or its complex and real-valued equivalents, which perform nearly the same if applied in combination with LLL reduction. The pseudo-LLL reduction shows the worst performance. However—even though respective theoretical bounds cannot be derived—it still seems to approach the same diversity behavior in practice.

2) *Bit Rates in Coded Transmission:* Finally, the performance is assessed w.r.t. coded transmission for which the rate according to (83)—depending on the particular noise enhancement (maximum squared norm) and the SNR—is the relevant quantity. In Fig. 13, both the expectations and the 0.01-quantiles of the achievable rates are illustrated, assuming  $\sigma_x^2/\sigma_n^2 \hat{=} 20$  dB (MMSE criterion). In particular, the latter represent the rates for which an outage of 1% can be expected.

In the complex-valued case (Fig. 13 (Top)), it is visible that the use of lattices over Eisenstein integers enables a slight gain w.r.t. the achievable rate, which increases with the dimensions



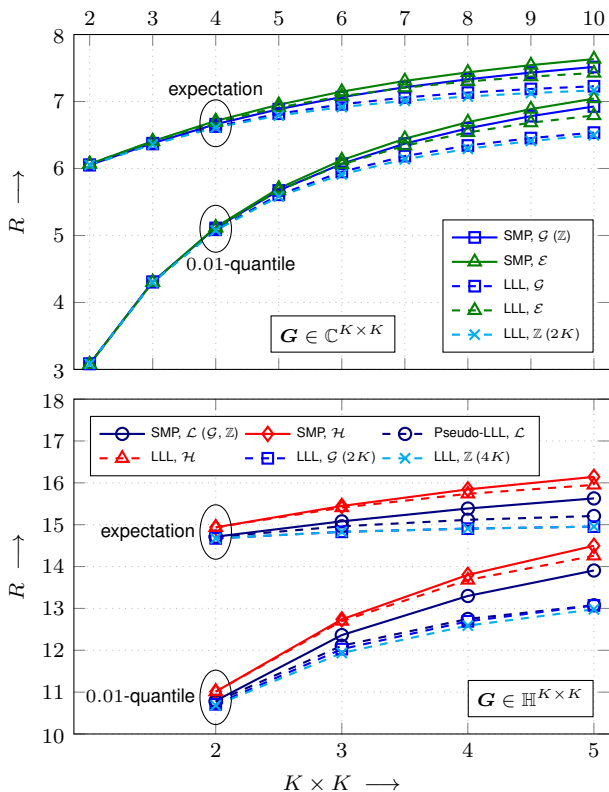


Fig. 13. Achievable rates for lattice-based linear equalization according to (83) in coded transmission ( $\sigma_x^2/\sigma_n^2 \cong 20$  dB, MMSE criterion) over the  $K \times K$  MIMO channel for different integer rings and algorithms obtained by numerical simulations. Both the expectations and the 0.01-quantiles are shown. Top: complex-valued transmission. Bottom: quaternion-valued transmission.

in accordance with Sec. IV. Just like in the numerical analysis of the maximum norms in Fig. 5 for i.i.d. Gaussian matrices, the RLLL algorithm performs the worst.

In quaternion-valued transmission (Fig. 13 (Bottom)), lattices over Hurwitz integers significantly enhance the achievable rates. The QLLL reduction over  $\mathcal{H}$  approximates the solutions to the SMP quite well. Moreover, it is quite interesting that—by analogy with the curves in Fig. 5—the pseudo-QLLL reduction over  $\mathcal{L}$  performs substantially better than its complex or real-valued “genuine” counterparts. Hence, in practice, its usage may be taken into account—even though no theoretical performance guarantees can be given.

Summarizing the above observations, we can conclude that the main results from Sec. IV also hold for the channel model at hand. This especially concerns the potential gains which increase with the dimensions of the MIMO channel. In addition, by performing a related complexity analysis, one would obtain results almost identical to the ones provided in Figs. 7 and 8.

## VI. SUMMARY AND OUTLOOK

In this paper, algorithms and bounds known from the field of *real-valued* lattice problems have been generalized and adapted to operate over complex and quaternion numbers. To this end, a review of the particular arithmetic and the properties

of these number sets has been given first. Then, generalized variants of LLL reduction and a list-based algorithm to determine the successive minima of a lattice have been given. In addition to lattices over the set of (real-valued) integers  $\mathbb{Z}$ , they can operate over the Gaussian (complex integers) as well as the Eisenstein integers for the complex case, and the Lipschitz as well as the Hurwitz integers for the quaternion-valued case. For all of these integers sets, bounds on the length of the first basis vector obtained from LLL reduction as well as on the first successive minimum have been derived. These bounds were complemented by bounds for the particular orthogonality defects, incorporating all basis or successive-minima vectors. The provided results indicate that lattices over the Eisenstein integers (instead of the Gaussian integers) may be beneficial in the complex-valued case, and that lattices over the Hurwitz integers (instead of the Lipschitz integers) may be of advantage in the quaternion-valued case. When running the presented successive-minima algorithm over these rings, the expected complexity is only increased a little bit in comparison to their counterparts. Moreover, when the LLL reduction is applied over these complex or quaternion-valued integer rings, the expected complexity is significantly decreased in comparison to an equivalent real-valued reduction. Finally, particular application scenarios have been identified. These considerations included their use in the field of MIMO communications, in particular in lattice-based equalization for the MIMO uplink channel, where gains can be expected if lattices and related constellations over Eisenstein and Hurwitz integers, respectively, are employed.

Future work could deal with the extension to the multi-dimensional, e.g., the eight-dimensional case, in which several time steps or frequencies could be combined to one symbol. In addition, the adaption of other criteria/algorithms for lattice basis reduction, e.g., HKZ [4] or Minkowski [5] reduction, could be studied and related bounds could be derived for the complex and/or quaternion-valued case. Moreover, since algebraic constellations are required for the use in the IF concept, the initial work on four-dimensional ones in [74]–[76] could be extended to derive constellations similar to the complex ones in [2], [24], [30], [41]. The same holds for quaternionic multilevel-coding schemes similar to [77]–[79]. Besides, a deeper analysis of the pseudo-QLLL algorithm and related bounds could be given and other non-Euclidean rings or algebraic structures similar to [42] be studied.

## APPENDIX A

### HELPER FUNCTIONS FOR THE LIST-BASED DETERMINATION OF THE SUCCESSIVE MINIMA

In this appendix, some procedures are listed which are incorporated in Algorithm 5 (determination of the successive minima).

Algorithm 6 creates the equivalent real-valued representation of the generator matrix  $\mathbf{G}$  depending on the integer ring  $\mathbb{I}$ . These representations have been derived in Sec. II.

In Algorithm 7, the candidate integer vectors are reconverted from the equivalent real-valued representation to the representation in the particular ring  $\mathbb{I}$ . To this end, for the Gaussian

**Algorithm 6** Equivalent Real-Valued Representation over  $\mathbb{Z}$ .

---

```

 $\mathbf{G}_{r,\mathbb{I}} = \text{RINGTOZ}(\mathbf{G}, \mathbb{I})$ 
1: switch  $\mathbb{I}$  do
2:   case  $\mathbb{Z}$ 
3:      $\mathbf{G}_{r,\mathbb{I}} = \mathbf{G}$ 
4:   case  $\mathcal{G}$ 
5:      $\mathbf{G}_{r,\mathbb{I}} = \begin{bmatrix} \mathbf{G}^{(1)} & -\mathbf{G}^{(2)} \\ \mathbf{G}^{(2)} & \mathbf{G}^{(1)} \end{bmatrix}$ 
6:   case  $\mathcal{E}$ 
7:      $\mathbf{G}_{r,\mathbb{I}} = \begin{bmatrix} \mathbf{G}^{(1)} & -\mathbf{G}^{(2)} \\ \mathbf{G}^{(2)} & \mathbf{G}^{(1)} \end{bmatrix} \begin{bmatrix} \mathbf{I}_K & -\frac{1}{2}\mathbf{I}_K \\ \mathbf{0}_K & \frac{\sqrt{3}}{2}\mathbf{I}_K \end{bmatrix}$ 
8:   case  $\mathcal{L}$ 
9:      $\mathbf{G}_{r,\mathbb{I}} = \begin{bmatrix} \mathbf{G}^{(1)} & -\mathbf{G}^{(2)} & -\mathbf{G}^{(3)} & -\mathbf{G}^{(4)} \\ \mathbf{G}^{(2)} & \mathbf{G}^{(1)} & -\mathbf{G}^{(4)} & \mathbf{G}^{(3)} \\ \mathbf{G}^{(3)} & \mathbf{G}^{(4)} & \mathbf{G}^{(1)} & -\mathbf{G}^{(2)} \\ \mathbf{G}^{(4)} & -\mathbf{G}^{(3)} & \mathbf{G}^{(2)} & \mathbf{G}^{(1)} \end{bmatrix}$ 
10:  case  $\mathcal{H}$ 
11:     $\mathbf{G}_{r,\mathbb{I}} = \begin{bmatrix} \mathbf{G}^{(1)} & -\mathbf{G}^{(2)} & -\mathbf{G}^{(3)} & -\mathbf{G}^{(4)} \\ \mathbf{G}^{(2)} & \mathbf{G}^{(1)} & -\mathbf{G}^{(4)} & \mathbf{G}^{(3)} \\ \mathbf{G}^{(3)} & \mathbf{G}^{(4)} & \mathbf{G}^{(1)} & -\mathbf{G}^{(2)} \\ \mathbf{G}^{(4)} & -\mathbf{G}^{(3)} & \mathbf{G}^{(2)} & \mathbf{G}^{(1)} \end{bmatrix} \cdot \begin{bmatrix} \mathbf{I}_K & \mathbf{0}_K & \mathbf{0}_K & \frac{1}{2}\mathbf{I}_K \\ \mathbf{0}_K & \mathbf{I}_K & \mathbf{0}_K & \frac{1}{2}\mathbf{I}_K \\ \mathbf{0}_K & \mathbf{0}_K & \mathbf{I}_K & \frac{1}{2}\mathbf{I}_K \\ \mathbf{0}_K & \mathbf{0}_K & \mathbf{0}_K & \frac{1}{2}\mathbf{I}_K \end{bmatrix}$ 
12: end switch

```

---

and the Lipschitz integers, the components are simply stacked in the matrix  $C$ . For the Eisenstein and the Hurwitz integers, the particular generator matrices according to (29) and (30), respectively, have to be incorporated first.

In Algorithm 8, the matrix of candidate vectors  $C$  is transformed to row-echelon form. To this end, for each candidate with the index  $l$ , it is checked if a new dimension is established. This is the case when one of the elements  $c_{k,l}, \dots, c_{K,l}$  is not zero; then, the vector does not depend on the previous ones. Given that case, the particular row with the non-zero element is interchanged with the row  $k$ . After normalization<sup>19</sup> to  $c_{k,l} = 1$ , all other elements  $c_{k+1,l}, \dots, c_{K,l}$  are set to zero by subtracting  $c_{n,l}$  times the row with index  $k$ . All multiplications are performed in such a way that the skew-field property of quaternions is taken into account.

## APPENDIX B

## COMPARISON OF THE UPPER BOUND ON THE FIRST VECTOR NORM FOR DIFFERENT LLL VARIANTS

In this appendix, the upper bound on the squared length of the first basis vector in case of LLL reduction as described in Sec. IV-A2 is compared for different Euclidean integer rings.

<sup>19</sup>Please note that linearly independent lattice vectors are required, i.e., independent vectors have to be present over  $\mathbb{R}$ ,  $\mathbb{C}$ , or  $\mathbb{H}$ . Hence, when calculating the row-echelon form for the integer vectors, non-integer elements may occur. Nevertheless, these non-integer elements are not relevant since only the “steps” within the row-echelon form are of interest. Alternatively, the calculation of the row-echelon form can directly be performed with the related lattice vectors.

**Algorithm 7** Reconversion from Representation over  $\mathbb{Z}$ .

---

```

 $\mathbf{C}_u = \text{ZTORING}(\mathbf{C}, \mathbb{I})$ 
1: switch  $\mathbb{I}$  do
2:   case  $\mathbb{Z}$ 
3:      $\mathbf{C}_u = \mathbf{C}$ 
4:   case  $\mathcal{G}$ 
5:      $\mathbf{C}_u^{(1)} = \mathbf{C}_{1:K,1:N_c}$ 
6:      $\mathbf{C}_u^{(2)} = \mathbf{C}_{K+1:2K,1:N_c}$ 
7:   case  $\mathcal{E}$ 
8:      $\tilde{\mathbf{C}} = \begin{bmatrix} \mathbf{I}_K & -\frac{1}{2}\mathbf{I}_K \\ \mathbf{0}_K & \frac{\sqrt{3}}{2}\mathbf{I}_K \end{bmatrix} \cdot \mathbf{C}$ 
9:      $\mathbf{C}_u^{(1)} = \tilde{\mathbf{C}}_{1:K,1:N_c}$ 
10:     $\mathbf{C}_u^{(2)} = \tilde{\mathbf{C}}_{K+1:2K,1:N_c}$ 
11:  case  $\mathcal{L}$ 
12:     $\mathbf{C}_u^{(1)} = \mathbf{C}_{1:K,1:N_c}$ 
13:     $\mathbf{C}_u^{(2)} = \mathbf{C}_{K+1:2K,1:N_c}$ 
14:     $\mathbf{C}_u^{(3)} = \mathbf{C}_{2K+1:3K,1:N_c}$ 
15:     $\mathbf{C}_u^{(4)} = \mathbf{C}_{3K+1:4K,1:N_c}$ 
16:  case  $\mathcal{H}$ 
17:     $\tilde{\mathbf{C}} = \begin{bmatrix} \mathbf{I}_K & \mathbf{0}_K & \mathbf{0}_K & \frac{1}{2}\mathbf{I}_K \\ \mathbf{0}_K & \mathbf{I}_K & \mathbf{0}_K & \frac{1}{2}\mathbf{I}_K \\ \mathbf{0}_K & \mathbf{0}_K & \mathbf{I}_K & \frac{1}{2}\mathbf{I}_K \\ \mathbf{0}_K & \mathbf{0}_K & \mathbf{0}_K & \frac{1}{2}\mathbf{I}_K \end{bmatrix} \cdot \mathbf{C}$ 
18:     $\mathbf{C}_u^{(1)} = \tilde{\mathbf{C}}_{1:K,1:N_c}$ 
19:     $\mathbf{C}_u^{(2)} = \tilde{\mathbf{C}}_{K+1:2K,1:N_c}$ 
20:     $\mathbf{C}_u^{(3)} = \tilde{\mathbf{C}}_{2K+1:3K,1:N_c}$ 
21:     $\mathbf{C}_u^{(4)} = \tilde{\mathbf{C}}_{3K+1:4K,1:N_c}$ 
22: end switch

```

---

**Algorithm 8** Transformation to Row-Echelon Form.

---

```

 $\mathbf{i} = \text{ROWECHOLON}(\mathbf{C})$ 
1:  $k = 1, l = 1, \mathbf{i} = [0, \dots, 0]$ 
2: while  $k \leq K$  do
3:   for  $m = k, \dots, K$  do
4:     if  $c_{m,l} \neq 0$  then
5:        $i_k = l$ 
6:        $\tilde{\mathbf{c}} = \mathbf{C}_{k,1:N_c}$ 
7:        $\mathbf{C}_{k,1:N_c} = \mathbf{C}_{m,1:N_c}$ 
8:        $\mathbf{C}_{m,1:N_c} = \tilde{\mathbf{c}}$ 
9:        $\mathbf{C}_{k,1:N_c} = c_{k,l}^{-1} \cdot \mathbf{C}_{k,1:N_c}$ 
10:      for  $n = k+1, \dots, K$  do
11:         $\mathbf{C}_{n,1:N_c} = \mathbf{C}_{n,1:N_c} - c_{n,l} \mathbf{C}_{k,1:N_c}$ 
12:      end for
13:       $k = k + 1$ 
14:      break
15:    end if
16:  end for
17:   $l = l + 1$ 
18: end while

```

---

## A. Derivation of Corollary 1

We start with the derivation of Corollary 1. It contains a generalized variant of the comparison between RLLL and CLLL algorithm that has been given in [40].

Considering the upper bound in (47), we can first state that its right-hand part,  $\text{vol}^{\frac{2}{K}}(\mathbf{\Lambda}(\mathbf{G}))$ , is irrelevant for the comparison of all considered LLL variants since  $\text{vol}^{\frac{2}{2K}}(\mathbf{\Lambda}(\mathbf{G}_r)) = \text{vol}^{\frac{2}{K}}(\mathbf{\Lambda}(\mathbf{G}))$  holds for the  $2N \times 2K$  real-valued representation of complex matrices and  $\text{vol}^{\frac{2}{4K}}(\mathbf{\Lambda}(\mathbf{G}_r)) = \text{vol}^{\frac{2}{2K}}(\mathbf{\Lambda}(\mathbf{G}_c)) = \text{vol}^{\frac{2}{K}}(\mathbf{\Lambda}(\mathbf{G}))$  for the  $4N \times 4K$  real-valued and the  $2N \times 2K$  complex-valued representations of quaternionic matrices.

Hence, given the first LLL variant with the maximum squared quantization error  $\epsilon_1^2$  that operates on a matrix of rank  $K_1$ , and the second variant with the error  $\epsilon_2^2$  operating over a matrix of rank  $K_2$ , the first one performs better if

$$\frac{(\delta - \epsilon_2^2)^{K_2-1}}{(\delta - \epsilon_1^2)^{K_1-1}} < 1 \quad (84)$$

since both terms within the braces are positive.

### B. Complex Matrices

Based on Corollary 1, the different LLL variants can be compared in an asymptotic manner. We start with the comparison given complex generator matrices  $\mathbf{G} \in \mathbb{C}^{N \times K}$ .

When comparing the ELLL ( $\mathbb{I} = \mathcal{E}$ ) with the CLLL ( $\mathbb{I} = \mathcal{G}$ ), we have  $K_1 = K_2$ ,  $\epsilon_1^2 = \frac{1}{3}$ , and  $\epsilon_2^2 = \frac{1}{2}$ . Hence, we obtain

$$\lim_{K_1 \rightarrow \infty} \frac{(\delta - \frac{1}{2})^{K_1-1}}{(\delta - \frac{1}{3})^{K_1-1}} < 1, \quad (85)$$

i.e., the ELLL performs better independently from  $\delta$ .

Given the CLLL ( $\mathbb{I} = \mathcal{G}$ ) and the RLLL ( $\mathbb{I} = \mathbb{Z}$ ),  $K_2 = 2K_1$ ,  $\epsilon_1^2 = \frac{1}{2}$ , and  $\epsilon_2^2 = \frac{1}{4}$ . Corollary 1 is given as

$$\frac{(\delta - \frac{1}{4})^{2K_1}}{(\delta - \frac{1}{2})^{K_1}} \cdot \underbrace{\frac{(\delta - \frac{1}{2})}{(\delta - \frac{1}{4})}}_{< 1}. \quad (86)$$

Hence, the CLLL bound is smaller if  $(\delta - \frac{1}{4})^2 < \delta - \frac{1}{2}$ . This condition is, however, never fulfilled for  $\delta \in (\frac{1}{2}, 1]$ , but at least equality can be achieved if and only if  $\delta = \frac{3}{4}$ , see also [40].

In the same way, the comparison ELLL ( $\mathbb{I} = \mathcal{E}$ ) vs. RLLL ( $\mathbb{I} = \mathbb{Z}$ ), with  $K_2 = 2K_1$ ,  $\epsilon_1^2 = \frac{1}{3}$ , and  $\epsilon_2^2 = \frac{1}{4}$  can be performed. By analogy with (86), the condition  $(\delta - \frac{1}{4})^2 < \delta - \frac{1}{3}$  is obtained. It is fulfilled if  $\frac{3}{4} - \frac{1}{\sqrt{6}} \approx 0.34 < \delta \leq 1$ .

### C. Quaternionic Matrices

We continue with the comparison for the case when quaternionic matrices  $\mathbf{G} \in \mathbb{H}^{N \times K}$  are present.

For the comparison QLLL ( $\mathbb{I} = \mathcal{H}$ ) vs. CLLL ( $\mathbb{I} = \mathcal{G}$ ), the parameters  $K_2 = 2K_1$  and  $\epsilon_1^2 = \epsilon_2^2 = \frac{1}{2}$  are given, leading to

$$\lim_{K_1 \rightarrow \infty} \frac{(\delta - \frac{1}{2})^{2K_1-1}}{(\delta - \frac{1}{2})^{K_1-1}} < 1. \quad (87)$$

Hence, independent from  $\delta$ , the QLLL gives a better result.

Comparing the QLLL ( $\mathbb{I} = \mathcal{H}$ ) with the ELLL ( $\mathbb{I} = \mathcal{E}$ ), we have  $K_2 = 2K_1$ ,  $\epsilon_1^2 = \frac{1}{2}$ , and  $\epsilon_2^2 = \frac{1}{3}$ . Hence, similar to (86), we obtain the condition  $(\delta - \frac{1}{3})^2 < \delta - \frac{1}{2}$ , which is fulfilled if  $\frac{5}{6} - \frac{1}{2\sqrt{3}} \approx 0.54 < \delta \leq 1$ .

Finally, for the comparison QLLL ( $\mathbb{I} = \mathcal{H}$ ) vs. RLLL ( $\mathbb{I} = \mathbb{Z}$ ), the parameters  $K_2 = 4K_1$ ,  $\epsilon_1^2 = \frac{1}{2}$ , and  $\epsilon_2^2 = \frac{1}{4}$  are present. Similar to above, we obtain the condition  $(\delta - \frac{1}{4})^4 < \delta - \frac{1}{2}$  that is fulfilled if  $0.504 < \delta \leq 1$ .

## APPENDIX C

### COMPARISON OF THE UPPER BOUND ON THE ORTHOGONALITY DEFECT FOR DIFFERENT LLL VARIANTS

In this appendix, the upper bound on the orthogonality defect of the basis obtained from LLL reduction (Sec. IV-B2) is asymptotically compared for different Euclidean integer rings. To this end, the inequality condition from Corollary 2

$$\frac{(\delta - \epsilon_2^2)^{K_2(K_2-1)}}{(\delta - \epsilon_1^2)^{K_1(K_1-1)}} < 1 \quad (88)$$

is analyzed that follows directly from (59) since both terms within the braces are positive. Noteworthy, the same condition also holds for the bound on the product of the basis vectors in (59) in which the volume of the lattice is additionally incorporated, see also the discussion in Appendix B.

#### A. Complex Matrices

First, the performance of different LLL variants is considered for the case when complex generator matrices  $\mathbf{G} \in \mathbb{C}^{N \times K}$  are given.

When comparing the ELLL ( $\mathbb{I} = \mathcal{E}$ ) with the CLLL ( $\mathbb{I} = \mathcal{G}$ ), with  $K_1 = K_2$ ,  $\epsilon_1^2 = \frac{1}{3}$ , and  $\epsilon_2^2 = \frac{1}{2}$ , we directly see that

$$\lim_{K_1 \rightarrow \infty} \frac{(\delta - \frac{1}{2})^{K_1(K_1-1)}}{(\delta - \frac{1}{3})^{K_1(K_1-1)}} < 1, \quad (89)$$

i.e., the ELLL performs better independently from  $\delta$ .

Given the CLLL ( $\mathbb{I} = \mathcal{G}$ ) and the RLLL ( $\mathbb{I} = \mathbb{Z}$ ),  $K_2 = 2K_1$ ,  $\epsilon_1^2 = \frac{1}{2}$ , and  $\epsilon_2^2 = \frac{1}{4}$ . Then, the term reads

$$\frac{(\delta - \frac{1}{4})^{4K_1^2}}{(\delta - \frac{1}{2})^{K_1^2}} \cdot \underbrace{\frac{(\delta - \frac{1}{2})^{K_1}}{(\delta - \frac{1}{4})^{2K_1}}}_{< 1}, \quad (90)$$

where the right part is less than or equal to one, cf. (86). The CLLL bound is lower if  $(\delta - \frac{1}{4})^4 < \delta - \frac{1}{2}$ . This condition is fulfilled for  $0.504 < \delta \leq 1$ .

The comparison ELLL ( $\mathbb{I} = \mathcal{E}$ ) vs. RLLL ( $\mathbb{I} = \mathbb{Z}$ ), with  $K_2 = 2K_1$ ,  $\epsilon_1^2 = \frac{1}{3}$ , and  $\epsilon_2^2 = \frac{1}{4}$  can be performed similar to (90). Then, for the left-hand term,  $(\delta - \frac{1}{4})^4 < \delta - \frac{1}{3}$  has to hold. However, the right-hand term is not necessarily less than one, i.e., the product of both terms will be less than one if the left one has this property and if  $(\delta - \frac{1}{4})^4 / (\delta - \frac{1}{3}) < (\delta - \frac{1}{4})^2 / (\delta - \frac{1}{3})$ . The latter condition is always true since  $\delta - \frac{1}{4} < 1$ . The left-hand one holds when  $0.3334 < \delta \leq 1$ .

#### B. Quaternionic Matrices

Finally, the bounds are compared for the case when quaternionic matrices  $\mathbf{G} \in \mathbb{H}^{N \times K}$  are present.

Comparing the QLLL ( $\mathbb{I} = \mathcal{H}$ ) with the CLLL ( $\mathbb{I} = \mathcal{G}$ ), the parameters  $K_2 = 2K_1$  and  $\epsilon_1^2 = \epsilon_2^2 = \frac{1}{2}$  result in

$$\frac{(\delta - \frac{1}{2})^{4K_1^2}}{(\delta - \frac{1}{2})^{K_1^2}} \cdot \frac{(\delta - \frac{1}{2})^{K_1}}{(\delta - \frac{1}{2})^{2K_1}}. \quad (91)$$

The QLLL generally results in a better bound: similar to above, the left-hand term is less than one; the same holds for the product of both terms due to  $(\delta - \frac{1}{2})^3 < (\delta - \frac{1}{2})$  as  $\delta - \frac{1}{2} < 1$ .

The comparison QLLL ( $\mathbb{I} = \mathcal{H}$ ) vs. ELLL ( $\mathbb{I} = \mathcal{E}$ ) is done with  $K_2 = 2K_1$ ,  $\epsilon_1^2 = \frac{1}{2}$ , and  $\epsilon_2^2 = \frac{1}{3}$ . Here, the conditions  $(\delta - \frac{1}{3})^4 < \delta - \frac{1}{2}$  and  $(\delta - \frac{1}{3})^4 < (\delta - \frac{1}{3})^2$  are obtained. The latter is true and the former is fulfilled if  $0.5008 < \delta \leq 1$ .

For the comparison QLLL ( $\mathbb{I} = \mathcal{H}$ ) vs. RLLL ( $\mathbb{I} = \mathbb{Z}$ ) with  $K_2 = 4K_1$ ,  $\epsilon_1^2 = \frac{1}{2}$ , and  $\epsilon_2^2 = \frac{1}{4}$ , the conditions read  $(\delta - \frac{1}{4})^{16} < \delta - \frac{1}{2}$  and  $(\delta - \frac{1}{4})^{16} < (\delta - \frac{1}{4})^4$ . Since the latter is again fulfilled, see above, the former is relevant. It holds if  $0.5000 < \delta \leq 1$ .

#### ACKNOWLEDGMENT

The authors would like to thank the associate editor and the anonymous reviewers for their valuable comments and suggestions that helped a lot to improve the quality of this work.

#### REFERENCES

- [1] S. Stern and R. F. H. Fischer, "Quaternion-valued multi-user MIMO transmission via dual-polarized antennas and QLLL reduction," in *25th Int. Conf. on Telecommun. (ICT)*, Saint Malo, France, Jun. 2018, pp. 63–69.
- [2] S. Stern, "Advanced equalization and coded-modulation strategies for multiple-input/multiple-output systems," Ph.D. dissertation, Ulm University, Ulm, Germany, May 2019.
- [3] C. Hermite, "Extraits de lettres de M.Ch. Hermite à M. Jacobi sur différents objets de la théorie des nombres," *Journal für die reine und angewandte Mathematik*, vol. 40, pp. 261–315, 1850.
- [4] A. N. Korkine and J. I. Zolotareff, "Sur les formes quadratiques," *Mathematische Annalen*, vol. 6, pp. 366–389, 1873.
- [5] H. Minkowski, "Über die positiven quadratischen Formen und über kettenbruchähnliche Algorithmen," *Journal für die reine und angewandte Mathematik*, vol. 107, pp. 278–297, 1891.
- [6] A. K. Lenstra, H. W. Lenstra, and L. Lovász, "Factoring polynomials with rational coefficients," *Mathematische Annalen*, vol. 261, pp. 515–534, Dec. 1982.
- [7] R. Kannan, "Improved algorithms for integer programming and related lattice problems," in *15th Annual ACM Symp. on Theory of Computing*, 1983, pp. 193–206.
- [8] C. P. Schnorr and M. Euchner, "Lattice basis reduction: Improved practical algorithms and solving subset sum problems," *Mathematical Programming*, vol. 66, no. 1, pp. 181–199, Aug. 1994.
- [9] W. Zhang, S. Qiao, and Y. Wei, "HKZ and Minkowski reduction algorithms for lattice-reduction-aided MIMO detection," *IEEE Trans. Signal Process.*, vol. 60, no. 11, pp. 5963–5976, Nov. 2012.
- [10] B. Helfrich, "Algorithms to construct Minkowski reduced and Hermite reduced lattice bases," *Theoretical Computer Science*, vol. 41, pp. 125–139, 1985.
- [11] D. Micciancio and O. Regev, *Lattice-based Cryptography*. Berlin, Heidelberg: Springer-Verlag, 2009, pp. 147–191.
- [12] D. N. Tse and P. Viswanath, *Fundamentals of Wireless Communication*. New York, NY, USA: Cambridge University Press, 2005.
- [13] E. Agrell, T. Eriksson, A. Vardy, and K. Zeger, "Closest point search in lattices," *IEEE Trans. Inf. Theory*, vol. 48, no. 8, pp. 2201–2214, Aug. 2002.
- [14] H. Yao and G. W. Wornell, "Lattice-reduction-aided detectors for MIMO communication systems," in *IEEE Global Telecomm. Conf. (GLOBECOM)*, Taipei, Taiwan, Nov. 2002, pp. 424–428.
- [15] C. Windpassinger and R. F. H. Fischer, "Low-complexity near-maximum-likelihood detection and precoding for MIMO systems using lattice reduction," in *IEEE Inf. Theory Workshop (ITW)*, Paris, France, Mar. 2003, pp. 345–348.
- [16] C. Windpassinger, "Detection and precoding for multiple input multiple output channels," Ph.D. dissertation, University of Erlangen-Nuremberg (FAU), Erlangen, Germany, 2004.
- [17] D. Wübben, R. Böhne, V. Kühn, and K.-D. Kammeyer, "Near-maximum-likelihood detection of MIMO systems using MMSE-based lattice-reduction," in *IEEE Int. Conf. on Commun. (ICC)*, vol. 2, Paris, France, Jun. 2004, pp. 798–802.
- [18] D. Wübben, D. Seethaler, J. Jaldén, and G. Matz, "Lattice reduction," *IEEE Signal Process. Mag.*, vol. 28, no. 3, pp. 70–91, May 2011.
- [19] R. F. H. Fischer, S. Stern, and J. B. Huber, "Lattice-reduction-aided and integer-forcing equalization: Structures, criteria, factorization, and coding," *Foundations and Trends® in Commun. and Inf. Theory*, vol. 16, no. 1-2, pp. 1–155, 2019.
- [20] M. Taherzadeh, A. Mobasher, and A. K. Khandani, "LLL reduction achieves the receive diversity in MIMO decoding," *IEEE Trans. Inf. Theory*, vol. 53, no. 12, pp. 4801–4805, Dec. 2007.
- [21] J. Zhan, B. Nazer, U. Erez, and M. Gastpar, "Integer-forcing linear receivers," *IEEE Trans. Inf. Theory*, vol. 60, no. 12, pp. 7661–7685, Dec. 2014.
- [22] R. F. H. Fischer, *Precoding and Signal Shaping for Digital Transmission*. New York, NY, USA: John Wiley & Sons, 2002.
- [23] H. L. Van Trees, *Detection, Estimation, and Modulation Theory: Part I—Detection, Estimation, and Filtering Theory*, 2nd ed. New York, NY, USA: Wiley, 2013.
- [24] K. Huber, "Codes over Gaussian integers," *IEEE Trans. Inf. Theory*, vol. 40, no. 1, pp. 207–216, Jan. 1994.
- [25] J. H. Conway and N. J. Sloane, *Sphere Packings, Lattices and Groups*, 3rd ed., ser. A Series of Comprehensive Studies in Mathematics. New York, NY, USA: Springer, 1999, vol. 290.
- [26] H. Jiang and S. Du, "Complex Korkine-Zolotareff reduction algorithm for full-diversity MIMO detection," *IEEE Commun. Lett.*, vol. 17, no. 2, pp. 381–384, Feb. 2013.
- [27] L. Ding, Y. Wang, and J. Zhang, "Complex Minkowski reduction and a relaxation for near-optimal MIMO linear equalization," *IEEE Wireless Commun. Lett.*, vol. 6, no. 1, pp. 38–41, Feb. 2017.
- [28] N. E. Tunali, Y.-C. Huang, J. J. Boutros, and K. R. Narayanan, "Lattices over Eisenstein integers for compute-and-forward," *IEEE Trans. Inf. Theory*, vol. 61, no. 10, pp. 5306–5321, Oct. 2015.
- [29] S. Stern and R. F. H. Fischer, "Advanced factorization strategies for lattice-reduction-aided preequalization," in *IEEE Int. Symp. on Inf. Theory (ISIT)*, Barcelona, Spain, Jul. 2016, pp. 1471–1475.
- [30] K. Huber, "Codes over Eisenstein-Jacobi integers," *Contemporary Mathematics*, vol. 168, pp. 165–165, 1994.
- [31] M. Karlsson and E. Agrell, *Multidimensional Optimized Optical Modulation Formats*. John Wiley & Sons, 2016, ch. 2, pp. 13–64.
- [32] Y. Cui, R. Li, and H. Fu, "A broadband dual-polarized planar antenna for 2G/3G/LTE base stations," *IEEE Trans. Antennas Propag.*, vol. 62, no. 9, pp. 4836–4840, Sep. 2014.
- [33] M. Li, Y. Ban, Z. Xu, G. Wu, C. Sim, K. Kang, and Z. Yu, "Eight-port orthogonally dual-polarized antenna array for 5G smartphone applications," *IEEE Trans. Antennas Propag.*, vol. 64, no. 9, pp. 3820–3830, Sep. 2016.
- [34] F. Ghaedi, J. Jamali, and M. Taghizadeh, "A wideband dual-polarized antenna using magneto-electric dipoles for base station applications," *AEU—Int. J. of Electronics and Commun.*, vol. 126, p. 153395, 2020.
- [35] S. M. Alamouti, "A simple transmit diversity technique for wireless communications," *IEEE J. Sel. Areas Commun.*, vol. 16, no. 8, pp. 1451–1458, Oct. 1998.
- [36] J. H. Conway and D. A. Smith, *On Quaternions and Octonions*. Boca Raton, FL, USA: A K Peters/CRC Press, 2003.
- [37] O. M. Isaeva and V. A. Sarytchev, "Quaternion presentations polarization state," in *2nd Topical Symp. on Combined Optical-Microwave Earth and Atmosphere Sensing*, Atlanta, GA, USA, Apr. 1995, pp. 195–196.
- [38] B. J. Wysocki, T. A. Wysocki, and J. Seberry, "Modeling dual polarization wireless fading channels using quaternions," in *Joint IST Workshop on Mobile Future and Symp. on Trends in Commun.*, Bratislava, Slovakia, Jun. 2006, pp. 68–71.
- [39] H. Napias, "A generalization of the LLL-algorithm over Euclidean rings or orders," *Journal de Théorie des Nombres de Bordeaux*, vol. 8, no. 2, pp. 387–396, 1996.
- [40] Y. H. Gan, C. Ling, and W. H. Mow, "Complex lattice reduction algorithm for low-complexity full-diversity MIMO detection," *IEEE Trans. Signal Process.*, vol. 57, no. 7, pp. 2701–2710, Jul. 2009.
- [41] S. Stern and R. F. H. Fischer, "Lattice-reduction-aided preequalization over algebraic signal constellations," in *9th Int. Conf. on Signal Process. and Commun. Systems (ICSPCS)*, Cairns, QLD, Australia, Dec. 2015.
- [42] S. Lyu, C. Porter, and C. Ling, "Lattice reduction over imaginary quadratic fields," *IEEE Trans. Signal Process.*, vol. 68, pp. 6380–6393, 2020.
- [43] L. Ding, K. Kansanen, Y. Wang, and J. Zhang, "Exact SMP algorithms for integer-forcing linear MIMO receivers," *IEEE Trans. Wireless Commun.*, vol. 14, no. 12, pp. 6955–6966, Dec. 2015.
- [44] R. F. H. Fischer, M. Cyran, and S. Stern, "Factorization approaches in lattice-reduction-aided and integer-forcing equalization," in *Int. Zurich Seminar on Commun.*, Zurich, Switzerland, Mar. 2016, pp. 108–112.

- [45] J. Wen, L. Li, X. Tang, and W. H. Mow, "An efficient optimal algorithm for the successive minima problem," *IEEE Trans. Commun.*, vol. 67, no. 2, pp. 1424–1436, Feb. 2019.
- [46] P. Nguyen and B. Vallée, *The LLL Algorithm: Survey and Applications*, ser. Information Security and Cryptography. Berlin, Heidelberg: Springer-Verlag, 2009.
- [47] P. M. Neumann, G. A. Stoy, and E. C. Thompson, *Groups and Geometry*, ser. Oxford Science Publications. Oxford, United Kingdom: Oxford University Press, 1994.
- [48] A. A. Karatsuba and Y. P. Ofman, "Multiplication of many-digit numbers by automatic computers," in *Doklady Akademii Nauk*, vol. 145, no. 2. Russian Academy of Sciences, 1962, pp. 293–294.
- [49] A. Cariow and G. Cariowa, "An unified approach for developing rationalized algorithms for hypercomplex number multiplication," *Electric Review*, vol. 91, no. 2, pp. 36–39, 2015.
- [50] H. Aslaksen, "Quaternionic determinants," *The Mathematical Intelligencer*, vol. 18, no. 3, pp. 57–65, 1996.
- [51] R. R. Müller and B. Cakmak, "Channel modelling of MU-MIMO systems by quaternionic free probability," in *IEEE Int. Symp. on Inf. Theory (ISIT)*, Cambridge, MA, USA, 2012, pp. 2656–2660.
- [52] S. H. Weintraub, *Factorization: Unique and Otherwise*, ser. CMS Treatises in Mathematics. Boca Raton, FL, USA: A K Peters/CRC Press, 2008.
- [53] T. H. Cormen, C. E. Leiserson, R. L. Rivest, and C. Stein, *Introduction to Algorithms*, ser. Computer Science. Cambridge, MA, USA: MIT Press, 2009.
- [54] M. Bossert, *Channel Coding for Telecommunications*. Chichester, United Kingdom: John Wiley & Sons, 1999.
- [55] J. Conway and N. Sloane, "Fast quantizing and decoding algorithms for lattice quantizers and codes," *IEEE Trans. Inf. Theory*, vol. 28, no. 2, pp. 227–232, Mar. 1982.
- [56] R. Zamir, B. Nazer, Y. Kochman, and I. Bistriz, *Lattice Coding for Signals and Networks: A Structured Coding Approach to Quantization, Modulation and Multiuser Information Theory*. Cambridge, United Kingdom: Cambridge University Press, 2014.
- [57] H. Daudé and B. Vallée, "An upper bound on the average number of iterations of the LLL algorithm," *Theoretical Computer Science*, vol. 123, no. 1, pp. 95–115, 1994.
- [58] W. H. Press, S. A. Teukolsky, W. T. Vetterling, and B. P. Flannery, *Numerical Recipes: The Art of Scientific Computing*, 3rd ed. Cambridge, United Kingdom: Cambridge University Press, 2007.
- [59] A. Akhavi, "The optimal LLL algorithm is still polynomial in fixed dimension," *Theoretical Computer Science*, vol. 297, no. 1, pp. 3–23, 2003.
- [60] R. F. H. Fischer, "From Gram–Schmidt orthogonalization via sorting and quantization to lattice reduction," in *Joint Workshop on Coding and Commun. (JWCC)*, Santo Stefano Belbo, Italy, Oct. 2010.
- [61] J. C. Lagarias, H. W. Lenstra, and C. P. Schnorr, "Korkin-Zolotarev bases and successive minima of a lattice and its reciprocal lattice," *Combinatorica*, vol. 10, no. 4, pp. 333–348, Dec. 1990.
- [62] H. Minkowski, "Diskontinuitätsbereich für arithmetische Äquivalenz," in *Ausgewählte Arbeiten zur Zahlentheorie und zur Geometrie, Mit D. Hilberts Gedächtnisrede auf H. Minkowski, Göttingen 1909*. Vienna, Austria: Springer, 1989, pp. 73–120.
- [63] H. F. Blichfeldt, "The minimum value of quadratic forms, and the closest packing of spheres," *Mathematische Annalen*, vol. 101, no. 1, pp. 605–608, 1929.
- [64] C. Siegel and K. Chandrasekharan, *Lectures on the Geometry of Numbers*. Berlin, Heidelberg: Springer-Verlag, 1989.
- [65] C. Ling and N. Howgrave-Graham, "Effective LLL reduction for lattice decoding," in *IEEE Int. Symp. on Inf. Theory (ISIT)*, 2007, pp. 196–200.
- [66] C. Ling, W. H. Mow, and L. Gan, "Dual-lattice ordering and partial lattice reduction for SIC-based MIMO detection," *IEEE J. Sel. Topics Signal Process.*, vol. 3, no. 6, pp. 975–985, Dec. 2009.
- [67] J. G. Proakis and M. Salehi, *Digital Communications*, 5th ed. New York, NY, USA: McGraw-Hill, 2008.
- [68] F. Frey, S. Stern, J. K. Fischer, and R. F. H. Fischer, "Two-stage coded modulation for Hurwitz constellations in fiber-optical communications," *J. Lightw. Technol.*, vol. 38, no. 12, pp. 3135–3146, Jun. 2020.
- [69] S. S. Qureshi, S. Ali, and S. A. Hassan, "Optimal polarization diversity gain in dual-polarized antennas using quaternions," *IEEE Signal Process. Lett.*, vol. 25, no. 4, pp. 467–471, Apr. 2018.
- [70] L. Zheng and D. N. Tse, "Diversity and multiplexing: A fundamental tradeoff in multiple-antenna channels," *IEEE Trans. Inf. Theory*, vol. 49, no. 5, pp. 1073–1096, May 2003.
- [71] B. Hassibi, "An efficient square-root algorithm for BLAST," in *IEEE Int. Conf. on Acoustics, Speech, and Signal Process.*, Istanbul, Turkey, Jun. 2000, pp. 737–740.
- [72] C. Stierstorfer, "A bit-level-based approach to coded multicarrier transmission," Ph.D. dissertation, University of Erlangen-Nuremberg (FAU), Erlangen, Germany, 2009.
- [73] G. D. Forney, M. D. Trott, and Sae-Young Chung, "Sphere-bound-achieving coset codes and multilevel coset codes," *IEEE Trans. Inf. Theory*, vol. 46, no. 3, pp. 820–850, May 2000.
- [74] M. Güzeltepe, "Codes over Hurwitz integers," *Discrete Mathematics*, vol. 313, no. 5, pp. 704–714, 2013.
- [75] M. Güzeltepe and O. Heden, "Perfect Mannheim, Lipschitz and Hurwitz weight codes," *Mathematical Communications*, vol. 19, no. 2, pp. 253–276, 2014.
- [76] D. Rohweder, S. Stern, R. F. Fischer, S. Shavgulidze, and J. Freudenberger, "Four-dimensional Hurwitz signal constellations, set partitioning, detection, and multilevel coding," *IEEE Trans. Commun.*, vol. 69, no. 8, pp. 5079–5090, 2021.
- [77] S. H. Chae, M. Jang, S.-K. Ahn, J. Park, and C. Jeong, "Multilevel coding scheme for integer-forcing MIMO receivers with binary codes," *IEEE Trans. Wireless Commun.*, vol. 16, no. 8, pp. 5428–5441, Aug. 2017.
- [78] R. F. H. Fischer, J. B. Huber, S. Stern, and P. M. Guter, "Multilevel codes in lattice-reduction-aided equalization," in *Int. Zurich Seminar on Inf. and Commun.*, Zurich, Switzerland, Feb. 2018, pp. 133–137.
- [79] S. Stern, D. Rohweder, J. Freudenberger, and R. F. Fischer, "Binary multilevel coding over Eisenstein integers for MIMO broadcast transmission," in *23rd Int. ITG Workshop on Smart Antennas (WSA)*, 2019, pp. 198–205.

**Sebastian Stern** (Member, IEEE) received the B.Sc. and M.Sc. degrees in Communications and Computer Engineering from Ulm University, Ulm, Germany, in 2010 and 2012, respectively, and the Dr.-Ing. (Doctor of Engineering) degree in 2019. He is currently working as a Senior Researcher at the Institute of Communications Engineering, Ulm University, where he received the teaching assignment for a lecture on multi-user communications and multiple-input/multiple-output (MIMO) systems. His main research interests are in the area of communication theory and especially concern lattice-based approaches and algorithms for MIMO communications and related fields, coded-modulation techniques, and massive MIMO schemes.

**Cong Ling** (Member, IEEE) received the B.Sc. and M.Sc. degrees in Electrical Engineering from the Nanjing Institute of Communications Engineering, Nanjing, China, in 1995 and 1997, respectively, and the Ph.D. degree in electrical engineering from Nanyang Technological University, Singapore, in 2005. He is currently a Reader (Associate Professor) with the Electrical and Electronic Engineering Department, Imperial College London. His research interests include coding, signal processing, and security, with a focus on lattices. Before joining Imperial College, he had been on the faculties of the Nanjing Institute of Communications Engineering and King's College. He served as an Associate Editor for IEEE TRANSACTIONS ON COMMUNICATIONS and IEEE TRANSACTIONS ON VEHICULAR TECHNOLOGY.

**Robert F.H. Fischer** (Senior Member, IEEE) received the Dr.-Ing. and Habilitation degrees from the University of Erlangen-Nuremberg, Erlangen, Germany, in 1996 and 2001, respectively.

From 1992 to 1996 he was a Research Assistant with the Telecommunications Institute, University of Erlangen-Nuremberg. In 1997, he was with the IBM Research Laboratory, Zürich, Switzerland. In 1998, he returned to the University of Erlangen-Nuremberg. In 2005, he spent a sabbatical with ETH Zürich. Since 2011 he has been a Full Professor at Ulm University, Ulm, Germany. He is currently teaching the undergraduate and graduate courses on signals and systems and digital communications. He authored the textbook *Precoding and Signal Shaping for Digital Transmission* (John Wiley & Sons, 2002). His current research interests include fast, reliable, and secure digital transmission, including single-carrier and multi-carrier modulation techniques, information theory, coded modulation, digital communications, signal processing, and especially precoding and shaping techniques.

Dr. Fischer was a recipient of the Dissertation Award from the Technical Faculty, University of Erlangen-Nuremberg, in 1997, the Publication Award of the German Society of Information Techniques in 2000, the Wolfgang Finkelburg Habilitation Award in 2002, and the Johann-Philipp-Reis-Preis in 2005.